Awareness and Localization of Explosives-Related Threats

A Department of Homeland Security Center of Excellence

Phase 2, Year 2 Annual Report
September 2015

ALERT
AWARENESS AND LOCALIZATION
OF EXPLOSIVES-RELATED THREATS

Table of Contents

R1-A.1: Characterization of Explosives & Precursors

I. PARTICIPANTS

Faculty/Staff			
Name	Title	Institution	Email
Jimmie Oxley	Co-PI	URI	joxley@uri.edu
Jim Smith	Co-PI	URI	jsmith@chm.uri.edu
Gerald Kagan	Post-Doc	URI	gkagan@chm.uri.edu
Graduate, Undergraduate and REU Students			
Name	Degree Pursued	Institution	Month/Year of Graduation
Maria Donnelly	PhD	URI	5/2015
Matt Porter	PhD	URI	5/2016
Austin Brown	PhD	URI	5/2016
Kevin Colizza	PhD	URI	5/2018
Lindsay McLennan	PhD	URI	5/2017
Stephanie Rayome	MS	URI	12/2015
Jon Canino	PhD	URI	5/2014
Devon Swanson	PhD	URI	5/2017

II. PROJECT DESCRIPTION

A.   Overview and Significance

All new materials require characterization; but in the case of explosives, complete characterization is especially important in terms of safety concerns--safety for those who handle the materials and safety for those with expectations that the materials perform. In the case of homemade explosives (HMEs), the materials may not be exactly new (many were reported in the late 1800's), but their "routine" handling by those involved in counterterrorism has resulted in accidents and raises questions about detectability.

To detect, destroy, handle safely or prevent the synthesis of HMEs, complete understanding of the following information is essential:

- How the HME is formed and what accelerates or retards its formation;
- How the HME decomposes and what accelerates or retards that decomposition;
- How the HME crystallizes;
- What is its vapor pressure and what is its headspace signature;
- What is its density;
- What is its sensitivity to accidental ignition as well as purposeful ignition;
- What is its performance under shock and fire conditions?

Admittedly this mission is too large and R1-A.1 has approached it material by material. In previous years, we have examined triacetone triperoxide (TATP) and erythritol tetranitrate (ETN) [1-11]. The detailed ex-

amination of TATP resulted in 10 publications and led to a method of preparing safe, long-lasting canine and instrument training aids. ETN, a compound chemically similar to the often used explosive PETN (pentaerythritol tetranitrate), is still being examined. Our present focus has been on hexamethylene triperoxide diamine (HMTD) [12, 13] and fuel/oxidizer (FOX) mixtures, in general [14].

Many laboratories which work directly or indirectly on homeland security issues are not able to purchase or store explosives, especially HMEs. Our database provides a valuable service to those laboratories. Standard chemical properties are measured and uploaded to a database for assessment by registered users. In addition, advice is available in terms of how to perform analyses in their own laboratory; and, in a few cases, personnel have been sent to train in the URI laboratory. Disposal of small quantities of HMEs can also be a concern. URI is a leader in the field of chemical digestion of unwanted HMEs. Research on FOX mixtures is a field where little definitive information is available but there is much speculation in terms of what "works" and what "ought to work". Our research in this area has two goals: (1) To allow the homeland security enterprise (HSE) to narrow or widen the list of threat oxidizers; and (2) To collect and match sufficient small-scale data to large-scale performance so that small-scale data has greater predictive value.

R1-A.1 is currently focused on HMTD formation and decomposition and on bounding the range of FOX mixtures which can be used as explosives. Publications regarding our findings can be found in section V.A. One of our first approaches to the study of HMTD was examining analysis methods. HMTD exhibits an unusual gas phase phenomenon in the presence of alcohols, and we used positive ion atmospheric pressure chemical ionization (APCI) mass spectrometry to examine this behavior. HMTD was infused with various solvents, including ^{18}O and ^{2}H labeled methanol, and based on the labeled experiments, it was determined that under APCI conditions, the alcohol oxygen attacks a methylene carbon of HMTD and releases H_2O_2 [12]. Our work continued to study synthesis and decomposition of HMTD in condensed phase. Mechanisms are proposed based on isotopic labeling and mass spectral interpretation of both condensed phase products and headspace products. Formation of HMTD from hexamine appeared to proceed from dissociated hexamine, as evident from the scrambling of the ^{15}N label when synthesis was carried out with equal molar labeled/unlabeled hexamine. The decomposition of HMTD was considered with additives and in the presence and absence of moisture. In addition to mass spectral interpretation, density functional theory (DFT) was used to calculate energy differences of transition states and the entropies of intermediates along the decomposition pathway. HMTD is destabilized by water and citric acid, making purification following initial synthesis essential in order to avoid an unanticipated violent reaction [13].

A survey of the stability and performance of FOX mixtures examined 11 solid oxidizers with 13 fuels by differential scanning calorimetry (DSC), simultaneous differential thermolysis (SDT) and hot-wire ignition. Sugars, alcohols, hydrocarbons, benzoic acid, sulfur, charcoal and aluminum were used as fuels; all fuels except charcoal and aluminum melted at or below 200°C. It was found that the reaction between the oxidizer and the fuel was usually triggered by a thermal event, i.e. melt, phase change or decomposition. Although the fuel usually underwent such a transition at a lower temperature than the oxidizer, the phase change of the fuel was not always the triggering event. When sugars or sulfur were the fuels, their phase change usually triggered their oxidation. However, 3 oxidizers, KNO_3, $KClO_4$, NH_4ClO_4, tended to react only after they underwent a phase change or began to decompose, which meant that their oxidization reactions, regardless of the fuel, was usually above 400°C. $KClO_4$/fuel mixtures decomposed at the highest temperatures, often over 500°C, with the ammonium salt decomposing almost 100°C lower. Mixtures with ammonium nitrate (AN) also decomposed at much lower temperatures than those with the corresponding potassium salt. With the exception of the oxidizers triggered to react by the phase changes of the polyols and sulfur, FOX mixtures generally decomposed between 230°C and 300°C, with AN formulations generally decomposing at the lowest temperature. In terms of heat release, potassium dichromate/fuel mixtures were the least energetic, generally releasing less than 200 Jg^{-1}. Most of the mixtures released 1000 to 1500 Jg^{-1}, with potassium chlorate, ammonium perchlorate and AN releasing significantly more heat, around 2000 Jg^{-1}. When the fuel was aluminum, most of the oxidizers decomposed below 500°C, leaving the aluminum to oxidize at over 800°C.

Only two oxidizers reduced the temperature of the aluminium exotherm: chlorate and potassium nitrite. To go to temperatures above 500°C, unsealed crucibles were necessary, but with these containers, the endothermic volatilization of reactants and products effectively competed against the exothermic decomposition so that heat release values were artificially low.

B.   State-of-the-Art and Technical Approach

Physical properties include infrared (IR), Raman, ^{1}H and ^{13}C NMR and mass spectroscopy. These properties are measured and made available to the HSE and forensic labs through an online database. Also available to the users are analytical methods. Other essential properties include thermal stability under a variety of conditions, heat of decomposition and detonation and destructive techniques. As discussed below our database has over 900 subscribers and is much appreciated. In the last year, we have been asked to review more than 40 papers dealing with explosives; this serves to keep us busy and updated with the latest research. In terms of studies of FOX materials, it is of interest that most papers in the last decade originated from India or Iran.

B.1.   HMTD studies

B.1.a.   Rationale and approach for HMTD studies

HMTD was first synthesized in 1881 [15, 16]; it forms from the oxidation of hexamine by hydrogen peroxide with an acid catalyst followed some decades later [17]. X-ray diffraction showed planar 3-fold coordination about the two bridgehead nitrogen atoms rather than a pyramidal structure (see Fig. 1) [18, 19]. This ring strain in HMTD may account for its low thermal stability and high sensitivity to impact, shock, and electrostatic discharge [20, 21]. Because there have been several accidents with counterterrorism personnel handling HMTD, we launched a study to better understand its chemistry and to identify its signature under a variety of conditions for the purposes of detection. The chemistry and decomposition of HMTD in the presence of a number of chemicals was probed. In addition, isotopically labeled HMTD was prepared and used to elucidate its mechanism of formation and decomposition
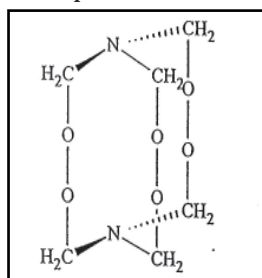

Figure 1: HMTD structure.

B.1.b.   HMTD headspace studies

HMTD has only limited solubility even in the most polar solvent so that large volumes of ethyl acetate and acetonitrile must be used for recrystallization, and these proved almost impossible to remove completely from HMTD. For that reason, many of the studies were conducted with both crude and recrystallized HMTD to ensure the presence of trace solvent had not biased results. Because HMTD decomposition can be readily observed at 60 °C, significant decomposition at ambient temperature is probable. In fact, when HMTD was removed from storage at -15 °C (freezer temperature), it developed a noticeable odor after a couple of hours.

Headspace samples of both crude and recrystallized HMTD, fresh and aged, were analyzed by GC/MS. Gases were analyzed from the headspace using gas-tight syringe or Solid Phase Microextraction (SPME) fiber. The former was used for permanent gases; the latter for volatile amines. When HMTD was heated under a variety of conditions the predominant decomposition products observed in the headspace were trimethylamine

(TMA) and dimethylformamide (DMF) with trace quantities of ethylenimine (EN), methyl formamide (MFM), formamide (FM), hexamine, with moisture, 1-methyl-1H-1,2,4-triazole and pyrazine. No oxygen nor nitrogen was found, but carbon monoxide and carbon dioxide were evolved in significant amounts. Surprisingly, no HMTD was observed under dry, moist, acidic, or basic conditions. This raised concerns about whether molecular HMTD could be found in its headspace or whether it had decomposed under our analytical protocols. Therefore, we used the same GC/MS conditions to inject a solution of HMTD; the molecular ion was observed, leading us to conclude that if it had been in the vapor headspace, we should have observed it. However, at the Trace Explosive Detection conference (April 2015), MIT Lincoln Labs reported with a specialized set up they were able to detect the molecular ion at the parts-per-trillion level. [21]

B.1.c. Reactivity of HMTD

The effect of additives on HMTD stability was screened by differential scanning calorimetry (DSC) (see Table 1) and by isothermal heating at 60°C or 80°C (see Table 2 on the next page). A general trend is readily observed: acids lower the temperature at which the exothermic maximum appeared. We had previously demonstrated that concentrated mineral acid could be used to destroy HMTD [22-26]. We and others also observed that aqueous basic solutions rapidly decompose HMTD [27]. To determine the effect of select additives, HMTD was held at 60 °C for a week at 30%RH; of the additives tested, only citric acid markedly accelerated HMTD decomposition. The fact that water and citric acid, both used in the synthesis of HMTD, lowered its thermal stability emphasizes the need to thoroughly rinse and dry HMTD. Headspace monitoring revealed that water, citric acid, or any acidity sped up the production of TMA and DMF in gas phase.

Material	pKa of Additive	pKb of Additive	Onset Temp. of Exotherm (°C)	Exotherm Temp. Maximum (°C)	Heat Released (J/g)
18.2MΩ H2O	14.0	0.0			
HMTD Crude	N/A	N/A	159	161	2300
HMTD Rec 70/30 EA/ACN	N/A	N/A	168	171	3100
HMTD + Aqueous Solution					
HMTD Crude + 2ul H2O	N/A	N/A	136	140	3100
HMTD Rec 70/30 EA/ACN + 2ul H2O	N/A	N/A	140	143	3200
HMTD Crude +2ul pH4 Buffer	N/A	N/A	126	129	3700
HMTD Crude + 2ul pH7 Buffer	N/A	N/A	134	137	3300
HMTD Crude + 2ul pH10 Buffer	N/A	N/A	137	139	3100
HMTD + Solvents					
HMTD Crude + 2ul ACN	N/A	N/A	152	178	3000
HMTD Crude + 2ul Benzene	N/A	N/A	166	172	3200
HMTD Crude + 2ul EtOH	N/A	N/A	153	164	2800
HMTD Crude + 2ul EtAc	N/A	N/A	156	169	2800
HMTD + Solid Acids					
HMTD Crude + KH2PO4 15%	7.2	6.8	163	165	2100
HMTD Crude + KH Phthalate 15%	5.4	8.6	156	157	1900
HMTD Crude + Benzoic Acid 15%	4.2	9.8	155	160	2600
HMTD Crude + Ascorbic Acid 15%	4.0	10.0	146	148	2000
HMTD Crude + Citric Acid 15%	3.1	10.9	134	137	2800
HMTD Crude + Sulfanilic Acid 15%	3.0	11.0	122	125	2400
HMTD Crude + O Phthalic Acid 15%	2.9	11.1	143	145	2000
HMTD + Solid Bases					
HMTD Crude + Melamine 15%	5.0	9.0	158	159	2000
HMTD Crude + NaHCO3 15%	6.4	7.7	163	164	1300
HMTD Crude + KH2PO4 15%	7.2	6.8	163	165	2100
HMTD Crude + NaOH 15%	14.0	0.0	160	161	2300
HMTD Crude + NaOH 30%	14.0	0.0	162	164	2100
HMTD Crude + K Tertbutoxide 15%	17.0	-3.0	159	160	2200

*NaHCO$_3$ has and endotherm which lowers the total heat released

Table 1: DSC of HMTD with additives (20 °C/min).

30%RH 60C 1 week	
HMTD Solid Additive (15%)	Average % Remaining
None	87
NaHCO3	87
KH2PO4	96
NaOH	75
KTButoxide	80
Citric Acid	13

Table 2: Solid additives with HMTD.

B.1.d.   Effect of humidity on HMTD decomposition

In 1924, it was reported:

"That H.M.T.D. is stable at temperatures up to at least 60 °C; it is not affected by storage under water; but it is slowly affected when subjected to high humidity at maximum summer temperature….It is practically non-hygroscopic."[27]

Because this statement does not support our DSC results (see Table 1 with added water), samples of crude HMTD were held at 60°C at fixed humidities of 0, 30, 75, or 100%RH and monitored each week for four weeks (see Fig. 2) [28]. After 2 weeks, the samples of HMTD at high humidities were completely degraded; no HMTD was observed by GC/MS.
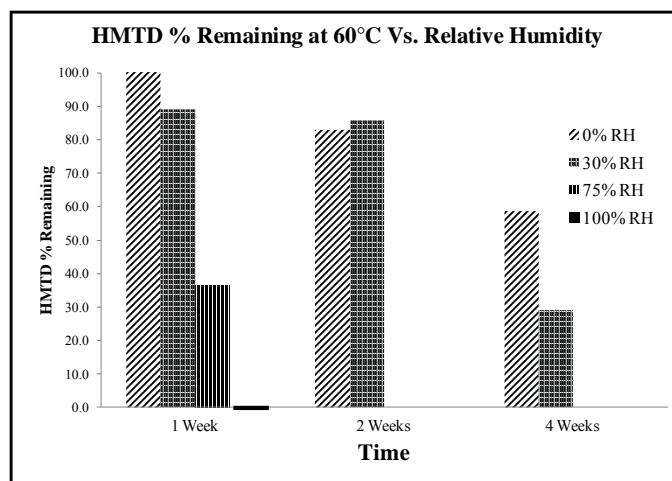

Figure 2: Effect of humidity on HMTD.

B.1.e.   Mass spectral analysis of condensed-phase decomposition products

HMTD was heated at 60°C under various conditions. Products were examined by GC/MS and LC/MS; and assignments are shown in Table 3 and Table 4, respectively, on the next page. Assignments are based on comparison with the authentic samples [4.2, 4.3, 4.5, 4.11, HMTD and hexamine] and on the high resolution mass spectrometric results where compositions could be determined within 5 ppm of their calculated mass (see Table 4 on the next page). Upon examining the HMTD decomposition products, it is tempting to suggest HMTD thermolysis produces a number of small molecular fragments, e.g. CH_2O, NH_3, CH_2NH, or $CH(O)NH_2$, which undergo further reaction, such as an aldehyde-amine condensation. The observed substituted triazine

species (3.10, 3.11, 3.12) and those containing four nitrogen have been reported to form from hexamethylenetetramine (hexamine) [29-31]. Indeed, hexamine was found when HMTD was decomposed at 60 °C at 75% or 100% RH or with added water or acidic buffer. Only tetramethylene diperoxide diamine dialdehyde (TMDDD) (4.22) (matched to an authentic sample), and the mono aldehyde (3.7) suggested the original HMTD structure and that HMTD was degraded stepwise.

In examining how HMTD decomposed, we asked how that degradation formed hexamine. Hexamine is made from ammonia and formaldehyde, and the route is via hexahydro-1,3,5-triazine[21, 32]. The conversion of hexamine to 2,4,6-cyclotrimethylene-1,3,5-trinitramine (RDX) has been the subject of several studies [33-35].
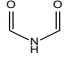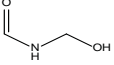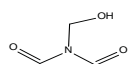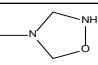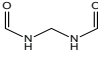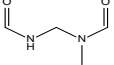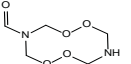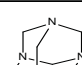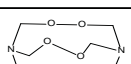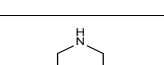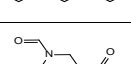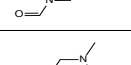
#	Mass	Identity	amount	
1	73	(structure)	L	DRY & HUMID
2	75	(structure)	L	MATCHED TO AUTHENTIC SAMPLE; MAINLY SEEN IN HUMID CONDITIONS
3	103	(structure)	M	MATCHED TO AUTHENTIC SAMPLE; MAINLY SEEN IN HUMID CONDITIONS
4	88	(structure)	S	
5	84, 102	(structure)	L	MATCHED TO AUTHENTIC SAMPLE; DRY CONDITIONS
6	116	(structure)	L	DRY CONDITIONS
7	178	(structure)	S	BOTH IN DRY & HUMID CONDITIONS
8	140	(structure)	M	MATCHED TO AUTHENTIC SAMPLE; MAINLY SEEN IN HUMID OR ACIDIC CONDITIONS
9	208	(structure)	L	
10	143	(structure)	S	
11	171	(structure)	L	MATCHED TO AUTHENTIC SAMPLE; MAINLY SEEN IN HUMID CONDITIONS
12	157	(structure)	S	MAINLY SEEN IN DRY CONDITIONS

Table 3: Decomposition Products GC/MS.
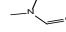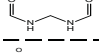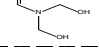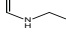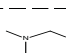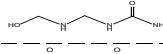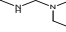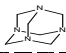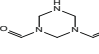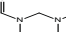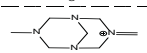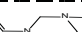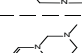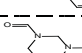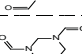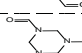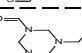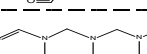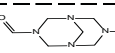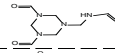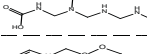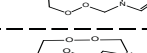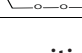
#	[M+H]+	Identity	amount	
1	74.06004	(structure)	L	C_3H_8ON
2	103.0501	(structure)	L	$C_3H_7O_2N_2$ MATCHED TO AUTHENTIC SAMPLE
3	106.0499	(structure)	S	$C_3H_8O_3N$
4	117.0659	(structure)	L	$C_4H_9O_2N_2$
5	117.1022	(structure)	L	$C_5H_{13}ON_2$
6	120.0768	(structure)	S	$C_3H_{10}O_2N_3$
7	133.0608	(structure)	S	$C_4H_9O_3N_2$
8	141.1131	(structure)	L	$C_6H_{13}N_4$
9	144.0768	(structure)	M	$C_5H_{10}O_2N_3$
10	145.0608	(structure)	M	$C_5H_9O_3N_2$
11	155.1289	(structure)	M	$C_7H_{15}N_4$
12	157.1083	(structure)	L	$C_6H_{13}ON_4$
13	158.0923	(structure)	L	$C_6H_{12}O_2N_3$
14	160.0717	(structure)	L	$C_5H_{10}O_3N_3$
15	172.0712	(structure)	L	$C_6H_{10}O_3N_3$ MATCHED TO AUTHENTIC SAMPLE
16	172.1078	(structure)	S	$C_7H_{14}O_2N_3$
17	174.0873	(structure)	M	$C_6H_{12}O_3N_3$
18	174.1235	(structure)	S	$C_7H_{16}O_2N_3$
19	185.1032	(structure)	S	$C_7H_{13}O_2N_4$
20	201.0982	(structure)	L	$C_7H_{13}O_3N_4$
21	205.0931	(structure)	S	$C_6H_{13}O_4N_4$
22	207.0611	(structure) TMDDD	M	$C_6H_{11}O_6N_2$
	209.0768	(structure) HMTD dependent		$C_6H_{13}O_6N_2$

Table 4: Decomposition Products LC/MS.

Bachman found that performing the nitration of hexamine in acetic anhydride with ammonium nitrate allowed two moles of RDX to be produced rather than one via direct nitration [21]. Using that example we questioned the stoichiometry in the synthesis of HMTD from hexamine. Under the normal synthetic route as it is describe in equation 1; our yield, based on hexamine, was not more than 60%. However, if excess formaldehyde was added to the reaction mixture, yields of greater than 100% (based on 1 HMTD to 1 hexamine) were observed (eq 2). If no extra formaldehyde is added, the reaction must wait for the degradation of part of the hexamine to form formaldehyde (see Fig. 3). Indeed, hexamine is frequently used as a source of formaldehyde [31, 36].

$$C_6N_4H_{12} + 3\ H_2O_2\ \rightarrow\ C_6N_2H_{12}O_6 + 2\ NH_3 \quad\quad\quad (1)$$

$$C_6N_4H_{12} + 6\ H_2O_2 + 6\ OCH_2\ \rightarrow\ 2\ C_6N_2H_{12}O_6 + 6\ H_2O \quad\quad\quad (2)$$
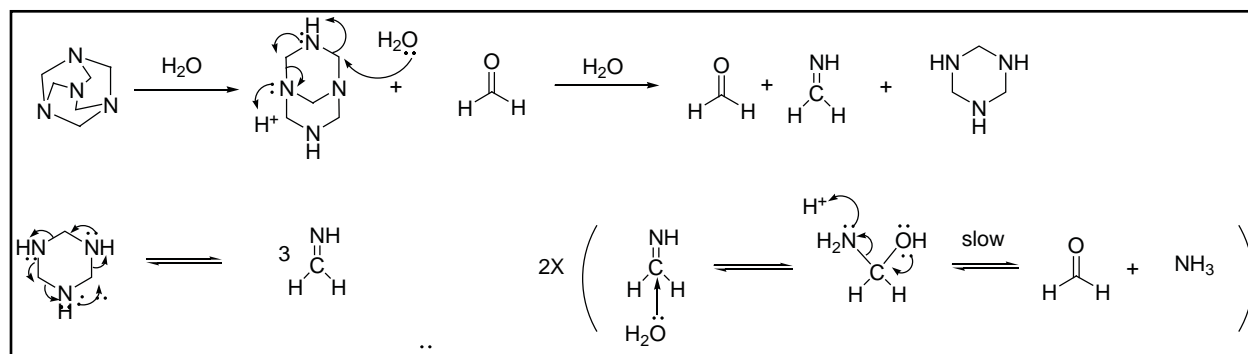
Figure 3: Proposed hexamine decomposition mechanism.

Without acid catalysis, formation of HMTD takes days. Furthermore, the reaction is sensitive to the type and amount of acid (see Table 5 on the next page). Diprotic and triprotic acids (e.g. sulfuric, phosphoric, and oxalic acids) could be used as direct replacements for citric acid. Monoprotic acids (e.g. acetic acid, trifluoroacetic acid, formic acid, and nitric acid) gave yields comparable to citric acid only if these acids were added in 2.2 mol acid to 1 mol hexamine ratio. This aspect of the acid effect warrants further examination.

To probe the importance of citric acid in catalyzing the reaction of hexamine with hydrogen peroxide, the reaction was run without acid. It took 7 days at room temperature, instead of a few hours with citric acid, for the first HMTD to precipitate. After 9 days, the yield of HMTD (assuming 1:1 molar ratio hexamine: HMTD) was only ~7%. Other diprotic and triprotic acids (vide supra) were added in 1.1 to 1 molar ratios hexamine: acid. Monoprotic acids gave poor yields (see Table 5 on the next page) if added in 1.1 to 1 molar ratios. If these (acetic acid, trifluoroacetic acid, formic acid, and nitric acid) were added in a 2.2 to 1 molar ratio hexamine:acid yields were comparable to those achieved with citric acid. The ratio of hexamine to HMTD became a point of interest.

HMTD Reaction #	Additive	Mol Ratio of HP (48.4wt%): Hexamine	Mol Ratio Acid (Citric): Hexamine	% Yield	MP (°C)	Purity by GC/MS
5	citric acid	8	1.1:1	44.5	149-150	87.4
6	citric acid	8	1.1:1	40.7	144-145	87.1
17	citric acid	8	1.1:1	52.7	153-157	95.8
14	anhydrous oxalic acid	8	1.1:1	45.0	151-153	94.4
15	85% o-phosphoric acid	8	1.1:1	26.9	149-150	91.3
32	50% sulfuric Acid	8	1.1:1	50.5	152-158	98.2
13	glacial acetic acid	8	1.1:1	7.4	152-153	94.3
30	glacial acetic acid	8	2.2:1	33.1	151-156	100.0
21	88% formic Acid	8	1.1:1	6.3	154-158	94.5
25	88% formic Acid	8	2.2:1	43.5	153-154	100.0
22	99% TFA	8	1.1:1	3.3	155-159	93.3
26	99% TFA	8	2.2:1	53.5	153-156	99.6
31	70% nitric Acid	8	2.2:1	51.1	155-157	100.0
Kin. #2	no acid	8	0:1	9.5	148-149	89.5
Kin. #3	no acid	8	0:1	7.2	152-160	92.4

Table 5: HMTD reactions with additives with scaled yield of 0.5g.

If HMTD was formed when hexamine breaks into small fragments, then it ought to incorporate carbon and nitrogen from outside sources. When HMTD was created in a ^{13}C formaldehyde solution, the label was observed in both the HMTD (m/z 209, 210, 211, 212, 213) formed and the hexamine (m/z 140, 141, 142, 143, 144) remaining early in the reaction (42min when precipitation was observed in 2 hr) (see Fig. 4 on the next page). This could be explained by the formation of bis(hydroxymethyl) peroxide (BHMP) and its incorporation into HMTD. Incorporation of formaldehyde into the hexamine can be explained by looking at the first step of decomposition of hexamine (see Fig. 5 on the next page). Excess formaldehyde may push this reaction in the reverse direction. However, when HMTD synthesis was performed in the presence of ^{15}N labeled ammonium sulfate, the resulting HMTD, when analyzed by LC-MS, showed little incorporation of the label.
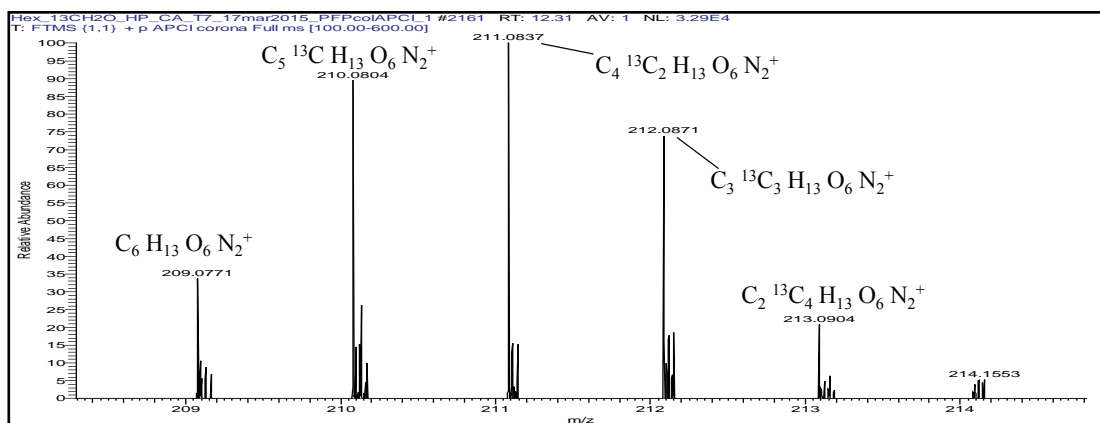
Figure 4: Mass spectrum of HMTD formed in the presence of 13C-Formaldehyde.
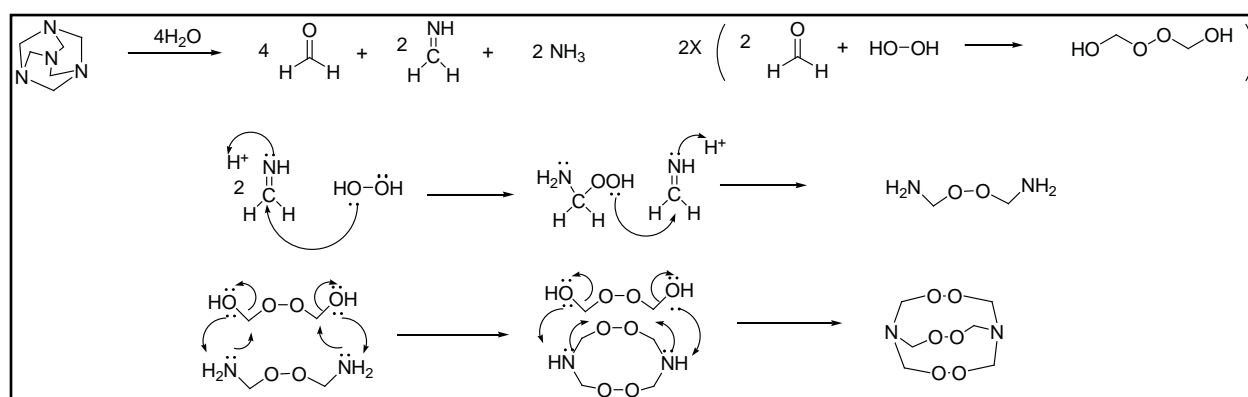
Figure 5: Formation of HMTD from completely dissociated hexamine.

In contrast to the lack of ^{15}N incorporation during HMTD synthesis, it was found that under humid decomposition conditions, the ^{15}N label was observed in the decomposition products (4.2, 4.13, 4.14, 4.15) as well as in hexamine (single, double, triple and quadruple label). Yet, when the same decomposition studies were performed dry, no hexamine was formed and the decomposition products 4.2 and 4.14 showed no label incorporation. In the presence of deuterium oxide, the HMTD decomposition products trimethylamine, dimethylformamide, hexamine, and triazines showed little incorporation of deuterium (m/z 157, 171 etc.). This suggested that the hydrogen transferred during the decomposition was part of the original HMTD molecule. In the water surrounding an open vial of HMTD, formic acid was observed. It has previously been suggested that formaldehyde and hydrogen peroxide form formic acid [38].

A mechanism for HMTD formation was proposed based on data from isotopic ratio mass spectrometry [37]. Because it required the formation of a triperoxy tertiary amine and protonated methylene imine, we looked for alternative pathways. Tentative proposals are illustrated in Figure 5 and Figure 6 on the next page. In Figure 5 hexamine is broken into small molecules, and from the formaldehyde/hydrogen peroxide reaction bis(hydroxymethyl) peroxide (BHMP) is formed, while from the imine/ hydrogen peroxide reaction bis(methylamine) peroxide is formed. The latter reacts with two molecules of BHMP to create HMTD. The mechanism in Figure 6 on the next page also postulates the formation of BHMP but allows HMTD to remain intact until fairly late in the reaction. Both mechanisms are in line with the fact that the reaction proceeds to HMTD faster in the presence of excess formaldehyde. The key to both mechanisms is the formation of BHMP, first synthesized in 1914 by Fenton from hydrogen peroxide and formaldehyde and later studied by Satterfield [38]. It is likely this species was generated in situ in the reported syntheses of several caged peroxides having planar bridgehead nitrogen atoms [39]. Once a methylene is lost from hexamine to form formaldehyde the

resulting octahydro-1,3,5,7-tetrazocine would be subject to rapid ring inversion and isomerization, which BHMP can bridge across two nitrogen atoms.
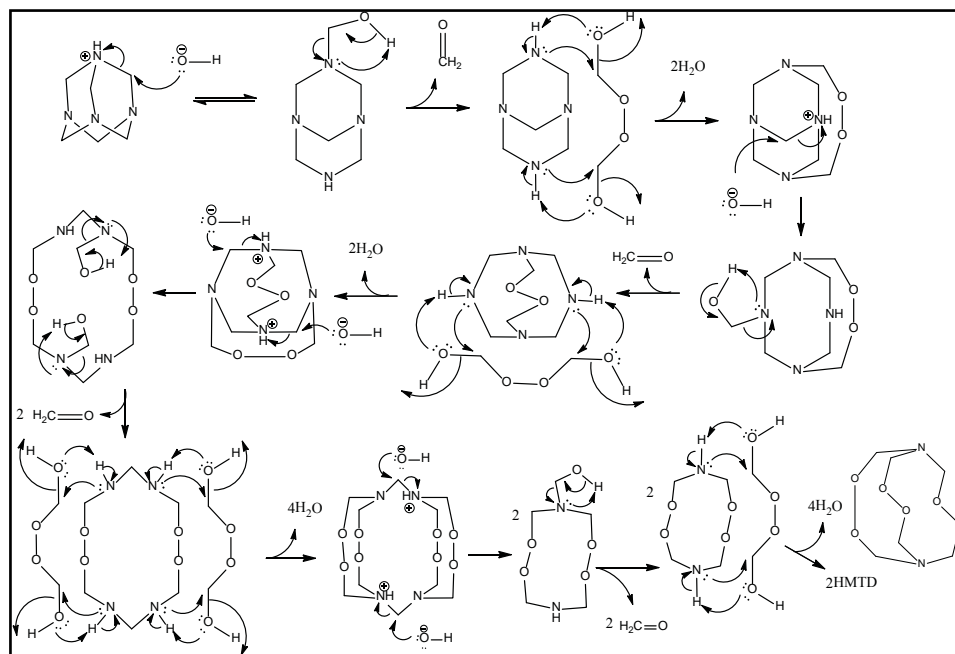
Figure 6: Formation of HMTD from intact of hexamine.

To distinguish between the mechanisms proposed in Figures 5 and 6, synthesis of HMTD was performed with a 1:1 mixture of ^{14}N hexamine and ^{15}N hexamine. If formation of HMTD proceeds through the route shown in Figure 5, then total scrambling of the label would be expected, i.e. the HMTD product should show the unlabeled, single-labeled and double-labeled species [M+H], 209 to 210 to 211, in a 1:2:1 ratio. This was observed (see Fig 7).
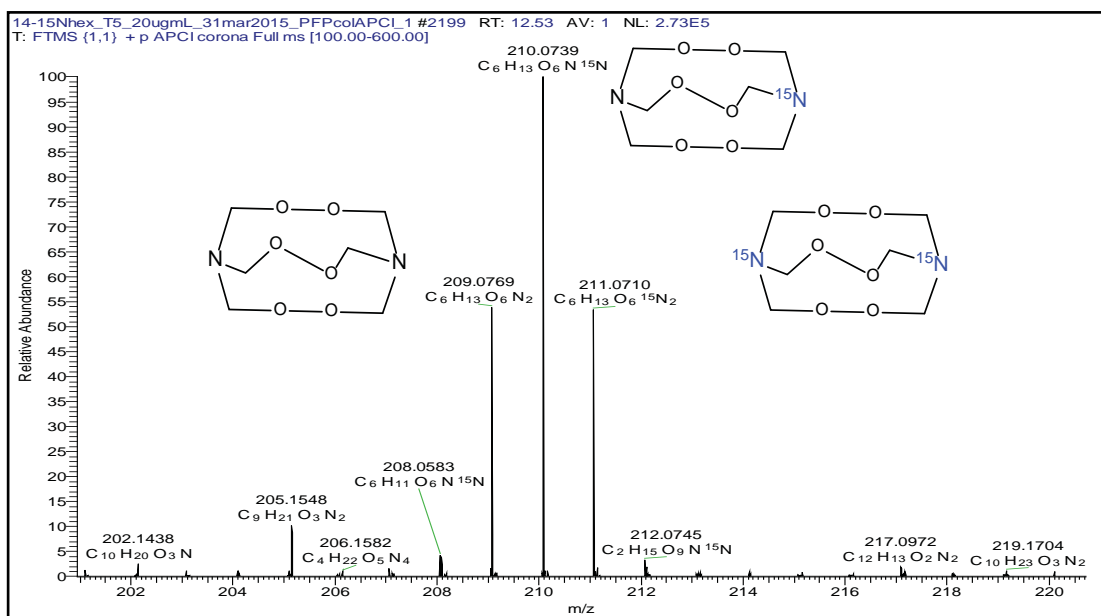
Figure 7: Mass spectrum of HMTD formed from a mixture of N-14 and N-15 labeled hexamine.

To shed light on how HMTD decomposes, density functional theory (DFT) calculations were performed by R1-C1 team (see their report or reference 4 in the overview).

B.1.f.   Summary/conclusions

Because HMTD is destabilized by water and citric acid, it is important to purify it after initial synthesis. Ignoring the degrading effects of acid and humidity can lead to an unexpected violent reaction. Precautions should be taken to see that HMTD remains dry. The headspace (signature) of HMTD is mainly trimethylamine (TMA) and dimethylformamide (DMF), and these might be used for canine and other vapor detection training instead of the more hazardous HMTD. Further work is underway to clarify mechanisms of HMTD decomposition. Studies to date indicate hexamine must break down to form formaldehyde, but the reverse reaction is only effective in the presence of moisture. Preventing the assembly of formaldehyde into the molecule HMTD will continue as the ultimate research goal.

B.2.   Studies on FOX mixtures

B.2.a.   Rationale for study of FOX mixtures

The scientific literature lacks information about fuel-oxidizer mixures; nevertheless, it is an essential first step to establishing limitations or potentials of individual oxidizers in Fuel Oxidizer Explosives (FOX). This study is part of an attempt to identify principles related to potential explosivity. This report provides an extensive survey of the stability and performance of 11 solid oxidizers with 13 fuels from differential scanning calorimetry (DSC), simultaneous differential thermolysis (SDT) and hot-wire ignition.

B.2.b.   Neat Species

Oxidizing power can be assessed in various ways. Intrinsic oxidizing ability, given by standard reduction potentials in Volts (1M aq solution against standard hydrogen electrode), is one approach to quantifying oxidizing power. Standard reduction potentials are listed in Table 6 starting from the left with species having most positive potential [40]:

$$H_2O_2 > IO_4^- > MnO_4^- > BrO_3^- > MnO_4^- > ClO_3^- > Cr_2O_7^- > ClO_4^- > IO_3^- > NO_3^- > NO_2^-$$
$$1.8 > 1.7\text{-}1.6 > 1.7\text{-}1.5 > 1.5\text{-}1.4 > \quad 1.5 \quad > \quad 1.5 \quad > 1.4\text{-}1.3 > 1.4\text{-}1.2 > 1.2\text{-}1.1 > 1.0\text{-}0.8 > -0.46$$
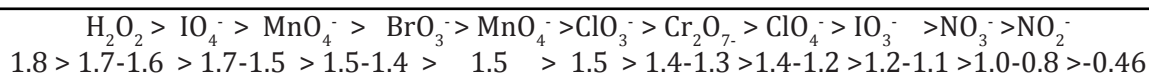
Table 6: Standard reduction potentials.

Actual potentials depend on the pH of the solution and the final products:

$NO_3^- \rightarrow NO$, HNO_2, NH_4^+, NO_2 0.96, 0.94, 0.87, 0.80 V, respectively

An alternative approach to rating oxidizing power is a burn test. The U.N. Manual of Tests and Criteria rates an oxidizer by comparing its burn rate in admixture with cellulose (2:3 and 3:7 ratios) to mixtures of potassium bromate/cellulose [41]. Our burn tests used 250mg instead of 30g oxidizer, and sucrose or aluminum powder instead of cellulose. Fuel-Oxidizer burn rates are shown in Table 7 on the next page.

Thermal stability was assessed via the temperature at peak maximum of the DSC exotherm. The higher the exotherm temperature, the more thermally stable the species. Some salts decomposed with exclusive endothermic responses (see Table 8 on the following page). Among salts releasing heat (exothermic response), the amount of heat varied from more than 1000 J/g for ammonium salts, which can undergo self-oxidation, to a few hundred joules per gram for other oxidizers. Thermal traces of the oxidizers alone were not simple; they included phase change(s), decompositions, and heats of fusion of the decomposition product. In systems where oxygen was not allowed to escape, the pairs perchlorate/ chlorate [42] and nitrate/nitrite [43] can establish a psuedo-equilibria (eq 1-2). [44]

$$O_2$$
$$KClO_4 \leftrightarrows KClO_3 \rightarrow KCl + 1.5\ O_2 \qquad (1)$$
$$KNO_3 \leftrightarrows KNO_2 +\ 0.5O_2 \qquad\qquad (2)$$
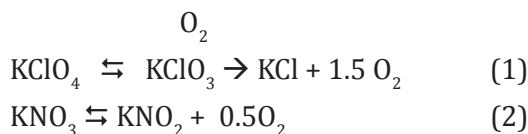
Table II. Burn time (seconds) of a 4:1 Oxidizer: Sucrose Mix											
Oxidizer	KIO_4	$KMnO_4$	$KBrO_3$	$KClO_3$	$K_2Cr_2O_7$	NH_4ClO_4	$KClO_4$	KIO_3	KNO_3	NH_4NO_3	KNO_2
anion potential 1M aq. H_2 0V	1.7-1.6	1.7-1.5	1.5-1.4	1.5	1.4-1.3		1.4-1.2	1.2-1.1	1.0-0.8		-0.46
wt % oxygen in oxidizer	28%	25%	29%	39%	16%	34%	46%	22%	40%	20%	28%
Decomp °C 8/2 oxidizer/sucrose	187	236	186	180	231	484	540	182	396	176	212
J/g heat released	1681	1741	1511	3195	157	1342	735	939	1108	2084	1777
Burn Test 8:2 Oxidizer:Al	KIO_4	$KMnO_4$	$KBrO_3$	$KClO_3$	$K_2Cr_2O_7$	NH_4ClO_4	$KClO_4$	KIO_3	KNO_3	NH_4NO_3	KNO_2
Ave Burn Time by Eye (s)	too fast	too fast	too fast	too fast	too fast	4.3	too fast	7.5	3.8	18.2	2.5
Std. Dev	too fast	too fast	too fast	too fast	too fast	1.0	too fast	2.1	0.7	1.6	0.6
Ave Peak Light Signal Thor Lab (mV)	2564	2360	1113	1129	140	144	2736	--	--	--	--
Std. Dev	232	297	437	286	54	73	11	--	--	--	--
Notes	bright flash	bright flash	bright flash	bright flash	bright flash	bright flash, strobes	bright flash	bubbled	bubbled	bubbled	bubbled
Burn Test 8:2 Oxidizer:Sucrose	KIO_4	$KMnO_4$	$KBrO_3$	$KClO_3$	$K_2Cr_2O_7$	NH_4ClO_4	$KClO_4$	KIO_3	KNO_3	NH_4NO_3	KNO_2
Ave Burn Time by Eye (s)	too fast	1.9	too fast	1.0	4.9	4.6	2.5	1.6	2.5	18.1	1.3
Std. Dev		0.2		0.4	1.7	0.8	0.4	0.4	0.7	2.7	0.3
Ave Peak Light Signal Thor Lab (mV)	56	25	346	104	--	3	11	--	--	--	32
Std. Dev	23	6	98	43	--	1	4	--	--	--	12
Notes	purple flickering	orange flame	purple flame	purple flame	charring, no flame	yellow flame	purple flame	charring, no flame	charring, no flame	dim yellow flame	yellow flame
Burn Test 5:5 Oxidizer:Sucrose	KIO_4	$KMnO_4$	$KBrO_3$	$KClO_3$	$K_2Cr_2O_7$	NH_4ClO_4	$KClO_4$	KIO_3	KNO_3	NH_4NO_3	KNO_2
Ave Burn Time by Eye (s)	3.1	10.4	too fast	2.6	15.9	9.2	8.1	9.0	0.9	21.4	2.6
Std. Dev	0.5	2.1	too fast	0.8	1.7	1.2	1.1	4.2	0.1	4.8	1.1
Ave Peak Light Signal Thor Lab (mV)	--	8	430	128	--	10	58	--	43	--	43
Std. Dev	--	7	164	41	--	2	13	--	13	--	13
Notes	no light, black snake	dim yellow flame	purple flame	purple flame	dim yellow flame	dim yellow flame	dim yellow flame	dim yellow flame	dim yellow flame	no light, black snake	dim yellow flame
Burn Test 8:2 Oxidizer:Benzoic Acid	KIO_4	$KMnO_4$	$KBrO_3$	$KClO_3$	$K_2Cr_2O_7$	NH_4ClO_4	$KClO_4$	KIO_3	KNO_3	NH_4NO_3	KNO_2
Ave Burn Time by Eye (s)	1.6	3.0	too fast	4.4	16.0	6.3	4.5	4.9	4.5	28.7	2.1
Std. Dev	0.5	0.8	too fast	1.7	1.6	1.0	0.6	1.2	1.8	6.2	0.5
Ave Peak Light Signal Thor Lab (mV)	1413	147	2228	762	26	226	737	221	91	14	160
Std. Dev	331	22	228	104	8	45	304	35	33	4	88
Notes	bright flash	orange flame	bright flash	bright yellow flame	yellow flame	bright yellow flame	white flame	white flickering	orange flame	yellow flickering	orange flame

Table 7: FOX burn rates.

Ammonium perchlorate (AP, NH_4ClO_4) did not melt but exhibited an endotherm around 245°C (~70 J/g) as a result of an orthorhombic to cubic phase change. [Ammonium chlorate is thermally unstable and has been reported to spontaneously ignite at temperatures as low as 100°C [45]; for this reason it was not used in this study.] Early in the study it was noted that thermal traces obtained from sealed DSC ampules did not necessarily match those obtained from the open SDT samples (see Fig. 8 on the next page). (An advantage of SDT was that it allowed scanning to higher temperatures. However, since the ampules were not sealed, thermal traces differed markedly from sealed DSC thermal analyses when decomposition products or moisture volatilized.)

All the fuels, except charcoal and aluminum, melted below 208°C; some showed exothermic decomposition especially when heated under air. Endothermic and exothermc temperature miniuma or maxima, onset temperatures for exotherm, and heat release as found by DSC (scan 20°/min) are shown in Table 8 on the following page.
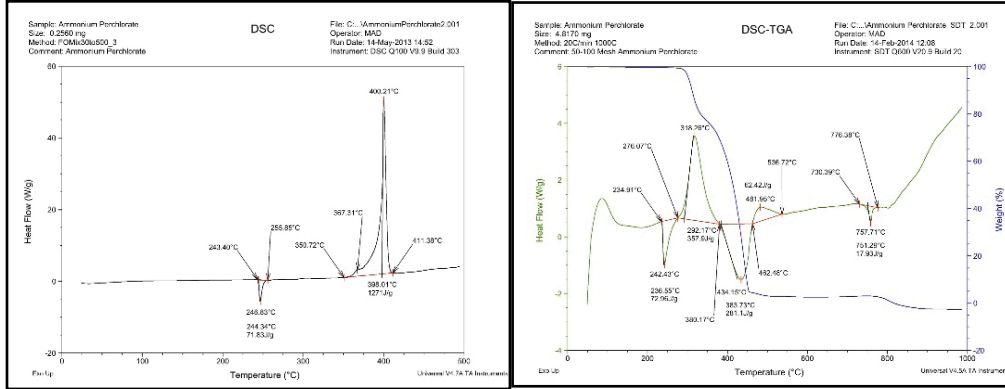
Figure 8: Ammonium Perchlorate DSC (left) vs SDT (right).

start	phase change endo	phase change onset	KIO4 endo	KIO4 onset	KIO4 max °C	KIO4 J/g	KIO4 #	KMnO4 endo	KMnO4 onset	KMnO4 max °C	KMnO4 J/g	KMnO4 #	KBrO3 endo	KBrO3 onset	KBrO3 max °C	KBrO3 J/g	KBrO3 #	KClO3 endo	KClO3 onset	KClO3 max °C	KClO3 J/g	KClO3 #	K2Cr2O7 endo	K2Cr2O7 onset	K2Cr2O7 max °C	K2Cr2O7 J/g	K2Cr2O7 #
phase change																											
melt			543					lit					415					358					402				D
melt KX			675					540					731					766			465	S					
decompose	258	433 (air)		348	355	94	3D		296	305	142	D		435	456	217	3D	517	580			6D					
Sucrose	185, 238		674	155	167	2054	2D 3S	183	225	236	1064	4 D	173, 730	186	206	1110	6D 3S	767	170	175	2037	D 3 S	191, 391	231	241	127	3 D 3S
Sucrose 20%			160, 675	170	183	1805	4D 3S	191, 893	232	237	1798	3 S	176, 770	176, 364	207, 368	1718, 694	4D 3S	766	191, 331	240, 342	2091, 165	3 S	193, 391	231	244	102	3 D
Fructose	129	254	115, 676	126	138	1620	3D 3S	99	177	200	1222	4 D	116, 730	180	196	1317	2D 3S	111, 766	133	166	2,296	3 3	111	105, 174	109, 190	80, 115	3 D 2S
Lactose	153, 208	279																151	183	197	1597	3 D					
Glucose	165, 233	285																149	205	243	2688	9 D					
penta-erythritol	190, 263, 359																										
erythritol	122	297 bp	115, 601, 665	118	145	1140	3S	108	140, 325	161, 358	1702, 204	4 D	190, 732	223	246	1427	2D 3S	191, 767	251	267	2058	5 D	193, 399, 800	385	390	129	3 D 2S
Cyclododecanol	78		77	197, 286, 354	212, 314, 366	19, 237, 496	3D	72	314	320	768	2 D	72	398	408	876	3D	119	235	258	2272	3 D	77	360	384	256	3 D
surfur	135, 179, 316 bp	341	114, 577	242	300	2353, 759, ~350	4D 3S	116, 581	298	309	2360	D 3 S	116, 186	213	320	815	2D	116, 316, 438	171	183	723	4 D					
naphthalene	80		81	292, 450	317, 481	759, (ends after	4D 3S	80	287	303	931	3 D	81	423	433	1779	2D	81, 351	437	461	ended past 500	4 D	81, 396	468	471	68	2 D
acid 20%	121		121	284, 404	299, 415	959, 544	3D	120	124, 288	159, 311	909, 430	3 D	124	368	369	835	3D	124	325	344	3648	3 S	119	385	387	138	3 D
charcoal		416 (air)	100	350, 444	356, 447	116, 240	4D	653	294	310	792	3D	654, 733	421	430			357, 654, 769	329	333	1585	4 D	395	397, 672	400, 702	74, 82	3 D 3S
Al 20%	541, 654, 676			347	356	76	2D 1S		789	819	726	1S		421	430	149	4D 1S		364	477	1499	3 D 1S					
			KIO4					**KMnO4**					**KBrO3**					**KClO3**					**K2Cr2O7**				

Table 8: Temperature endotherms and exotherms DSC & SDT (20o/min, Heat Release J/g).

Fuel	NH4ClO4 endo	onset	max °C	J/g	#	KClO4 endo	onset	max °C	J/g	#	KIO3 endo	onset	max °C	J/g	#	KNO3 endo	onset	max °C	J/g	#	NH4NO3 endo	onset	max	J/g	#	KNO2 endo	onset	max °C	J/g	#
phase	248											nothing in DSC				132					128				3D	45				4D
melt																331					167				3S	419				4D
melt KX dec	758	398	402	1233	3D	613, 769	645	654	293	3S	555d, 680				5S	703				3S		282	311	1407	3D	731, 903	512	519	2	4S
Sucrose	164, 245, 756	176, 268	184, 341	199, 2253	3D, 3S	183, 306, 766	249, 497	281, 501	138, 1125	3D, 3S	154, 678	165	187	1243	D, 4S	133, 178	238, 391	262, 397	242, 1016	4D	55, 128	152	172	2092	3D		225	248	1281	3D
Sucrose 20%	172, 246, 758	476	477	1357	3D, 3S	186, 304, 768	506, 602	538, 622	869, 217	3D, 3S/4S	160, 670	169	185	838	D, 3S	133, 179, 331	377	386	681	3D	55, 130	163, 324	162, 334	1793, 839	4D, 3S	171, 407, 878	180	210	1689	2D, 3S
Fructose	122, 244, 756	173, 277	181, 338	222, 1638	7D, 3S	125, 309, 767	506	508	993	4D, 3S	124, 678	143	156	1442	D, 4S	154	227, 396	248, 404	205, 391	3D	55, 120	155	169	2652	5D		148	168	987	2D
Lactose																152, 212	253, 389	271, 393	276, 696	3D	55, 105	170	182	1480	4D					
Glucose																133, 164	258, 394	285, 398	299, 363	3D	55, 114	166	186	2277	3D					
penta-erythritol											121, 608, 666	156	181	871	D, 4S	187, 351, 677	450	469	1638	7D, 3S	130, 171, 190	263	267	2118	4D					
erythritol	112, 246	362	404	3822	4D	119, 305, 768	324, 450, 627	348, 477, 642	397, >500, 176	4D, 4D, 3S	75	444	452	354	3D	115, 132	397	413	2438	3D	90	265	267	1758	3D	109	288	315	1009	3D
cyclodo decanol	76, 249	361	404	1877	2D	77, 307	NR <500			2D						73, 129, 326	NR	<500		4D										4D
surfur	116, 249, 670	416	422	1747	3D, 3S	116, 306, 765	458	468	1612	3D, 3S	116, 195, 581	324	350	2299	3D, 3S	117, 190	324	336	1,054	6D	54, 116	204	213	2328	3D	120, 169	255	300	2094	2D
naphthalene	81, 247	435	470	1527	3D	82, 308	NR <500			2D	81	NR <500			3D	81, 131, 334	NR	<500			82, 129	305	328	829	3D					
benzoic acid 20%	125, 246	446	457	2347	2D	125, 306	395	>500		3D	124	418	426	476	2D	129, 318	NR <500				127, 166	313	335	1879	2D		NR			
charcoal	246	447	451	1718	4S	307, 765	510	525	1172	3D, 7S	555, 654, 676	443	448	300	3D	129, 324	461	474	1361	5D, 3S	54, 124	222	223	1607	4D	102	358	381	625	3D
Al 20%	247, 654	439, 872	479, 902	1887, 1279	4D, 1S	303, 654, 769	594	626	796	1S	676	581	590	45	iS	331, 572, 653	795	857	1377	3D, 1S	171, 277, 654	320, 864	331, 883	825, 216	2D, 1S	423, 654	695	762	2597	1S

Table 8: Temperature endotherms and exotherms DSC & SDT (20o/min, Heat Release J/g).

B.2.c. Oxidizer/fuel mixtures

Several kinetic and mechanistic studies exist that have examined the oxidization of alcohols by iodate and periodate [46-49], bromate [50, 51], chlorate and perchlorate [52, 53], permanganate [54-56], and dichromate [57] (see Table 9). Most of the oxidizers (KIO_4, $KMnO_4$, $KBrO_3$, $KClO_3$, K_2Cr_2O7, KIO_3, AN, KNO_2) reacted with the sugars immediately after the sugar melt, and a large exotherm was observed, as can be seen in Figure 9 (DSC thermogram of KIO_4 mixed with 50wt% sucrose). This behavior was observed regardless whether the sugar was a disaccharide, i.e. sucrose and lactose, or a monosaccharride, i.e. glucose and fructose (see Figs. 10 and 11 on the next page).

Oxidizer	Alcohol	Products	Reference
$KBrO_3$	propan-2-ol	acetone	19
$KClO_3$	Sucrose	KCl, CO_2, H_2O	21
$KClO_3$	Lactose	KCl, CO_2, H_2O, CO, H_2, C, CH_4	20
$KClO_4$	Sucrose	KCl, CO_2, H_2O	21
KIO_4	pea cannery waste	cleaved sugars, KIO_3	25
KIO_4	diacetyl, diisobutyryl, benzil, camphorquinone	iodate, carboxylic acid	26
$KMnO_4$	fructose, glucose, galactose, maltose, sucrose	formic acid & lower sugars	23
$NaIO_4$	dextran (an anhydroglucose polymer)	formic acid	27
$NaIO_4$	salicyl alcohol	dimer of intermediate via Diels-Alder	28
$NaIO_4$	Glucose	HCO_3H, HCHO, IO_3^-	16
$NaIO_4$	crystalline cellulose	dialdehyde	29
$NaIO_4$	glucose, ethylene glycol	formaldehyde	30
$NaIO_4$	Cellulose	dialdehyde	31
$NaIO_4$	Catechol	*o*-benzoquinone	32

Table 9: Oxidation products of some alcohols.
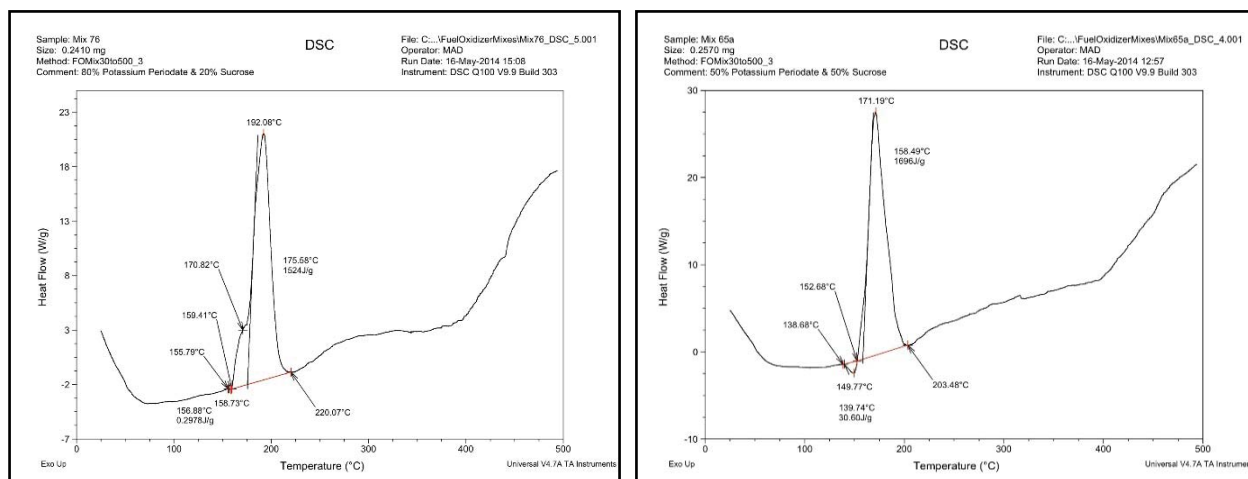
Figure 9: KIO4 with 50wt% Sucrose (left) and with 20wt% Sucrose (right).
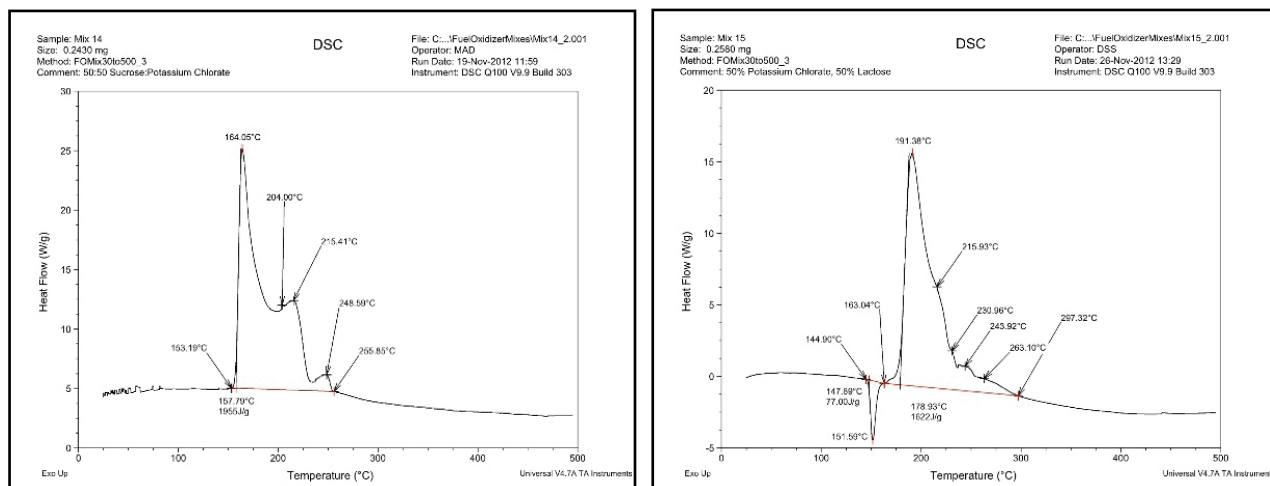
Figure 10: KClO3 + 50wt% disaccharide: sucrose (left) & lactose (right).
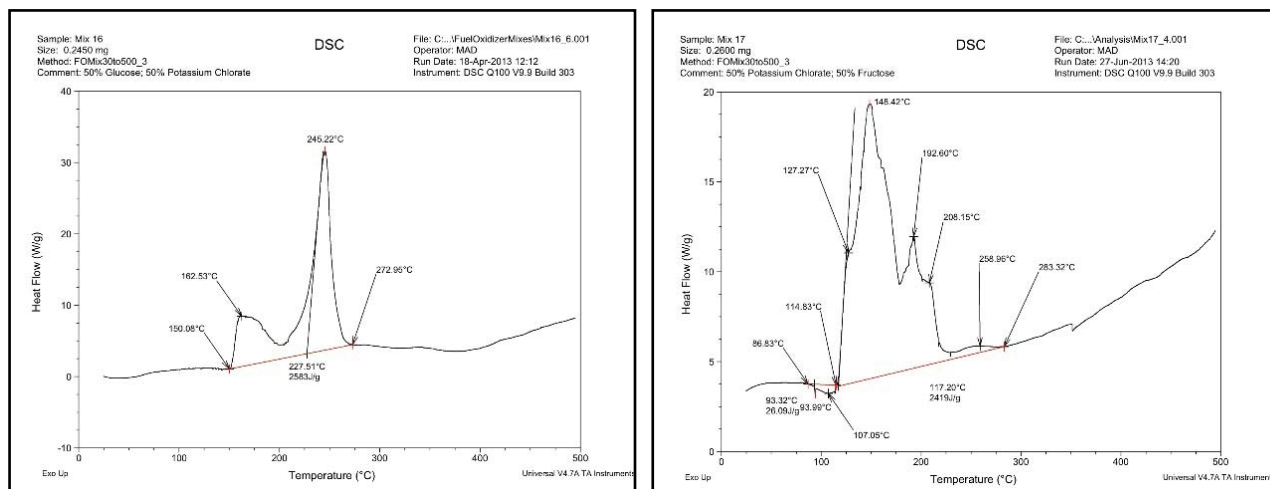
Figure 11: KClO3 + 50wt% monosaccharride: glucose (left) & fructose (right).

The majority of oxidizers reacted immediately after the melt of the sugar suggesting that molten sugars can solublize, mobilizing the oxidizer and promoting reactions. We labeled these oxidizers "sugar-controlled." A detailed examination of the reaction between $KClO_3$ and lactose noted the importance of liquid lactose and its solubilization of the chlorate; it also noted no disporportionation into perchlorate [52, 53]. For three oxidizers, this general trend with sugars was not observed. These oxidizers may have exhibited a small exotherm immediately after the sugar melt, but the majority of the exothermic reaction only occurred after the oxidizer underwent a melt, phase change, or decomposition; we labeled them "oxidizer-controlled." The two resistant anions were perchlorate and nitrate, but for the latter, nitrate, only the potassium salt failed to react immediately after the sugar melt. Ammonium nitrate melted in the same range as the sugars; thus, it was difficult to determine which melt had triggered the reaction. Figures 12 and 13 on the next page suggest this counter-trend exhibited by potassium nitrate was true regardless of the type of sugar.
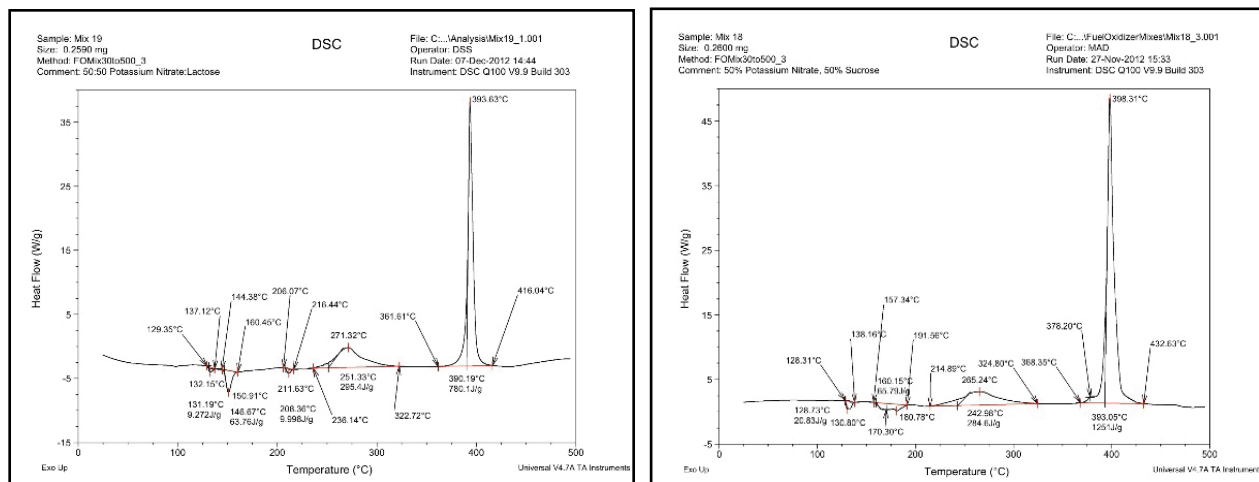
Figure 12: KNO3 + 50wt% disaccharide: sucrose (left) & lactose (right).
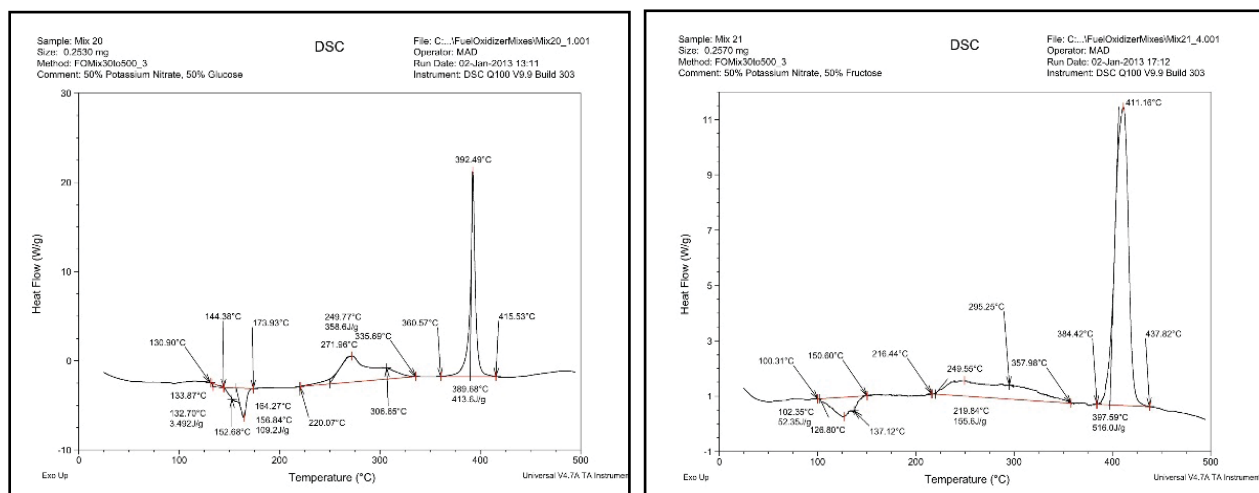
Figure 13: KNO3 + 50wt% monosaccharide: glucose (left) & fructose (right).

Generally, the thermograms did not change drastically in appearance when 20wt% rather than 50wt% sucrose was used (see Fig. 10 on the previous page).

With AN and the sugars, it was difficult to assign the decomposition trigger since both the sugars and AN both melted in the 150 to 170°C range. With the higher level of sucrose (50wt%), the main exotherm was observed around 180°C, while with sucrose closer to stoichiometric (20%), large exotherms were observed at 170 and 340°C, with the latter at the normal decomposition temperature of AN (see Fig. 14 on the next page).
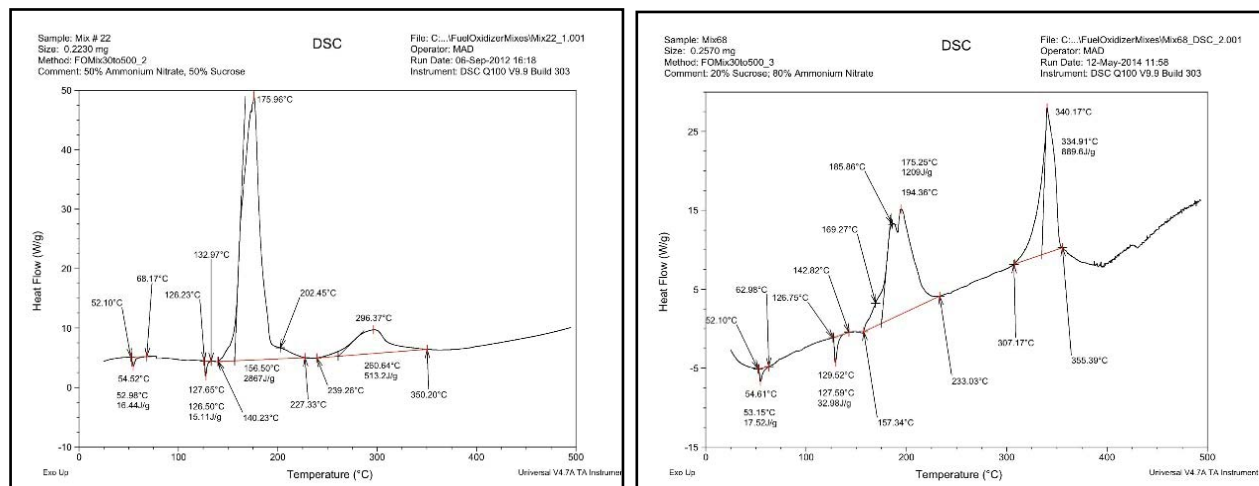
Figure 14: AN + 50wt% sucrose (left) & 20wt% sucrose (right).

The heat released from the oxidizers with 20wt% sucrose was comparable (~1400 J/g) to the heat released with 50wt% sucrose (see Table 10). There was a large deviation in observed heat released (±25%) run to run which we have attributed to the slow response of the DSC thermocouples. $K_2Cr_2O_7$ fuel mixtures were notably low in energy release, averaging less than a tenth of the other fuel/oxidizer mixtures.

	KIO4	KMnO4	KBrO3	KClO3	K2Cr2O7	AP	KClO4	KIO3	KNO3	AN	KNO2
exotherm J/g	94	142	217	465		1233	293			1407	SDT
Sucrose	2054	1064	1110	2037	127	**2253**	**1125**	1243	**1016**	2092	1281
Sucrose 20%	1805	1798	1718	2091	102	**1357**	**869**	838	**681**	1793	1689
Fructose	1620	1222	1317	2296	115	**1638**	**993**	1442	**596**	2652	987
Lactose				1597					**696**	1480	
Glucose				2688					**697**	2277	
Pentaerythritol			1427	2058					1638	2118	
Erythritol	1140	1702		2272	129	3822	573	871	2438	1758	1009
Cyclododecanol	790	768	876	1129	256	1877	not seen	354	not seen		
surfur	2353	2360	815	723		1747	1612	2299	1054	2328	2094
naphthalene	1205	931	1779	ended past 500	68	1527	not seen		?	829	
benzoic acid 20%	1500	1339	835	3648	138	2400	not seen	476	?	1879	?
charcoal	600	792		1585	156	1718	1172	300	1361	1607	625
Aluminum 20% all SDT	170	726	454	38, 1499 DSC		1600	800	490	1300	640	2400
Average all fuel - Al	1452	1331	1235	2011	136	2038	1057	978	1131	1892	1281

Table 10: Heat released (J/g) below 500oC from oxidizer/fuel mixes.

Since there was not much differentiation among the sugars, we chose to examine a more diverse group of alcohols: erythritol (mp 122oC), pentaerythritol (mp 190oC), and cyclododecanol (mp 78oC). Only two oxidiz-

ers with erythritol ($KMnO_4$ and KIO_4) showed immediate decomposition after the melt of erythritol, although all the "sugar-controlled "oxidizers except $K_2Cr_2O_7$ decomposed at lower temperatures than their own phase changes or decomposition point (see Figs. 15 and 16). Dichromate reactions were notable for their lack of heat produced (see Table 10), and because the reaction with erythritol occurred after the melt of dichromate.
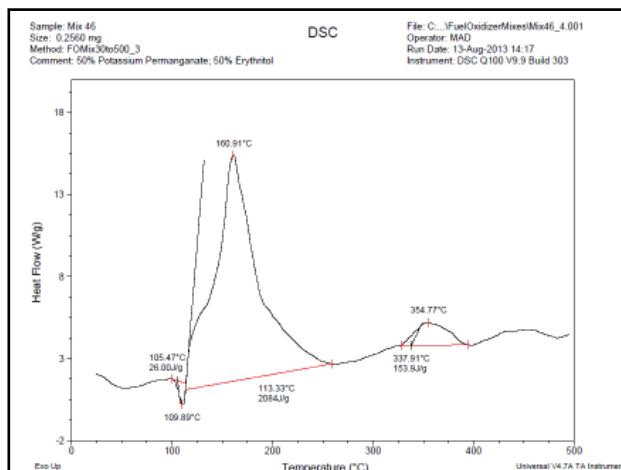
Figure 15: KMnO4 + erythritol.
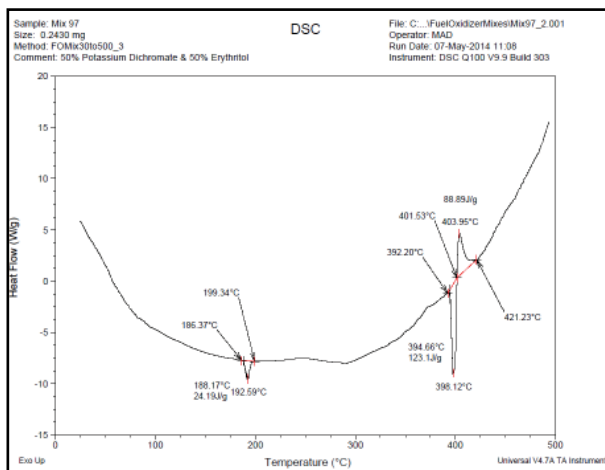
Figure 16: K2Cr2O7 + erythritol.

Four oxidizers were heated with pentaerythritol. $KClO_3$ and $KBrO_3$, which had been labeled "sugar-controlled", remained triggered by the fuel, while KNO_3 remained oxidizer controlled. AN, which with the four sugars exhibited an exotherm around 170°C, did not react with the melt of pentaerythritol (PE) at 190°C. Instead it began to release heat around 260°C, a phase change for PE. In some thermograms that exotherm was the only peak; in others a second peak was observed at the normal decomposition temperature of AN (see Fig. 17).
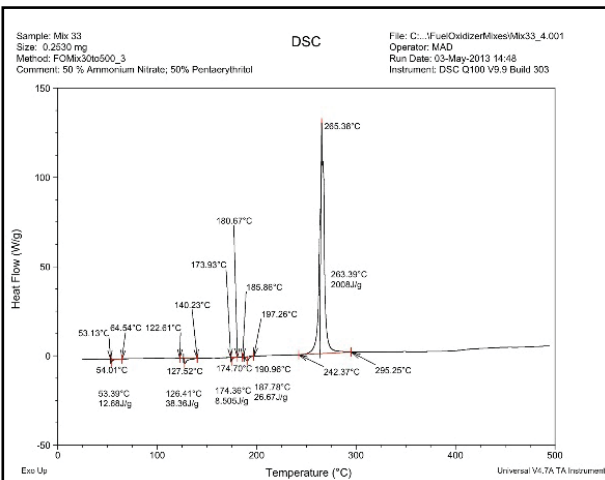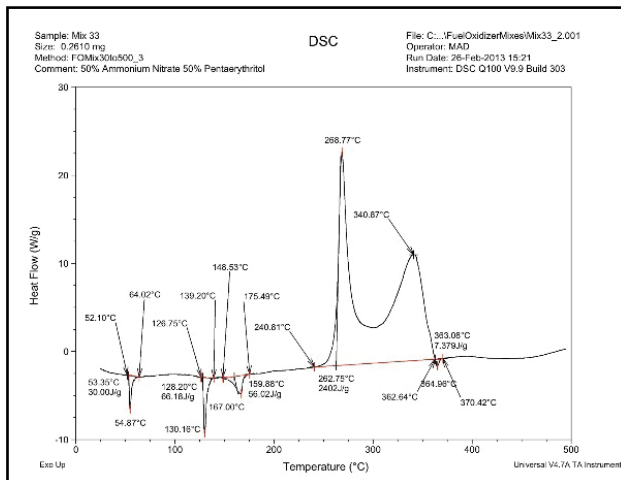
Figure 17: Two examples of AN + 50wt% pentaerythritol.

Cyclododecanol had a melting point lower than the other alcohols, but as a mono-alcohol it appeared to have little ability to solvate the oxidizers. A few oxidizers, $KClO_4$ and KNO_3, showed no reaction with cyclododecanol when monitored up to 500°C.

In an attempt to examine samples which did not exhibit heat releases below the 500°C cut off for DSC, many samples were also examined on the SDT. Because the SDT was designed to allow monitoring of weight loss and heat flow simultaneously, samples are scanned unsealed. This proved to be a dilemma. In some cases exothermic events appeared as endothermic events; the classic example is a scan of an unsealed sample of AN. When not contained in a sealed ampoule, AN will show an endotherm around its 300°C decomposition rather

than the actual exotherm (see Fig. 18). Occassionally the exothermic event was only partially countered by the endothermic evaporation of the reactant or products; in such cases the exotherm was observed, but heat release was significantly lower than it would have been in a sealed sample. Therefore, whenever possible, sealed samples were examined by DSC. To date we have found no satisfactory method for sealing DSC samples that remains gas tight over 550°C.
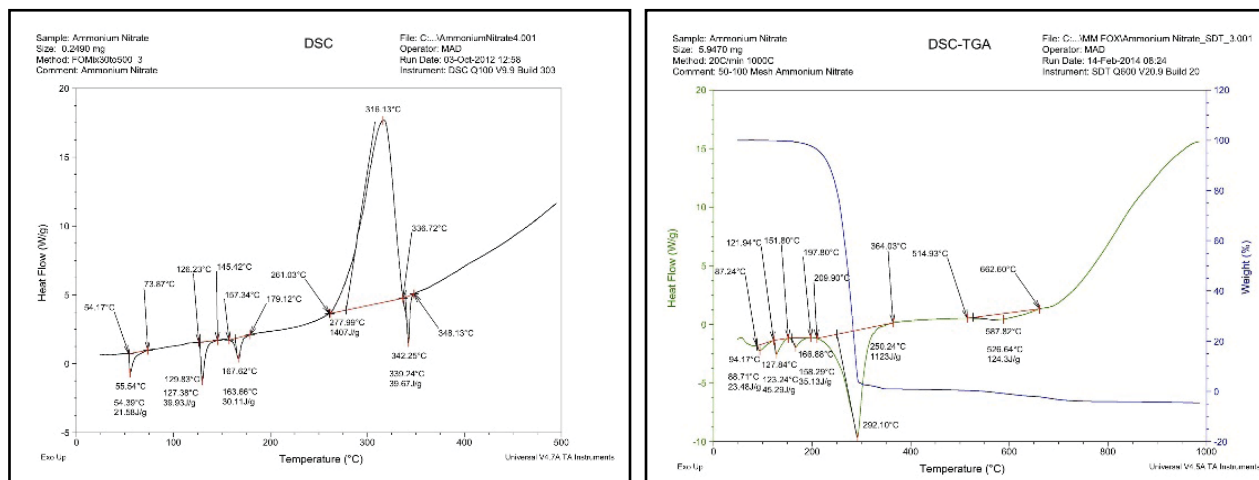
Figure 18: Ammonium nitrate in sealed DSC cell (left) vs. in open SDT cell (right).

To examine fuels other than alcohols, naphthalene, benzoic acid, charcoal, sulfur and aluminum were added to the study. Sulfur has long been used in energetic formulations [58, 59]. It exists as a number of allotropes [60]. With neat sulfur we observed two, sometimes three endotherms between 107 and 120°C, assigned to phase change and melting; there was also a small endotherm around 180°C. The oxidizers that were initiated by the sugar melt also showed exothermic decomposition with sulfur beginning around 180°C. A common characteristic of this exothermic decomposition was slow heat release rising to a recognizable exotherm (see Fig. 19). The same three oxidizers classified as oxidizer-controlled did not show an exotherm with sulfur until higher temperatures (see Fig. 20).
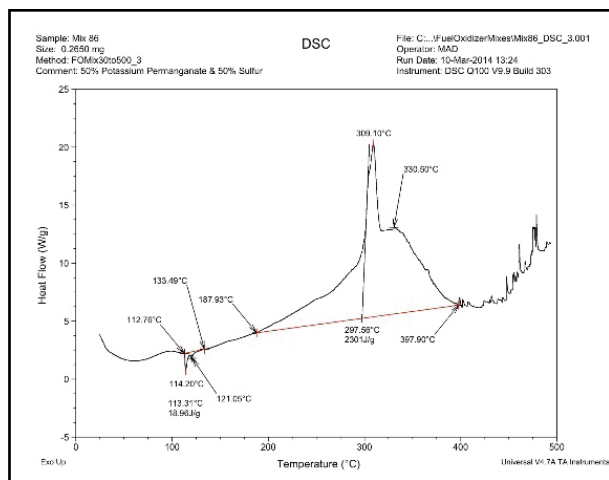
Figure 19: KMnO4 + 50wt% Sulfur.
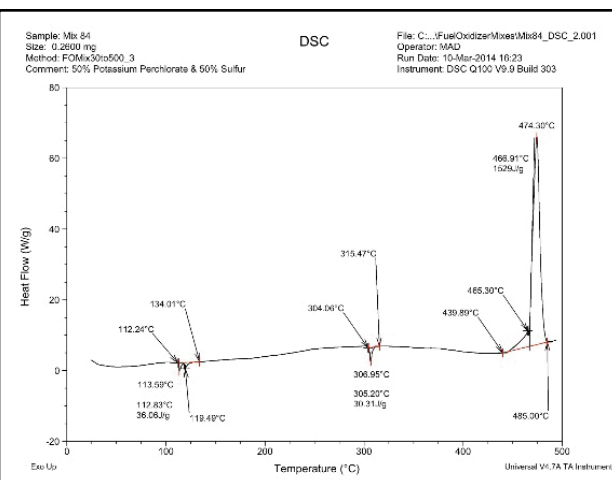
Figure 20: KClO4 + 50wt% Sulfur.

Table 11 on the next page records the temperature at which the exotherms were first observed to rise above the baseline (ramp rate of 20°/min). These temperatures were different than those recorded in Table 8, which tabulates the onset temperatures of the exothermic peaks as calculated by the TA Universal Analysis

software. As can be seen from the traces in Figures 21 and 22, when DSC exotherms are very broad, onset temperatures are often misleading. For example, when $KBrO_3$ is mixed with naphthalene (see Fig. 21), the difference between the onset and first deviation from baseline is not large ($\sim 30^o$), but for KIO_3 and sulfur (see Fig. 22) the difference between onset and deviation is huge ($\sim 160^o$). (Note that trace shown in Figure 22 is typical for sulfur mixtures.)

		KIO4	KMnO4	KBrO3	KClO3	K2Cr2O7	AP	KClO4	KIO3	KNO3	AN	KNO2
Oxidizer phase change		543	[240]	415	358	402	248	307, 613		132,331	128,167	45, 419
Oxidizer decomposition endo		**330**	**277**	**428**	**474**		**359**	**630**	**555**	**703**	**254**	**510**
Sucrose	**185, 238**	148	194	179	167	224	263	443	159	372	142	204
Pentaerythritol	**359**			211	209					420	242	
Erythritol	**122, 297**	119	112		192	383	258	313, 593	141	350	260	261
Surfur	**107, 119,**	182	189	193	149		391	428	169	294	172	189
Cyclododecanol	**78**	185, 251	196	379	397	321	323		414	NR<500		
Cyclododecanol		334					264					
Naphthalene	**80**	255	265	391	397	420	356		600	600	279	
Benzoic acid 20%	**121**	259	123	355	189	381	393	395	403	NR<500	270	NR<500
Charcoal		344	277		300	397	353	470	436	409	203	346
Al (20%)	**660**	830?	750	850?	364		902	563	830?	747	846	679
Al		339	280	419			280		581		291	

Table 11: Temperature at which principle exotherm is first observed (oC).
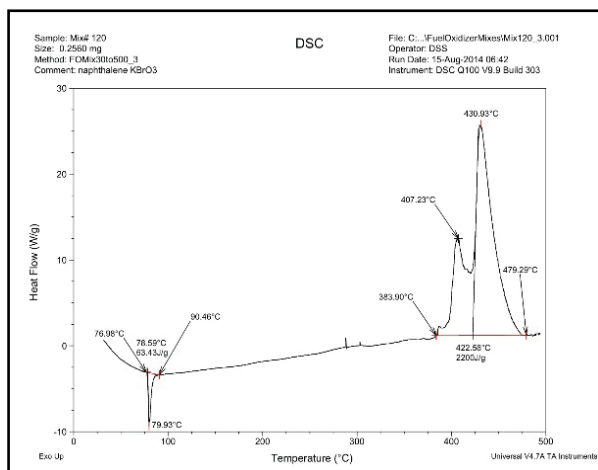
Figure 21: KBrO3 + 50wt% naphthalene.
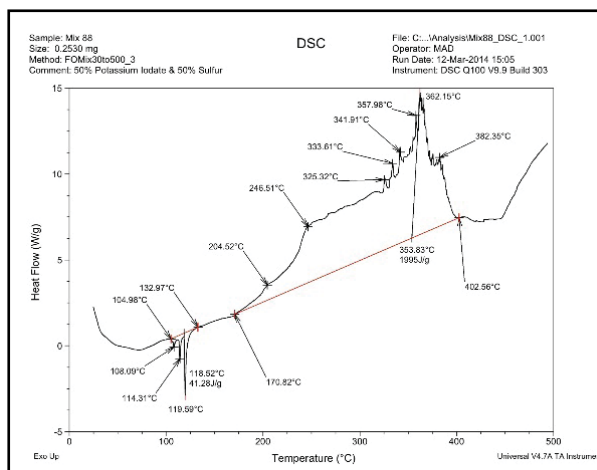
Figure 22: KIO3 + 50wt% Sulfur.

Obviously, the temperature at which an oxidizer/fuel mixture begins to react depends on both the susceptibility of the fuel to oxidation and the oxidizer's tendency to reduce. In comparing the carbonaous fuels, cyclododecanol, naphthalene, benzoic acid and charcoal, we had hoped to see a reactivity trend across all oxidizers, and, indeed, the following trend in the initiation temperature of the decomposition exotherm was observed with over half the oxidizers:

benzoic acid < cyclododecanol < charcoal < napththalene

It was also observed that with fuels other than aluminum, ammonium perchlorate mixtures decomposed at lower temperatures than those with potasssium perchlorate.

Aluminum, which has been used as a fuel in mixtures with ammonium nitrate and perchlorate, was used as

the highest melting fuel. With two exceptions, the oxidizers decomposed long before the aluminum reacted, and aluminum did not react until over 800°C (see Figs. 23 and 24 on the next page). In two cases ($KClO_3$, KNO_2) the exotherm appeared at significantly lower temperatures indicating they react readily with the aluminum (see Figs. 25 and 26). All the oxidizer/Al samples were examined by SDT, and a few were also examined by DSC. The low temperature exotherm observed for KIO_4 was its conversion into KIO_3. The low temperature (i.e. under 800°C) exotherms recorded for other oxidzers reflect the decomposition of the oxidizer.
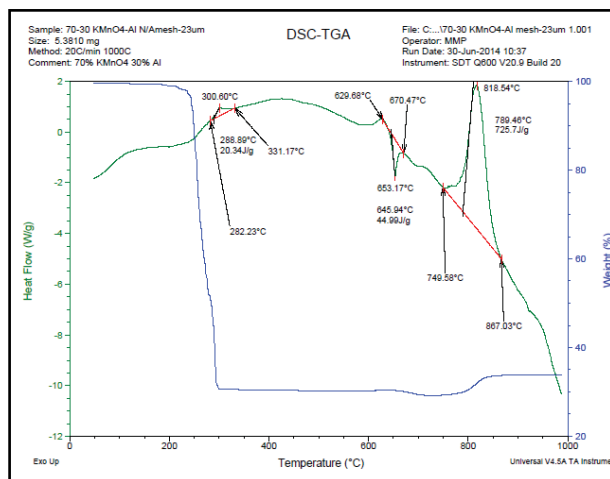
Figure 23: KMnO4 + 20wt% Aluminum.
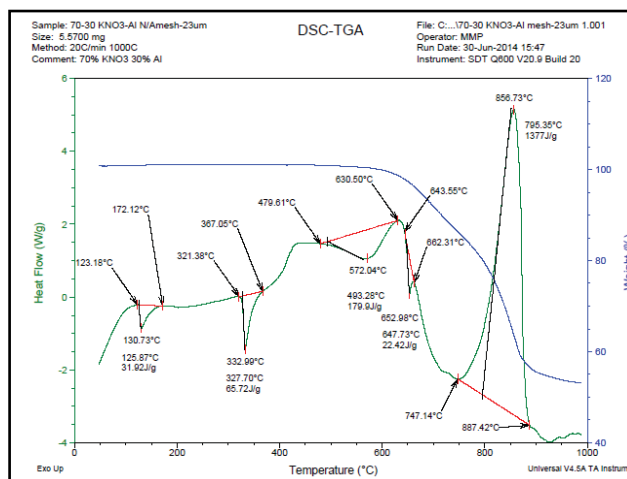
Figure 24: KNO3 + 20wt% Aluminum.
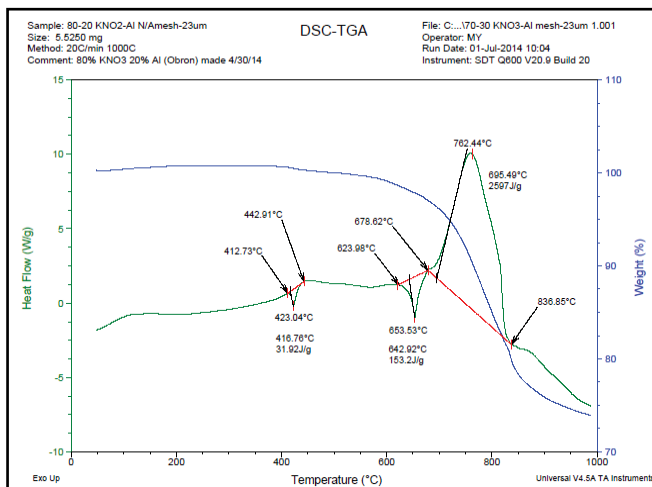
Figure 25: KNO2 + 20wt% Aluminum.
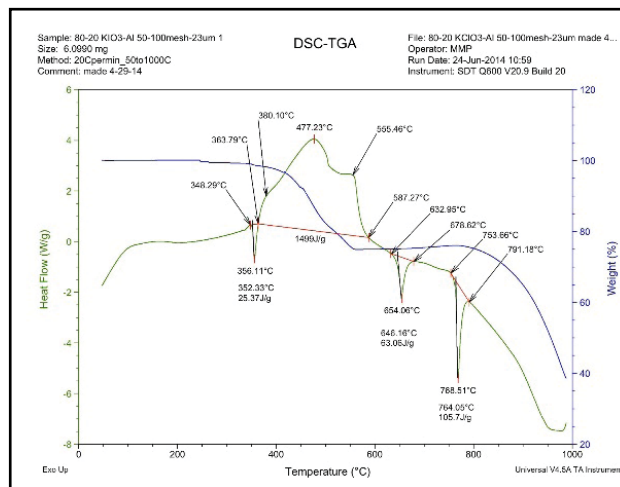
Figure 26: KClO3 + 20wt% Aluminum.

B.2.d. Summary of FOX studies

Neat oxidizers appeared to undergo decomposition roughly in line with standard reduction potentials (Table 1 and 2) [40]. Most oxidizers produced some heat when decomposed without fuel, but it was a few hundreds of joules per gram compared to 1500 to 3000 J/g when decomposed with fuel. The exceptions, of course, were the ammonium salts which produce 1000 to 1500 J/g without fuel and double that with fuel. The oxides of chlorine released the most heat, which is in line with the general trend that the larger the electronegative difference between oxygen and the central element, the more stable the oxy-halide. When anions containing the same central atom are compared, the order of stability is attributed to the degree of pi-bonding in each

species: $ClO_4^- > ClO_3^-$ and NO_3^- / NO_2^- [42, 61]. Between the oxo-chlorine or oxo-nitrogen species, perchlorate and nitrate are more stable and less sensitive than the less highly oxidized chlorate and nitrite.

A survey of the stability and performance of eleven solid oxidizers and thirteen fuels was performed by differential scanning calorimetry (DSC), simultaneous differential thermolysis (SDT) and hot-wire ignition. Sugars, alcohols, hydrocarbons, benzoic acid, sulfur, charcoal, and aluminum were used as fuels; all fuels except charcoal and aluminum melted at or below 200°C. When fuels were added to the oxidizer, the phase changes of the individual oxidizers and fuels were often still observed. Most of the fuels were added at the 50wt% level, but thermograms of 20wt% sucrose were examined and shown to be very similar to 50wt% sucrose in terms of appearance and heat release. Variations in terms of appearance and heat release were observed among runs of a sample; this was attributed to inhomogeneity in the tiny samples and variation in particle size [62-65]. DSC heat release values had standard deviations of over 25%; some variability may have been due to poor mixing; however, in the past we have found that even neat ammonium nitrate exhibited 15% variation in heat release. We suspect that with energetic materials it is difficult for the DSC thermocouples to accurately track fast release of heat. Experimentally, it was found that differences in DSC and SDT traces appeared to be related to the ability of reactants/products to vaporize in the open or lightly capped SDT containers.

We found that a phase change in the fuel or a phase change or decomposition of the oxidizer was typically the trigger that caused a reaction between the oxidizer and the fuel, and have therefore classified the reactions as fuel-controlled or oxidizer-controlled. With the exception of charcoal and aluminum, all fuels used in the study melted below 200°C. The melt or phase change of the sugars or sulfur triggered the reaction to proceed with most of the oxidizers. Three oxidizers, KNO_3, $KClO_4$, and NH_4ClO_4, most often triggered their own reaction, and typically exhibited the highest reaction temperatures, i.e. above 400°C, regardless of the fuel. With the exception of the oxidizers triggered to react by the phase changes of the polyols (i.e. sugars) and sulfur and all oxidizer/aluminum mixes, the oxidizer/fuel mixtures generally decomposed between 230°C and 300°C.

In terms of heat release, potassium dichromate/fuel mixtures were the least energetic, generally releasing less than 200 J/g. Most of the mixtures released 1000 to 1500 J/g, with potassium chlorate, ammonium perchlorate, and ammonium nitrate releasing significantly more heat, around 2000 J/g. When the fuel was aluminum most of the oxidizers decomposed below 500°C leaving the aluminum to oxidize at over 800°C. Only two oxidizers reduced the temperature of the aluminium exotherm—chlorate and potassium nitrite. No fuel stood out as clearly the 'best," in terms of releasing the most heat; they averaged 1500 J/g by DSC analysis.

Response to hot-wire ignition was assessed by the length of the burn and the light output. Table 2 orders the oxidizers left to right as highest oxidizing power to lowest in terms of electromotive potential. This trend is roughly followed by thermal stability. Light output, when the fuel was sucrose, did not show a clear trend. However, when the fuel was aluminium, the trend was roughly followed. Work continues on these correlations.

C.   Major Contributions

In April 2015, we were thanked by a National Institute of Standards & Technology (NIST) senior scientist for allowing them to use our database of explosive properties. They stated: "It was all we had, in many cases." This is high praise from an organization which maintains the "Chemistry Webbook." In the past, we have also received similar acclaim from military labs, both in CONUS and OCONUS. Other outreach of our information occurs by publication.

Contributions include:

• Baseline information about chemical properties and reactivity.

• Identifying the hazards of humidity to HMTD.

- Formation mechanism of HMTD; the limitations of certain oxidizers in terms of terrorist use.
- Gentle destruction methods for HMTD.

We have characterized the headspace over HMTD; the amount of HMTD in the vapor is less than parts-per-trillion. The odor associated with HMTD is due to amine decomposition products. Thus, the amine decomposition products can be used to generate the odor, making canine training aids from non-explosive components feasible. In contrast to historic reports [27], HMTD should not be stored under water. It rapidly decomposes in the presence of moisture.

HMTD is so thermally unstable that it can decompose in weeks if held at 60°C; in one week, if the humidity is high. This is in strong contrast to all military explosives and most HMEs. A number of decomposition and formation experiments have been performed with HMTD (see section V.A). Most notable were the studies using isotopically labeled species. Among those, the examination of the formation of HMTD using hexamine labeled with ^{15}N as well as unlabeled ^{14}N hexamine suggested that the formation of HMTD might be accomplished from any source of formaldehyde. While this is not necessarily good news for the forces of counterterrorism, at least it helps define the range of the problem.

A dozen FOX mixtures have been examined via both DSC and SDT and, for a few, burn characteristics were determined. This is the start of an initiative to determine the range of the threat in terms of oxidizers for use in FOX explosives. Materials, such as dichromate, appear to have little energy to contribute to an explosion, but other properties are being explored.

D.   Milestones

Studies suggest that thwarting the synthesis of HMTD will be challenging. Further mechanistic studies are underway in order to devise the best approach to this problem.

We believe that, ultimately, detonation testing, albeit on the small-scale (see project R1-B.1), will be necessary to prove whether or not a formulation is detonable, but we also believe that aspects of laboratory characterization can suggest the final outcome. It would be a useful contribution to the counterterrorism community to determine these characteristics.

E.   Future Plans

Greater understanding of HMTD formation and destruction remains the primary goal. Secondary milestones are to prevent its formation and to gently destroy it. Field work continues in an attempt to determine hazards associated with proposed methods of destruction. Work on safe, long-lived canine training aids for HMTD is making progress.

Thermal properties of FOX mixtures have been characterized. Yet, energy release alone does not appear to separate potential explosive precursors from other oxidizers; thus, the characterizations of gas release and rate of reaction (see project R1-B.1) are planned. A new method of assessing oxidizing power is being explored as well as the link between behaviors that can be observed in the lab and field performance.

III.   EDUCATION AND WORKFORCE DEVELOPMENT ACTIVITY

A.   Course, Seminar or Workshop Development

An explosive analysis class entitled "Advanced Studies in Explosives" was offered for the first time in spring of 2015 with 15 graduate students in attendance.

In May 2015, a hands-on course entitled "Explosives Analysis" was offered for the first time; six members of the HSE came to URI to attend.

Graduate student Devon Swanson was selected to give an award talk at the Trace Explosive Detection conference for his work on AFM of explosives (April 2015, Pittsburgh).

Dr. Smith presented "An Introduction to the Properties of Explosive and Trace Detection" at the IEEE HST '15 ALERT Tutorial Session: Introduction to Explosives/Threat Screening Tools and Technologies in April 2015.

Courses were presented for the Army, Navy, Air Force, and the Transportation Security Administration (TSA-TSIF, 10 classes and 200 people) and TSA explosive specialists (TSA-TSS-E, 5 classes and 110 people) (see Table 12).

New or Existing	Course/Module/ Degree/Cert.	Title	Description	Student Enrollment
New	Certificate	Explosive Analysis	Lab Analysis of Explosives	6*
New	Graduate credit	Explosive Analysis	Mass Spectroscopy; Thermal; Shock	15
Existing	Certificate	Pyrotechnics	Raytheon K-Tech ABQ	12
Existing	Certificate	Fundamentals	Fundamentals - Alcoa	12
Existing	Certificate	Air Blast	Air Blast - Huntsville	14
Existing	Certificate	Materials Characterization	Picatinny	14
Existing	Certificate	Fundamentals	TSIF Fundamentals	50
Existing	Certificate	Fundamentals	Fundamentals Eglin	28
Existing	Certificate	Fundamentals	URI Fundamentals	32
Existing	Certificate	Air Blast	Air Blast - LANL	15
Existing	Certificate	Materials Characterization	Materials Characterizations - Navy	18
Existing	Certificate	Stability, Compatibility	Stability, Compatibility - Navy	18

* Included DHS personnel

Table 12: Courses offered in Year 2.

A.1.   Invited lectures

- Thermal Stability and Chemistry of Difficult Energetic Materials", New Trends in Research Energetic Materials; Pardubice, CZ, April 11, 2015.

- JANNAF, December 10, 2014, Academic Research to Real Life Application, ABQ.

- 7th Annual CBRNe Convergence, Oct 28-30, 2014, New York, NY, tutorial to first responders.

- Recognizing Improvised Drug vs Explosive Labs, 23rd Annual Haz-Mat Training Conf. September 18, 2014, Plymouth, MA, tutorial to first responders.

B.   Student Internship, Job or Research Opportunities

Each URI project supports one or more graduate students. This is their best learning experience. Undergraduates are also supported on the projects as their class schedules permit. A newly minted PhD from our group, Dr. Jon Canino, accepted a position at Signature Science and is working at the Transportation Security Laboratory (TSL) in New Jersey.

C.   Interactions and Outreach to K-12, Community College, Minority Serving Institution Students or Faculty

We have continued our K-12 outreach by hosting high school teachers in the summer and providing chemical magic shows at K-12 schools. High school teachers conduct research in URI labs for 8 to 10 weeks under the mentorship of a graduate student. As a result, 2 teachers have gone back to seek advanced degrees.

In addition, in the summer of 2014, we hosted 2 forensic scientists from Qatar and a West Point cadet for several weeks. For the summer of 2014, we also hosted a professor from Tuskegee University and one of her students. In summer of 2015, we hosted two Navy midshipmen and a Penn State engineer. An air force employee will be placed at URI to begin work on a master's degree, which involves conducting ALERT research, in fall 2015.

D.   Training to Professionals or Others

We trained 110 TSS-Es in five classes and approximately 230 other people involved in the HSE in 12 classes, one of which was created to meet the needs of the U.S. Army forensic laboratory.

IV.   RELEVANCE AND TRANSITION

A.   Relevance of Research to the DHS Enterprise

- R1-A.1 addresses the characterization of HMEs. Metrics include:
    - o   Downloads of our papers;
    - o   Users of the explosive database; and
    - o   Requests to license the database.
    - o   Requests for classes

- R1-A.1 addresses safe samples of explosives. Metrics include:
    - o   Requests from explosive trace detection (ETD) instrument vendors for the scent product. Product is currently provided for free and we are under licensing negotiations;
    - o   Requests to license the product; and
    - o   A $10,000 award for this technology in student innovation contest April 2014.

- R1-A.1 addresses the safe disposal of explosives.

- R1-A.1 addresses the sampling of explosives and a new DHS award in this area is in the process of being awarded.

B.   Potential for Transition

- R1-A.1 addresses the characterization of HMEs. We receive requests to license the database.

- R1-A.1 addresses safe samples of explosive. We receive requests to license our safe source of explosive vapor.

- R1-A.1 addresses the sampling of explosives. We received a DHS BAA award with transition partners, FLIR and DSA.

C.   Data and/or IP Acquisition Strategy

This is ongoing and will continue.

D.   Transition Pathway

- R1-A.1 addresses the characterization of HMEs. There are requests to license the database; however, we are considering whether this would remove the present control we have on who can access the database.

- R1-A.1 addresses safe samples of explosive. We have received requests to license the product and are working with potential vendor, although the product is presently available for free to those requesting it.

- R1-A.1 has aligned with potential vendors, FLIR and DSA, for transitioning new sampling techniques.

E.   Transition Partner Connections

There is a substantial interest associated with the Explosives Database. U.S. subscribers to the Explosives Database include Coast Guard, ATF, DHS, TSA, DOT, NIST, NASA, most national labs (LANL, SNL, PNNL, BNL Savannah River, Oak Ridge) and various army, navy and air force laboratories in the CONUS and OCONUS.

V.   PROJECT DOCUMENTATION

A.   Peer Reviewed Journal Articles

1. Colizza, Kevin M Porter, J. Smith, J. Oxley "Gas Phase Reactions of Alcohols with Hexamethylene triperoxide diamine (HMTD) under Atmospheric Pressure Chemical Ionization Conditions" Rapid Communications in Mass Spectrometry, December 2014, 29(1), 74 10.1002/rcm.7084

2. Oxley, "Explosive Detection: How We Got Here and Where Are We Going?" International Journal of Energetic Materials and Chemical Propulsion; 2014, 13(4): 373-381. 10.1615/IntJEnergeticMaterialsChemProp.2014011493

3. Oxley, J.; Smith, J.; Donnelly, M.; Porter, M. "Fuel-Oxidizer Mixtures: Their Stabilities and Burn Characteristics; International Journal of Energetic Materials and Chemical Propulsion 2014, 13(6): 517-558. 10.1007/s10973-015-4589-x (J Therm Anal Calorim)

4. Oxley, J.C.; Smith, J.L.; Canino, J.N. "Insensitive TATP Training Aid by Microencapsulation" J. Energetic Materials; 2015, 33(3), 215-228. 10.1080/07370652.2014.985857

Pending-

1. Oxley, J.C.; Smith, J.L.; Porter, M.; Colizza, K.; McLennan, L. ; Zeire, Y.; Kosloff, R.; Dubikova, F. "Synthesis and Degradation of Hexamethylene triperoxide diamine (HMTD)" submitted to Propellants, Explosives, Pyrotechnics.

2. Oxley, J.C.; Smith, J.C.; Swanson, D.; Kagan, G. "Adhesion Forces of Energetic Materials on Polymer Surfaces, submitted to Propellants, Explosives, Pyrotechnics.

B.   Other Conference Proceedings

1. Donnelly (presenter) with J Oxley; J Smith; M. Porter, Fuel-Oxidizers Mixtures: Their Stabilities and Burn Characteristics, North American Thermal Analysis Society; 2014.

2. Smith, J. "An Introduction to the Properties of Explosive and Trace Detection." IEEE HST '15 Tutorial Session: Introduction to Explosives/Threat Screening Tools and Technologies, April 2015.

C.   Other Presentations

1. Seminars

   a. Devon Swanson (presenter) with J Oxley; J. Smith; G. Kagan "Adhesion Forces of Energetic Materials on Polymer Surfaces" Trace Explosive Detection April 2015; Pittsburgh

   b. Maria Donnelly, "Fuel-Oxidizer Mixtures: Evaluating the Hazard Potential," North American Thermal Analysis Society, Oct 2014.

2. Poster Sessions—for ALERT events

3. Short Courses-listed under education

D.   *Student Theses or Dissertations*

1. PhD Chemistry: Jon Canino Dec. 2014 Polymer Systems and Explosives

2. PhD Chemistry: Maria Donnelly May 2015 Thermal Stability & Sensitivity of Energetic Formulations

E.   *New and Existing Courses Developed and Student Enrollment*

See table in section III.A.

F.   *Requests for Assistance/Advice*

1. From DHS

    a. On call for a variety of TSA TSS-ES personnel

    b. Oxley is part of the DHS-formed Inter-Agency Explosive Terrorism Risk Assessment Working Group (IExTRAWG)

2. From Federal/State/Local Government

    a. Singapore, India, Turkey Defense groups ask questions, request classes; class request from India in review at Dept of State.

    b. We have been asked to support Brookhaven National Lab is some of their international outreach.

VI.   REFERENCES

[1] Oxley, J.C.; Smith, J.L.; Brady, J.; Steinkamp, F.L. "Factors Influencing Destruction of Triacetone Triperoxide (TATP)," Propellants, Explosives, Pyrotechnics, 2014, 39(2), 289-298., 10.1002/prep.201300063

[2] Oxley, J.C.; Smith, J.L.; Canino, J.N. "Insensitive TATP Training Aid by Microencapsulation" J. Energetic Materials; 2015, 33(3), 215-228.

[3] Oxley, J.C.; Smith, J.L.; Steinkamp, L.; Zhang, G. "Factors Influencing Triacetone Triperoxide (TATP) and Diacetone Diperoxide (DADP) Formation: Part 2," Propellants, Explosives, Pyrotechnics, 2013, 6, 841-851.

[4] Oxley, J.C.; Smith, J.L.; Bowden, P.; Ryan Rettinger "Factors Influencing TATP and DADP Formation: Part I" Propellants, Explosives, Pyrotechnics 2013, 38(2), 244-254.

[5] Brady, J.E.; Oxley, J.C.; Smith, J.L.; Hart, C.E. Estimating Ambient Vapor Pressure of Low Volatility Explosives by Rising-Temperature Thermogravitmetry; Propellants, Explosives, Pyrotechnics 2012 37(2), 215-222.

[6] Oxley, Jimmie C.; Brady, Joseph; Wilson, Steven A.; Smith, James L. "The risk of mixing dilute hydrogen peroxide and acetone solutions," J Chemical Health & Safety 2012 19(2), 27-33.

[7] Fan, W, Young, M, Canino, J, Smith, J, Oxley, J, Almirall, JR "Fast Detection of Triacetone Triperoxide (TATP) from Headspace using Planar Solid Phase Microextraction (PSPME) Coupled to an IMS Detector" Anal Bioanal Chem. 2012 403(2), 401-408.

[8] Oxley, J.C.; Smith, J.L.; Kirschenbaum, L.; Marimiganti, S.; Efremenko, I.; Zach, R; Zeiri,Y Accumulation of Explosive in Hair: Part 3: Binding Site Study; J Forensic Sci 2012 57(3), 623-35.

[9] Dubnikova, Faina; Kosloff, Ronnie; Oxley, Jimmie C.; Smith, James L.; Zeiri, Yehuda "Role of Metal Ions in the Destruction of TATP: Theoretical Considerations" J Phys Chem A 2011 115(38), 10565-10575.

[10] Oxley, J.C., Smith, J.L.; Huang, J.; Luo, W. "Destruction of Peroxide Explosives," J. Forensic Sci.,

2009 54(5), 1029-33.

[11] Oxley, J.C.; Smith, J.L.; Brady, IV, J.E.; Brown, A.C. Characterization and Analysis of Tetranitrate Esters, Propellants, Explosives, Pyrotechnics, 2012, 37(1), 24-39.

[12] Colizza, Kevin M Porter, J. Smith, J. Oxley "Gas Phase Reactions of Alcohols with Hexamethylene triperoxide diamine (HMTD) under Atmospheric Pressure Chemical Ionization Conditions" Rapid Communications in Mass Spectrometry 2014, 29(1), 74, 10.1002/rcm.7084.

[13] Oxley, J.; Smith, J.; Porter, M.; Colizza, K.; McLennan, L.; Zeiri, Y; Kosloff, R.; Dubnikova, F "Mechanisms of Synthesis and Degradation of Hexamethylene triperoxide diamine (HMTD)" submitted PEP.

[14] Oxley, J.; Smith, J.; Donnelly, M.; Porter, M. "Fuel-Oxidizer Mixtures: Their Stabilities and Burn Characteristics; International Journal of Energetic Materials and Chemical Propulsion 2014, 13(6): 517-558.10.1007/s10973-015-4589-x (J Therm Anal Calorim)

[15] Legler, L. Chem. Ber. 1881, 14, 602-604. or 1885, 18 3343.

[16] Baeyer, A; Villiger, V. Chem. Ber, 1900, 33 2479 or 2779.

[17] Von Girsewald, C., Berichte, 1912, 45, 2571-2576.

[18] Schaefer, W.P.; Fourkas, J.T.; Tiemann, b.G. "Structure of Hexamethylene Triperoxide Diamine" J. Am. Chem. Soc. 1985, 107, 2461-2463.

[19] Wierzbicki, A.; Salter, E.A.; Cioffi, E.A.; Stevens, E.D. "Density Functional Theory and X-ray Investigations of P- and M-Hexamethylene Triperoxide Diamine and Its Dialdehyde Derivative" J. Phys. Chem. A, 2001, 105 (38), pp 8763–8768 DOI: 10.1021/jp0123841

[20] Oxley, J.C.; Smith, J.L.; Bowden, P.; R. Rettinger "Factors Influencing TATP and DADP Formation: Part I" Propellants, Explosives, Pyrotechnics 2013, 38(2), 244-254.[7] Matyas, R.; Selesovsky, J.; Musil, T "Decreasing the Friction Sensitivity of TATP, DADP, and HMTD" Central Europ. J Energetic Mat. 2013, 10(2), 263-275.

[21] Mendum, Ted Trace Explosive Detection Conference; Pittsburgh April 2015.

[22] Colizz, K.; Porter, M.; Smith, J.L.; Oxley, J.C. "Gas Phase Reactions of alcohols with hexamethylene triperoxide diamine (HMTD) under atmospheric pressure chemical ionization conditions" Rapid Commun. Mass Spectrom. 2015, 29, 74-80.

[23] Oxley, J.C.; Smith, J.L.; Chen, H.; Cioffi, E. "Decomposition of Multi-Peroxidic Compounds: Part II: Hexamethylene Triperoxide Diamine (HMTD)" Thermochemica Acta 2002, 388(1-2), 215-225.

[24] Oxley, J.; Zhang, J.; Smith, J., Cioffi, E. "Mass Spectra of Unlabeled and Isotopically Labeled Hexamethylene Triperoxide Diamine (HMTD)" Propellants, Explosives and Pyrotechnics, 2000, 25, 1-4

[25] Oxley, J.C.; Smith, J.L.; Lou, L.; Brady, J. "Determining Vapor Pressures of Diacetone Diperoxide (DADP) and Hexamethylene Triperoxide Diamine (HMTD)" Propel Explos. Pyrotech. 2009, 34, 539-43

[26] Oxley, J.C.; Smith, J.L.; Brady, J.; Steinkamp, F.L. "Factors Influencing Destruction of Triacetone Triperoxide (TATP)," Propellants, Explosives, Pyrotechnics, 2014,39(2), 289-298.

[27] Taylor, C.A.; Rinkenbach, W. "H.M.T.D. A New Detonating Explosive" Army Ordnance; J Army Ordnance Assoc. 1924, 5, 436-66 Taylor, C.A; Rinkenbach,W "Sensitivities of Detonating Compounds to Frictional Impact, Impact, and Heat" J Franklin Institute., 1927, 204 369-76.

[28] Wexler, A. Constant Humidity Solutions, CRC Handbook of Chemistry Physics 85th ed.

[29] Nielsen, A.T. "Structure and Chemistry of the Aldehyde Ammonias. 3. Formaldehyde-Ammonia Reaction. 1,3,5,-Hexahydrotriazine" J. Org. Chem.; 1979, 44(10), 1678-84.

[30] Gilbert, E.E.; Leccacorvi, J.R.; Warman, M. "The Preparation of RDX from 1,3,5-Triacylhexahydro-s-triazines" Ind. Lab. Nitrations, Symp. 1 1976, 22, 327-340.

[31] Siele, V.I.; Warman, M.; Gilbert, E.E.; "The Preparation of 3,7-Diacyl-1,3,5,7-tetraazabicylco [3.3.1] nonanes" J. Heterocyc. Chem. 1974, 11(2), 237-239.

[32] Richmond, H.H.; Myers, G.S.; Wright, G.F. "The Reaction between Formaldehyde and Ammonia" J. Am. Chem. Soc., 1948, 70, 3659-64.

[33] Stefaniak, L; Urbanski, T.; Witanowski, M.; Januszewski, H. "NMR Conformational Study of Cyclic Products from Degadation of Hexamethylenetetramine Hexahydro-1,3,5-triazines and Octahydro-1,3,5,7-Tetrazocines" Roczniki Chemii Ann. Soc. Chim. Polonorum 1969, 43, 1687-92.

[34] Bachmann, W.E.; Sheehan, J.C. "A New Method of Preparing the High Explosives RDX" J. Am. Chem. Soc. 1949, 71 (5): 1842–1845.

[35] Aristoff, E.; Graham, J.A.; Meen, R.H.; Myers, G.S.; Wright, G.F. "Nitrolysis of Hexamethylenetetramine" Can J. Res. 1949, 27B, 520.

[36] Dreyfors, J.M.; Jones, S.B.; Sayed, Y. "Hexamethylenetetramine: A Review" Am. Ind. Hygiene Assoc. J 1989, 50(11), 579-585.

[37] Lock, C.M.; Brust, H.; van Breukelen, M.; Dalmolen, J.; Koeberg, M.; Stoker, D.A. "Investigation of Isotopic Linkages between Precursor Materials and the Improvised High Explosive Product Hexamethylene Triperoxide Diamine" Analytical Chem. 2012, 84, 4984-92.

[38] Satterfield, C.N.; Case, L.C. "Reaction of Aldehyde and hydrogen peroxide in Aqueous Solution" Ind. And Eng. Chem. 1954, 46 (5), 998-1001. Satterfield, C.N.; Wilson, R.E.; LeClair, R.M.; Reid, R.C. "Analysis of Aqueous Mixtures of Hydrogen Peroxide and Aldehydes" Anal Chem. 1954, 26 (11), 1792-1797.

[39] Edward, J.T.; Chubb, F. L.; Gilson, D.F.R.; Hynes, R.C.; Sauriol, F.; Wiesenthal, A. "Cage Peroxides have Planar Bridgehead Nitrogen Atoms" Can. J. Chem. 1999, 77(5/6) 1057-1065.

[40] Ayres GH. Quantitative Chemical Analysis Appendix V 2nd ed. New York: Harper & Row Publishers; 1968. Weast RC, Astle MJ, Beyer WH, editors. Handbook of Chemistry and Physics. 64th ed. Boca Raton: CRC Press; 1983.

[41] U.N. Manual of Tests and Criteria, section 34. 5th rev. ed.; 2010.

[42] Chantry GW, Plane RA. Raman Intensities of the A1 Lines of Oxyanions. J. Chem. Phys. 1960; 32(2):319-21.

[43] Stern K. High Temperature Properties and Decomposition of Inorganic Salts. J Phys Chem. Ref. Data 1972; 1(3):747-72.

[44] Olivares RI. The thermal stability of molten nitrite/nitrates salt for solar thermal energy storage in different atmospheres. Solar Energy 2012; 86:2576-83.

[45] Fairbrother F. The Spontaneous Decomposition of Ammonium Chlorate. J. Am.Chem. Soc. 1922; 44(11):2419-22.

[46] Hughes G, Nevell TP. The mechanism of the oxidation of glucose by periodate. Trans. Faraday Soc. 1948; 44:941-8.

[47] Honeyman J, Shaw CJG. Periodate oxidation. Part III. The mechanism of oxidation of cyclic glycols. J Chem. Soc. 1959; 2451-4.

[48] Muraleedharan K, Kannan MP. Thermal decomposition kinetics of sodium metaperiodate. React. Kinet. Catal. Lett. 1989; 39(2):339-44.

[49] Muraleedharan K, Kannan MP, Ganga Devi T. Thermal decomposition kinetics of potassium iodate. J. Therm. Anal. Calorim. 2011; 103:943-55.

[50] Diefallah E-HM, Basahl SN, Obaid AY, Abu-Eittah RH. Kinetic analysis of thermal decomposition reactions: I. Thermal decomposition of potassium bromate. Thermochimica Acta 1987; 111:49-56.

[51] Natarajan R, Venkatasubramanian N. Kinetics and mechanism of oxidation of secondary alcohols by

potassium bromate. Tetrahedron 1974; 30(16):2785-9.

[52] Scanes FS, Martin RAM. Heats of Reaction of Pyrotechnic Compositions Containing Potassium Chlorate. Combustion and Flame 1974; 23:357-62. Scanes FS. Thermal Analysis of Pyrotechnic Compositions Containing Potassium Chlorate & Lactose. Combustion and Flame 1974; 23:363-71.

[53] Hosseini SG, Pourmortazavi SM, Hajimirsadeghi SS. Thermal decomposition of pyrotechnic mixtures containing sucrose with either potassium chlorate of potassium perchlorate. Combustion and Flame 2005; 141:322-6.

[54] Herbstein FH, Kapon M, Weissman A. Old and new studies of the thermal decomposition of potassium permanganate. J. Thermal Analysis 1991; 41:303-22.

[55] Odebunmi EO, Owalude SO. Kinetics and Mechanism of Oxidation of Some Simple Reducing Sugars by Permanganate Ion in Alkaline Medium. J. Iran. Chem. Soc. 2008; 5(4):623-30.

[56] Odebunmi EO, Iwarere SA, Owalude SO. Kinetics of oxidation of fructose, sucrose, and maltose by potassium permanganate in NaHCO3/NaOH buffer and iridium (IV) complex in sodium acetate / acetic acid buffer. Int. J. Chem. 2006; 16(3):167-76.

[57] Charsley EL, Chen C-H. Differential thermal analysis and temperature profile analysis of pyrotechnic delay systems: ternary mixtures of silicon, boron and potassium dichromate. Thermochimica Acta 1980; 35(2):141-52.

[58] Pakkirisamy SV, Mahadevan S, Paramashivan SS, Mandal AB. Adiabatic thermokinetics and process safety of pyrotechnic mixtures. J. Therm. Anal Calorim. 2012; 109:1387-95.

[59] Tanner HG. Instability of Sulfur-Potassium Chlorate. J. Chem. Ed. 1959; 36(2):58-9.

[60] Meyer B. Elemental sulfur. Chem. Rev. 1976; 76(3):367–88.

[61] Wagner EL. Bond Character in XYM-Type Molecules: Chlorine-Oxygen Compounds. J. Chem. Phys. 1962; 37(4):751-9.

[62] Pourmortazavi SM, Hajimirsadeghi SS, Kohsari I, Fathollahi M, Hosseini SG. Thermal decomposition of pyrotechnic mixtures containing either aluminum or magnesium powder as fuel. Fuel 2008; 87:244-51.

[63] Pourmortazavi SM, Hajimirsadeghi SS, Hosseini SG. Characterization of the Aluminum/Potassium Chlorate Mixtures by Simultaneous TG-DTA. J. Thermal Analysis and Calorimetry. 2006; 84(3):557-61.

[64] Shafirovich E, Mukasyan AS, Varmak A, Kshirsagar G, Zhang Y, Cannon JC. Mechanism of Combustion in Low-Exothermic Mixtures of Sodium Chlorate and Metal Fuel. Combustion & Flame 2002; 128:133-44.

[65] Barton TJ, Williams N, Charsley EL, Ramsey J, Ottaway MR. Factors Affecting the Ignition Temperature of Pyrotechnics. 8th International Pyrotechnics Symposium, Steamboat Springs, CO, 12-18 July, 1982; 99-111.

R1-B.1: Metrics for Explosivity, Inerting & Compatibility

I.   PARTICIPANTS

Faculty/Staff			
Name	**Title**	**Institution**	**Email**
Jimmie Oxley	Co-PI	URI	joxley@uri.edu
Jim Smith	Co-PI	URI	jsmith@chm.uri.edu
Graduate, Undergraduate and REU Students			
Name	**Degree Pursued**	**Institution**	**Month/Year of Graduation**
Ryan Rettinger	PhD	URI	5/2016
Matt Porter	PhD	URI	5/2017
Tailor Busbee	PhD	URI	5/2020
Devon Swanson	PhD	URI	5/2017
Maria Donnelly	PhD	URI	5/2015
Jon Canino	PhD	URI	12/2014

II.   PROJECT DESCRIPTION

A.   Overview and Significance

Determining if a material or formulation is detonable and determining if an adulterant has inerted a detonable material are extremely difficult problems that cannot be properly addressed unless better metrics are developed. That development is the goal of this project. Because the potential matrix of threatening combinations of fuels and oxidizers is large, we seek to determine the characteristics required for detonability; bounding the problem in terms of oxidizer and its ratio with each fuel. In the laboratory, we probe characteristics such as heat and gas release, and a full suite of chemical, thermal and sensitivity analyses to correlate to larger scale detonation performance tests. A method which can successfully determine what formulations are potentially detonable would also reveal if "inerting" of an explosive had successfully made it non-detonable or just "safer". Either question, what is potentially detonable and if adulteration has achieved non-detonability, currently requires very large-scale testing or a reliable small-scale test. The goal of the R1-B projects is development of the latter-a reliable small-scale test which screens large scale threat combinations quickly and inexpensively. We have taken here a number of approaches to this problem. They are discussed below.

Approach 1: How well an explosive functions is highly dependent on bulk properties, e.g. density, lattice structure, but whether a chemical can detonate at all, requires that the molecule have certain molecular features. To be an explosive, the molecule must be able to react with chemistry that produces heat and gas; and this must happen rapidly enough that the detonation front is supported by the energy release. Examination of the atoms making up the molecule allows prediction of whether heat and gas can be produced. This aspect of the molecule is being investigated under Approach 1 with full details as referenced in paper [1] and in R1-A.1. The thermal and burn behaviors of 11 solid oxidizers and combinations of 13 fuels were determined; burn rate was found to roughly correlate with standard reduction potentials. The thermal studies highlighted the

importance of a melt or phase change of one component of the formulation in triggering the reaction. These studies also indicated that the choice in oxidizer, outweighed the choice in fuel, in determining the total energy released. These exciting observations are the first steps in finding behaviors observed on the milligram scale that may correlate with detonability measured on the kilogram scale. Figure 1 is a plot of temperature of decomposition vs heat of decomposition [2, 3]. The fact that explosives clearly group in a different region than non-explosives suggests we can use thermal analysis of small samples as one metric to rate detonability.
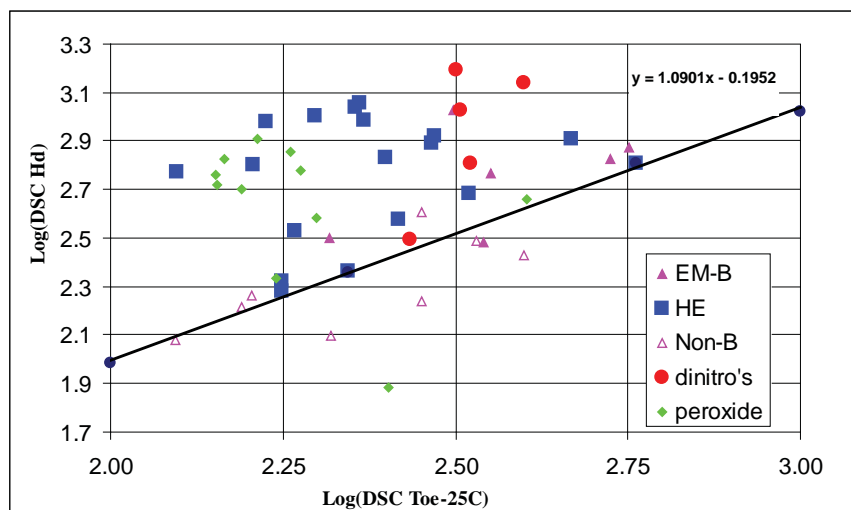
Figure 1: Plotting DSC (differential scanning calorimetric) response for peroxides (green diamonds), high explosives (blue square), dinitroarenes (red circles) and various energetic salts (pink triangles).

The critical question of whether the reaction can happen fast enough to support detonation is usually found experimentally. Other approaches in this project are examining the reaction that may or may not support steady detonation.

Approach 2 is looking at one of the fundamental molecular properties--dissociation energies during gas phase ion impact with an inert gas. By examining a variety of explosive and non-explosive compounds in an ion-trap or a triple-quadrupole mass spectrometer, a correlation may be observed between ease of fragmentation from the energy input required and the rank order of detonability.

In the past researchers developed a method for mass spectrometeric (MS) applications which was termed survival yield. The basic idea behind it was to supply enough energy to the molecule to see when only 50% of it was left over and the rest was gone due to fragmentation [4]. Recently, with the advent of new technologies and the progress in MS field resulted in reviving of this application as a proof of a concept for established ionization methods such as desorption electrospray ionization (DESI)[5, 6], electrospray ionization (ESI)[7, 8], and the newly developed accessories (mainly ionization probes) such as laser electrospray MS (LEMS) [9]. However, most of these applications are being performed on very simple molecules termed *thermometer ions* [10], which in the process produce only one or two fragments that can be easily identified and analyzed. Unfortunately, for most compounds (including virtually all energetic materials), this is not the case. Usually an array of fragments is formed; some cannot even be accounted for because of the constraints of the instrument, itself. Therefore, a new method must be developed which still has similar basis of the survival yield approach, but accounts for its limitations.

The concept is to produce and isolate ions of individual molecules within either an ion trap or a collision cell of a triple quadrupole mass spectrometer (MS). Once the ion has been isolated from the matrix (liquid phase, impurities, fragments or other unwanted ions), the collision energy provided by the MS can be gradually increased to observe several unique molecular properties: 1) the minimum energy eliciting initial fragmentation; 2) 50 % dissociation; 3) 100 % dissociation; 4) the window of energy associated with fragmentation;

and 5) a product ion spectrum. Each analysis requires less than 500 micrograms and presently takes 5 to 40 minutes to produce up to 6 full scans from 0 to 50 normalized collision energy units (eV). Initially, the ion trap MS is being used for method development and proof of principle. A quick-look experiment shows that innocuous compounds (see Table 1) can be differentiated from energetic ones (see Table 2), the latter being fragmented with much less energy. Once this method is optimized, we will attempt to establish consistent parameter sets across all compounds, e.g., solvent selection, tune conditions, percent of ion trap fill, etc. At what concentration a compound fills the ion trap may provide additional information about the ionization efficiencies. Because the ion-trap is attached to an exact mass detector (Orbitrap), molecular fragments can be assigned molecular formulas within 10 ppm accuracy.

Stable compounds	Mode	Ion	m/z	Time (sec)	E(eV) onset
2,4-Dichlorophenoxyacetic acid	ESI-	[M-H]-	218.9618	89.8	9.2
Hexamine	ESI+	[M+H]+	141.1128	118.8	11.0
DiNBenzA	ESI-	[M-H]-	210.9983	102.7	11
Sucrose	ESI+	[M+Na]+	365.1050	43.4	11.2
Dimedone	ESI+	[M+H]+	141.0904	104.2	14.8
Caffeine	APCI-	[M-H]-	195.0874	91.2	15.4
Gallic Acid	ESI-	[M-H]-	169.0132	58.5	15.8
Chrysiodine	ESI+	[M+H]+	213.1135	49.6	17.8
Aleuritic acid	ESI-	[M-H]-	303.2181	76.3	18.8
Tolidine	ESI+	[M+H]+	213.137	53.5	22
AVERAGE				78.80	14.70

Table 1: Ionization energies required for non-explosive compounds.

Energetic compounds	Mode	Ion	m/z	Time (sec)	E(eV) onset
PETN	ESI-	[M+formate]-	361.0097	29.5	2.6
Tetryl	ESI-	[M-H]-	286.0055	25.5	6.4
HMX	ESI-	[M+formate]-	341.0430	71.4	7.0
RDX	ESI-	[M+formate]-	267.0310	25.5	7.0
R-salt	ESI-	[M+formate]-	219.0491	59.8	7.4
TNT	APPI/APCI-	[M-H]-	226.0097	44.5	14.0
TATB	ESI-	[M-H]-	257.0260	49.6	15.6
DNAN	ESI-	[M-CH3]-	183.0042	50.9	17.8
AVERAGE				44.59	9.73

Table 2: Ionization energies required for explosive compounds.

Approach 3: Materials characterized as "explosives" release sufficient energy to "support" or "propagate" a detonation. Military explosives have been classified as such using detonation tests of prescribed size and initiating charge [11]. Homemade explosives (HMEs) often fail these tests because they release too little energy to support detonation in the prescribed tests; therefore, they are not recognized as real explosive threats. However, these HMEs will perform as explosive materials if the charge size is increased beyond a material-specific size, the critical diameter (D_{cr}). At sizes less than D_{cr}, an explosive will not propagate detonation; any conventional explosivity or detonability test performed under the critical diameter of the material will indicate that the material is not an explosive. The critical charge size of many potential threat materials is so

large that they are frequently not perceived as threats, when in reality they were simply tested below D_{cr}. For example, as dictated by shipping regulations, ammonium nitrate (AN) is not classed as an explosive, rather as DOT 5.1, because it does not propagate detonation at a diameter of 3.65 cm [11]. However, with sufficient AN (e.g. when the diameter exceeds 100 cm) it becomes detonable [12], as was accidentally demonstrated by the explosion in West Texas in April, 2013 [13]. Field testing at large scales is hazardous, expensive and slow. Thus, the goal of the R1-B projects is to determine whether a material is detonable at any scale by performing experiments with less than a few pounds of the material in question. A further complication exists in screening a material for explosivity. To confirm that a material is an explosive, traditional testing must be done well above critical diameter and with a sufficient initiating charge [14]. Thus, detonation failure can occur for several reasons including: (1) The material is too small in size; (2) It is insufficiently initiated; or (3) It is not an explosive. Traditional detonability tests do not differentiate.

For non-ideal explosives, a term which describes most HMEs, small-scale testing necessarily means studying these materials well below their critical diameters (D_{cr}). When steady detonation is not possible, conventional metrics, such as detonation velocity, yield little information. New diagnostics must be devised. Several approaches to this problem have been considered. Our initial approach was over-compensating for edge losses [15].

Approach 4 was actively soliciting other groups to join us in this effort. As a result, a group at Los Alamos National Lab (LANL) successfully probed evidence of detonable characteristics using 25 mL samples of hydrogen peroxide aqueous solutions of varying concentrations. While they were successful at that scale, they used instrumentation unique to that lab [16]. It has also been demonstrated by LANL researchers that the reaction zone of detonating nitromethane (NM) can be observed using photon Doppler velocimetry (PDV) [17]. We believe that a similar approach used to characterize a failing detonation can yield useful information about the material's capacity to detonate, i.e. confirming or denying the existence of a critical diameter [18].

B. State-of-the-Art and Technical Approach

Non-ideal detonation is difficult to study because, to date, no elegant, inexpensive approach exists. To determine if the rate at which a material releases energy is sufficient to support detonation, detonation testing is required at the sub-microsecond temporal- and millimeter spacial-scales. At this scale, resolved temporal resolution of run-up to detonation and failure can be observed. At present, state-of-the-art velocity measurements include microwave interferometry (MI) [19], Velocity Interferometer System for Any Reflector (VISAR) [20-22], Fabery-Perot interferometry (FPV) [23, 24] and PDV [25-28]. Microwave interferometry follows the reflection of a moving impedance discontinuity as a shock (or detonation) wave sweeps through an energetic material. However, the spatial resolution is poor ($\sim$cm) and the technique relies on the ability of the explosive to act as a waveguide (i.e. the explosive must be transparent to microwaves); likewise, the microwaves themselves require a large diameter waveguide ($\sim$1/4") which is invasive to small shots and will only average radial instabilities. Some explosives (e.g. H_2O_2 mixtures or aluminized mixtures) absorb or reflect microwave radiation and, therefore, cannot be examined by MI. VISAR uses a Michelson interferometer to measure the phase-interfered Doppler shift in the light frequency of a laser beam as it is reflected from a moving reflector. Unfortunately, amplitudes of returned light can vary greatly during a single experiment, and this technique has been largely replaced by PDV. FPV can be considered as a modified version of VISAR that requires the use of a streak camera to record fringe patterns; however, these are subject to various distortions caused by the camera, itself. PDV is a relatively new technological breakthrough that directly measures the beat frequency between the incident laser and the reflected light. The beat frequency is linearly proportional to the velocity of a moving reflector, which in our experiments, is either the shock or detonation front or a reflective interface between the explosive charge and a polymer window. PDV is useful for measuring velocities ranging from a few meters per second to roughly 50 km/s, with high accuracy and nanosecond resolution, and will work well for any index of refraction discontinuity in free space or within the fiber itself.

Characterizing detonation behavior for sub-critical quantities of non-ideal explosives is extremely challenging. Unless supported by special device design, detonation fronts fail for lack of sufficient and timely energy release from the reaction, which prevents traditional metrics from predicting the potential of a threat which failed at a small diameter to detonate above the tested configuration size. Steady detonations are achieved with very small diameters using military explosives, but many HMEs, especially fuel/oxidizer explosives (FOX) mixtures, may only perform as explosives on very large scales. If the material fails to support a steady detonation, meaning a 'no-go' result, the only meaningful conclusion is that the material is not explosive at that scale. Using conventional metrics, a failure to detonate may only mean that the size of the test was insufficient.

Detonation velocity is used as a measure of explosive performance; high detonation velocities reflect the high rate of energy release of conventional explosives. However, if the energy release lags in time (i.e., the reaction cannot keep up with the shock), the shock wave will decouple from the chemical conversion process, and the detonation will "fail". Thus, an accurate detonation velocity profile gives critical insight into the chemical reaction zone structure of high explosives. A versatile array of techniques will enable in-situ monitoring of both ignition and this delicate failure transition both temporally and spatially, beginning with a sample's overdriven detonation through failure and decoupling of the shock wave from chemistry. Using high speed photography and PDV, we may also be able to visually discern the decoupling frame-by-frame. We intend to use a collection of traditional, readily-accessible technologies with modified techniques and strategies to examine detonation structure and probe explosive behavior far below the critical diameter of the potential threat materials.

Since hydrogen peroxide was our chosen characterization challenge, PDV was the metric of choice. The first hurdle was that a data acquisition system that could sample at a rate of 18 GHz was required. Outside funding eventually supplied that requirement, but in the meantime, we investigated a novel approach to using PDV with a lower bandwidth acquisition system and modern telecommunications components. These successful investigations are making this technique available to a wide number of users; they are described in detail in reference [15]. Figure 2 on the next page and the discussion of the content below gives further details of the concept.

Typical detonation velocities are between 5-9 km/s for most military high explosives and typical particle velocities at the detonation condition range from 1-5km/s. Configuring an interferometric experiment to measure these relatively high speeds requires the capacity to measure the beat frequency of the incident light (usually vis-NIR: 200-600THz) with the Doppler-shifted reflected signal governed by:

$$f_{Doppler\ beat} = 2\frac{v_{reflector}}{c}f_0$$

where $f_{doppler\ beat}$ is the Doppler-shifted beat frequency, f_0 is the incident laser frequency, c is the speed of light, and $v_{reflector}$ is the speed of the reflecting surface. This sets the native Doppler beat frequency at 10s of gigahertz for visible-NIR wavelengths at typical explosive velocities. The limitation of PDV is mostly determined by the bandwidth of instruments, e.g. the high speed oscilloscope and photo receiver, which implies high instrument costs. However, by introducing a modulation frequency carried by the input laser beam, the beat frequency generated by the original PDV mixes with the modulation frequency, which allows a second beat to bring down the measurement frequency. This modified PDV extends the current system capability with little change, and far less expensive digitizers and receivers can be used. Short-time fast Fourier transform is performed to map the velocity change among the times.

Fig.1 Interferometer schematic by the PDV with fiber end.
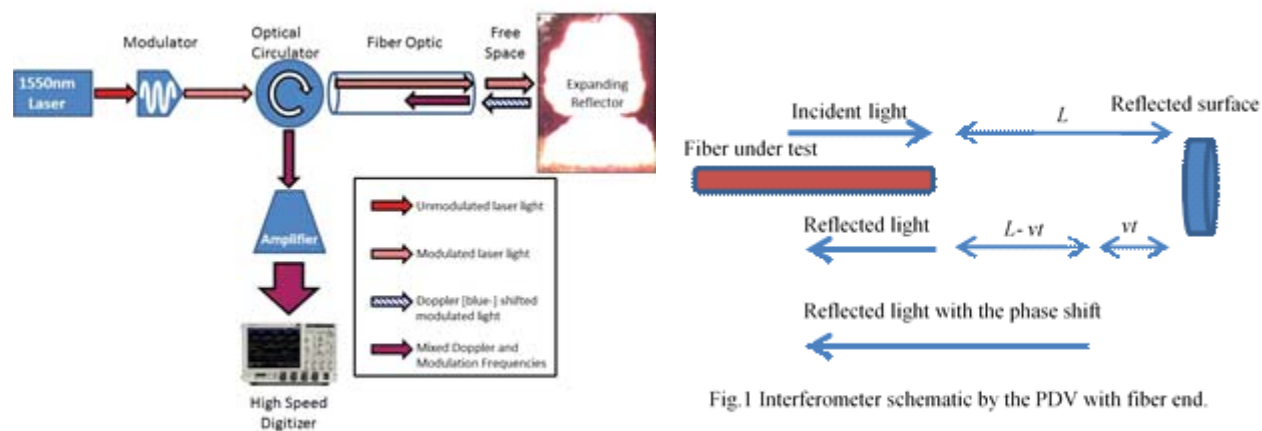
Figure 2: The concept of microwave-modulated Photon Doppler Velocimetry.

The second hurdle was created by our desire to use embedded PVD probes, a technique which has only been attempted occasionally and with little success. [29, 30] As PVD is normally used, it observes the optical response at the surface of the charge. For this, the optical fiber used is normally glass (for expense) and single-mode fiber (SMF) for distance. However, because glass is not a good acoustic impedance match with explosives, pressure fluctuations can propagate ahead of the shock front (see Fig. 3 on the next page). A better match would be plastic fibers, but these are generally only manufactured as multi-mode. We would like to run glass fiber to the explosive test article and then change to plastic fiber for the embedded section. Unfortunately, there is not a good way to connect the glass fiber (9 micron diameter) to the plastic fiber (62.5 micron). This is a diameter as well as optical impedance mismatch. Our approach to this (in collaborating with the T. Wei in electrical engineering at URI) is lensing to handle the diameter problem and a refractive index fluid to ameliorate the optical impedance problem (see Fig. 4 on the next page).

The third hurdle is interpretation of shock velocity data below actual detonation. Our approach is to begin testing with a well-characterized material, such as nitromethane (NM), and to use an end-on interfacial surface velocity PDV probe with the amount of NM large enough to achieve detonation. This test will then be repeated with the embedded PDV probe. Further tests in that configuration will be performed with smaller diameters or concentrations of NM. Streak photography will be used to record detonation curvature and assess the structure of the failed detonation. In addition, ultra-high speed photography (>300 million frames per second or <3ns interframe time) will allow observation of the reaction wave directly as it forms (run-up)

and dies (failure). This total characterization will provide a failure fingerprint which will characterize exactly how non-ideal materials perform at known fractions of critical diameter. At this point, this technique will be used to examine hydrogen peroxide.
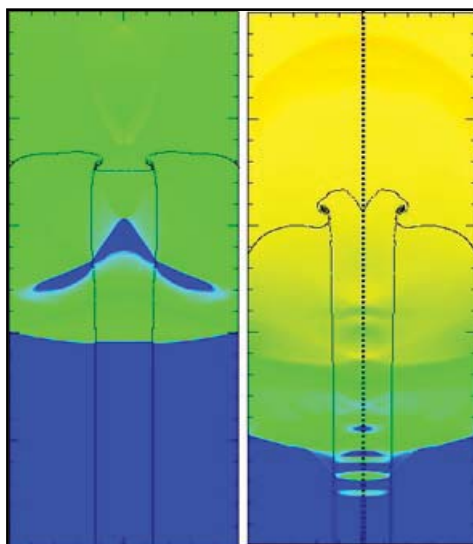
Figure 3: Modeling of shock in plastic (left) fiber vs. glass (right) fiber in explosive reaction.
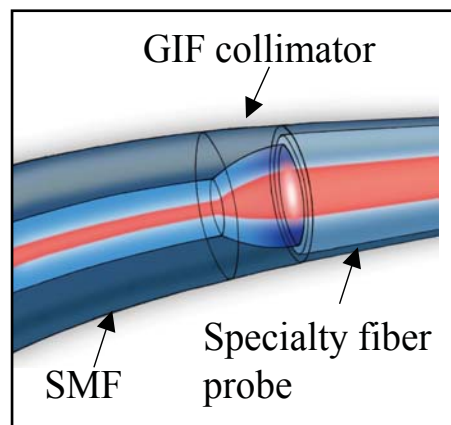
Figure 4: Proposed Graded Index Fiber (GIF) connecting glass SMF to plastic multi-mode fiber.

Visualizing the reaction wave should be straightforward with clear liquid explosives, such as NM or hydrogen peroxide because they should be radiating brilliantly but that has yet to be proved with ultra-high speed photography. The premise is that the initial shock wave will be unreactive for some time, and the superdetonation wave will be visible as it runs through the shocked nitromethane or hydrogen peroxide and catches the shock front. It is unclear whether the PDV probe will survive (and be optically functional) after the initial shock-up, but if it does, the superdetonation velocity may also be visible.

C. Major Contributions

Laboratory studies have shown the importance of low-melting fuels, such as sugars or sulfur, in creating reactive FOX mixtures. Field tests have yet to correlate these results with detonability.

Important differences in results arising from instrumental methodology, i.e. differential scanning calorimetry (DSC) vs. simultaneous differential thermolysis (SDT), have been revealed. Results point out the value of sealed DSC runs for evaluating heat release and open SDT runs for evaluating heat absorbed.

Determining the appropriate approach to detonability and equipping and familiarizing ourselves with the tools for the necessary metrics has been a significant part of this effort.

Work to date has resulted in one student obtaining staff status at LANL (Los Alamos National Lab), a poster at JANNAF, an award from the National Science Foundation (NSF, Low-cost velocimetry for ultra-fast shock wave measurements) and a Center report and a paper in review.

D. Milestones

We intend to use a compilation of previous ideas to approach a small scale test suite that can qualify the failure of explosives below their critical diameter. The first technique is similar to LANL's use of end-on interfacial surface velocity to measure reaction zone structure. Our preliminary surface velocity tests have proven successful. Because of the acoustic impedance challenge, few experimenters have successfully implemented

embedded PDV silica fibers. We are experimenting with ways to optically couple polymer fiber embedded probes (impedance more closing matching the explosive and its detonation products) with single-mode silica fibers that compose the rest of the optical system.

Recording detonation curvature with streak photography is well established. Visualizing the reaction wave with ultra-high speed photography should be straightforward with clear liquid explosives but that has yet to be proved. As mentioned above, the premise is that the initial shock wave will be unreactive for some time and the superdetonation wave will be visible as it runs through the shocked NM and catches the shock front. It is unclear whether the PDV probe will survive (and be optically functional) after the initial shock-up but, if it does, the superdetonation reaction wave may also be visible.

Theoretically, PDV can be adapted as an embedded probe inside the explosive material; thus, it would act as a time-resolved velocimeter similar to MI but without the size constraints of microwave waveguides and with very high spacial and temporal resolution. Fiber optic probes are non-intrusive and, potentially, they can be assembled using commercially available telecom components, making them extremely inexpensive. In contrast to VISAR/FPV, the derived velocity measurement is directly related to the observed beat frequency, reducing the need for extra components and complex data analysis. The main disadvantage of the PDV system is its critical demand on the sampling speed of the digitizer. Most PDV experiments are currently conducted with a sampling rate above 80 GSa/s. The cost for such large bandwidth has limited the wide adoption of PDV. Some approaches to making PDV more affordable are being investigated in collaboration with URI electrical engineering Professor Tao Wei under a program funded by NSF.

E.   Future Work

NM will be used for the proof-of-concept of the PDV experiment. Once the literature values for NM have been successfully replicated, NM will be successively diluted with chemicals known to increase the sensitivity of NM without providing more energy to the detonation front. The adulterated samples are expected to exhibit shorter reaction zones due to their increased sensitivity. As the adulterant concentration is increased, the reaction zone will eventually begin to spread apart because the active explosive ingredient is diminishing. At some critical amount, detonation will fail to propagate. The study will examine the failure point as well as points of dilution beyond detonation failure in conjunction with larger scale tests, at our outdoor test facility, to measure the actual D_{cr} for the samples below their critical diameter in the small-scale tests.

Once proof-of-concept tests are successfully completed, tests are planned with both hydrogen peroxide-fuel mixtures and solid oxidizer-fuel mixtures. Project R1-A.1 has already begun performing the laboratory characterization of FOX combinations. Characterizing the detonability of these mixtures will then be combined in correlation with other small-scale tests and may allow certain materials to be deleted from the threat list. This test will also allow us to assess the effectiveness of a given diluent or adulterant in an explosive mixture. True safe limits for materials can be established.

III.   EDUCATION AND WORKFORCE DEVELOPMENT ACTIVITY

A.   Course, Seminar or Workshop Development

"Advanced Studied in Explosives" course was offered for the first time in spring of 2015 with 15 graduate students in attendance.

In May 2015, a hands-on course entitled "Explosives Analysis" was offered for the first time; six members of the HSE came to URI to attend.

Graduate student Devon Swanson was selected to give an award talk at the Trace Explosive Detection conference for his work on AFM of explosives (April 2015, Pittsburgh).

Dr. Smith presented "An Introduction to the Properties of Explosive and Trace Detection" at the IEEE HST '15 ALERT Tutorial Session: Introduction to Explosives/Threat Screening Tools and Technologies in April 2015.

Courses were presented for the Army, Navy, Air Force, and the Transportation Security Administration (TSA-TSIF, 10 classes and 200 people) and TSA explosive specialists (TSA-TSS-E, 5 classes and 110 people).

A.1.   Invited lectures

- Thermal Stability and Chemistry of Difficult Energetic Materials" New Trends in Research Energetic Materials; Pardubice, CZ, April 11, 2015.

- JANNAF, December 10, 2014, Academic Research to Real Life Application, ABQ.

- 7th Annual CBRNe Convergence, October 28-30 2014, New York, NY, tutorial to first responders

- Recognizing Improvise Drug vs Explosive Labs, 23rd Annual Haz-Mat Training Conf. September 18, 2014, Plymouth, MA, tutorial to first responders

B.   Student Internship, Job or Research Opportunities

Each URI project supports one or more graduate students. This is their best learning experience. Undergraduates are also supported on the projects as their class schedules permit. A newly minted PhD from our group, Jon Canino, accepted a position at Signature Science and is working at the Transportation Security Laboratory in New Jersey.

C.   Interactions and Outreach to K-12, Community College, Minority Serving Institution Students or Faculty

We have continued our K-12 outreach by hosting high school teachers in the summer and providing chemical magic shows at schools K-12. High school teachers conduct research in URI labs for 8 to 10 weeks under the mentorship of a graduate student. As a result, two have gone back to seek advanced degrees.

In addition, in the summer of 2014, we hosted 2 forensic scientists from Qatar and a West Point cadet for several weeks. For the summer of 2014, we hosted a professor from Tuskegee University and one of her students. In summer of 2015, we will host two Navy midshipmen and a Penn State engineer, and air force employee will be placed at URI to begin work on a master's degree.

D.   Training to Professionals or Others

We trained 110 TSS-E (TSA explosive specialists) in five classes and approximately 230 other people involved in the HSE in twelve classes, one of which was created to meet the needs of the U.S. Army forensic laboratory.

IV.   RELEVANCE AND TRANSITION

A.   Relevance of Research to the DHS enterprise

There are, potentially, hundreds of explosive threat materials. Distinguishing between actual threats and benign chemicals is of high interest. This effort also extends to the question of concentration, e.g. absolute safe concentrations of hydrogen peroxide- the type of questions incoming from TSA and explosive trace detection (ETD) vendors. When the proposed tests are developed and executed, they will be available as screening tools to forge the answers to these problems.

This understanding of non-ideal detonation is an ongoing security research effort; URI's Energetics Laboratory was the only academic institution invited to the DHS Chemical Security Analysis Center & Explosives Division 1st inter-agency Explosives Terrorism Risk Assessment working group meetings established in May

2015. The characterization of non-ideal detonation is also of valuable interest to insensitive munitions (IM) research efforts, which also require better metrics and diagnostics to track detonation kinetics.

B.   Potential for Transition

- R1-B.1 addresses the characterization of HMEs. We have received requests to license the database.
- R1-B.1 addresses safe samples of explosive. We have received requests to license our safe source of explosive vapor.
- Traditional transition methods such as publication and presentation will also be used to transmit our new methodologies.

C.   Data and/or IP Acquisition Strategy

As the data from the program becomes available it will be provided to the community through DHS, publications, and presentations.

D.   Transition Pathway

R1-B will primarily be transferred to the user community by publications and presentations.

V.   PROJECT DOCUMENTATION

A.   Peer Reviewed Journal Articles

1. Colizza, Kevin M Porter, J. Smith, J. Oxley "Gas Phase Reactions of Alcohols with Hexamethylene triperoxide diamine (HMTD) under Atmospheric Pressure Chemical Ionization Conditions" Rapid Communications in Mass Spectrometry 2014, 29(1), 74, 10.1002/rcm.7084

2. Oxley, "Explosive Detection: How We Got Here and Where Are We Going?" International Journal of Energetic Materials and Chemical Propulsion; 2014, 13(4): 373-381. 10.1615/IntJEnergeticMaterialsChemProp.2014011493

3. Oxley, J.; Smith, J.; Donnelly, M.; Porter, M. "Fuel-Oxidizer Mixtures: Their Stabilities and Burn Characteristics; International Journal of Energetic Materials and Chemical Propulsion 2014, 13(6): 517-558. 10.1007/s10973-015-4589-x (J Therm Anal Calorim)

4. Oxley, J.C.; Smith, J.L.; Canino, J.N. "Insensitive TATP Training Aid by Microencapsulation" J. Energetic Materials; 2015, 33(3), 215-228. 10.1080/07370652.2014.985857

Pending –

1. Oxley, J.C.; Smith, J.L.; Porter, M.; Colizza, K.; McLennan, L. "Mechanisms of Synthesis and Degradation of Hexamethylene triperoxide diamine (HMTD)" submitted to Propellants, Explosives, Pyrotechnics.

2. Oxley, J.; Smith, J.; Donnelly, M.; Rayome, S. "Thermal Stability Studies on IMX-101 (Dinitroanisole/ Nitroguanidine/NTO)" accepted to Propellants, Explosives, Pyrotechnics.

B.   Other Conference Proceedings

1. Donnelly (presenter) with J Oxley; J Smith; M. Porter Fuel-Oxidizers Mixtures: Their Stabilities and Burn Characteristics North American Thermal Analysis Society (see paper), 2014

2. Smith, J. "An Introduction to the Properties of Explosive and Trace Detection." IEEE HST '15 Tutorial Session: Introduction to Explosives/Threat Screening Tools and Technologies, April 2015.

3. Phase 2, Year 2, DHS Annual Program Review, Northeastern University, March 2015.

C.   Other Presentations

1. Seminars

   a. Devon Swanson (presenter) with J Oxley; J. Smith; G. Kagan "Adhesion Forces of Energetic Materials on Polymer Surfaces" Trace Explosive Detection April 2015; Pittsburgh

   b. Maria Donnelly, "Fuel-Oxidizer Mixtures: Evaluating the Hazard Potential," North American Thermal Analysis Society, Oct 2014.

2. Poster Sessions

   a. Bowden, P., Rettinger, R., Oxley, J., Smith, J., Stewart, S., Kennedy, J., "Attempts at Overdriven Detonations in no-ideal Explosives" JANNAF poster with LANL Dec 2014

3. Short Courses - listed under education

D.   Student Theses or Dissertations

1. PhD Chemistry: Jon Canino Dec. 2014 Polymer Systems and Explosives

2. PhD Chemistry: Maria Donnelly May 2015 Thermal Stability & Sensitivity of Energetic Formulations.

E.   New and Existing Courses Developed and Student Enrollment

New or Existing	Course/Module/ Degree/Cert.	Title	Description	Student Enrollment
New	Certificate	Explosive Analysis	Lab Analysis of Explosives	6*
New	Graduate credit	Explosive Analysis	Mass Spectroscopy; Thermal; Shock	15
Existing	Certificate	Pyrotechnics	Raytheon K-Tech ABQ	12
Existing	Certificate	Fundamentals	Fundamentals - Alcoa	12
Existing	Certificate	Air Blast	Air Blast - Huntsville	14
Existing	Certificate	Materials Characterization	Picatinny	14
Existing	Certificate	Fundamentals	TSIF Fundamentals	50
Existing	Certificate	Fundamentals	Fundamentals Eglin	28
Existing	Certificate	Fundamentals	URI Fundamentals	32
Existing	Certificate	Air Blast	Air Blast - LANL	15
Existing	Certificate	Materials Characterization	Materials Characterizations - Navy	18
Existing	Certificate	Stability, Compatibility	Stability, Compatibility - Navy	18

* Included DHS personnel

F.   Requests for Assistance/Advice

1. From DHS

   a. On call for a variety of TSA TSS-ES personnel

   b. Oxley is part of the DHS-formed Inter-Agency Explosive Terrorism Risk Assessment Working Group (IExTRAWG)

2. From Federal/State/Local Government

   a. Singapore, India, Turkey Defense groups ask questions, request classes; class request from India

in review at Dept of State.

b. We have been asked to support Brookhaven National Lab in some of their international outreach.

VI.   REFERENCES

[1] J. Oxley, J Smith, M. Donnelly, M Porter "FOX Mixtures: Stabilities and Burn Characteristics; International Journal of Energetic Materials and Chemical Propulsion 2014, 13(6): 517-57.

[2] Yoshida, Yoshizawa, Itoh, Matsunaga, Watanabe, Tamura Kogyo Kayaku, 1987, 48, 311-316.

[3] Bodman, G.T. "Use of DSC in Screening for Explosive Properties" NATAS abstracts Sept 2002 p605-610.

[4] Derwa, F., De Pauw, E., Natalis, P. New basis for a method for the estimation of secondary ion internal energy distribution in soft ionization techniques. Org. Mass Spectrom. 1991; 26: 117.

[5] Takats, Z., Wiseman, J.M., Cooks, R.G. Ambient mass spectrometry using desorption electrospray ionization (DESI): instrumentation, mechanisms and applications in forensics, chemistry, and biology. J. Mass Spectrom. 2005, 40, 1261-1275.

[6] Nefliu, M., Smith, J.N., Venter, A., Cooks, R.G. Internal Energy Distributions in Desorption Electrospray Ionization (DESI). J. Am. Soc. Mass Spectrom. 2008, 19, 420–427.

[7]   Liang, Y., Neta, P., Simon-Manso, Y., Stein, S.E. Reaction of arylium ions with the collision gas N_2 in electrospray ionization mass spectrometry. Rapid Commun. Mass Spectrom. 2015, 29, 629-636.

[8] Naban-Maillet, J., Lesage, D., Bossee, A., Gimbert, Y., Sztaray, J., Vekey, K., Tabet, J-C. Internal energy distribution in electrospray ionization. J. Mass Spectrom. 2005, 40, 1-8.

[9] Flanigan IV, P.M., Shi, F., Archer, J.J., Levis, R.J. Internal Energy Deposition for Low Energy, Femtosecond Laser Vaporization and Nanospray Post-ionization Mass Spectrometry using Thermometer Ions. J. Am. Soc. Mass Spectrom. 2015, 26, 716-724.

[10] Collette, C. and De Pauw, E. Calibration of the Internal Energy Distribution of Ions Produced by Electrospray. Rapid Commun. Mass Spectrom. 1998, 12, 165-170.

[11] United Nations, Recommendations on the Transport of Dangerous Goods, Manual of Tests and Criteria, ST/SG/AC.10/11/Rev 5, Section 34, Classification Procedures, Test Methods and Criteria Relating To Oxidizing Substances of Division 5.1 2009

[12] CTTSO BAA 14-Q-3272 R3826; March 19, 2014

[13] U.S. Chemical Safety Board http://www.csb.gov/west-fertilizer-explosion-and-fire-/

[14] Most energetic materials capable of detonation can be initiated with the help of a high explosive booster charge, but if the sample energetic is below its critical diameter, the chemical reaction will quickly (less than an inch) decouple from the shock front and the shock will propagate as an inert pressure wave through the rest of the non-reacting material, giving the appearance that the material is non-explosive. This detonation failure phenomenon can be very delicate; many detonations near the critical diameter are very unstable, which means conventional explosive testing must be done well above the critical diameter.

[15] Bowden, P., Rettinger, R., Oxley, J., Smith, J., Stewart, S., Kennedy, J., "Attempts at Overdriven Detonations in no-ideal Explosives" JANNAF poster with LANL Dec 2014

[16] Sheffield, S.A.; Dattelbaum, D.M.; Stahl, D.B.; Gibson, L.L.; Bartram, B.D.; Engelke, R. "Shock Initiation and Detonation Study of High Concentration H2O2/H2O Solutions using In-Situ Magnetic Gauges" 14th International Detonation Symposium, Coeur d'Alene, ID, April 2010. LA-UR-10-01464.

[17] Bouyer, V; Sheffield, S.A. Dattelbaum, D.M; Gustavsen, R.L.; Stahl, D.B; Doucet, M.; Decaris, L,

"Experimental Measurements of the Chemical Reaction Zone of Detonating Liquid Explosives" Shock Compression of Condensed Matter 2009 p177-180.

[18] Chen, B.; Wei, T.; Rettinger, R.; Oxley, J. "Microwave-modulated Photon Doppler Velocimetry" in review.

[19] V. M. Bel'skii, A. L. Mikhailov, A. V. Rodionov, and A. A. Sedov, "Microwave diagnostics of shock-wave and detonation processes," Combustion Explosion and Shock Waves, vol. 47, pp. 639-650, Nov 2011.

[20] L. M. Barker and Hollenba.Re, "Laser interferometer for measuring high velocities of any reflecting surface," Journal of Applied Physics, vol. 43, pp. 4669-&, 1972.

[21] W. F. Hemsing, "Velocity sensing interferometer (VISAR) modification" Review of Scientific Instruments, vol. 50, pp. 73-78, 1979.

[22] L. M. Barker and K. W. Schuler, "Correction of velocity-per-freinge relationship for VISAR interferometer," Journal of Applied Physics, vol. 45, pp. 3692-3693, 1974.

[23] A. Courteville, Y. Salvade, and R. Dandliker, "High-precision velocimetry: optimization of a Fabry-Perot interferometer," Applied optics, vol. 39, pp. 1521-1526, Apr 2000.

[24] C. F. McMillan, D. R. Goosman, N. L. Parker, L. L. Steinmetz, H. H. Chau, T. Huen, R. K. Whipkey, and S. J. Perry, "Velocimetry of fast surfaces using Fabry–Perot interferometry," Review of Scientific Instruments, vol. 59, pp. 1-21, 1988.

[25] P. Mercier, J. Benier, A. Azzolina, J. M. Lagrange, and D. Partouche, "Photonic doppler velocimetry in shock physics experiments," Journal De Physique Iv, vol. 134, pp. 805-812, Aug 2006.

[26] P. Mercier, J. Bénier, P. A. Frugier, A. Sollier, M. R. Le Gloahec, E. Lescoute, J. P. Cuq Lelandais, M. Boustie, T. de Rességuier, A. Claverie, E. Gay, L. Berthe, and M. Nivard, "PDV measurements of ns and fs laser driven shock experiments on solid targets," AIP Conference Proceedings, vol. 1195, pp. 581-584, 2009.

[27] D. H. Dolan and S. C. Jones, "Push-pull analysis of photonic Doppler velocimetry measurements," Review of Scientific Instruments, vol. 78, Jul 2007.

[28] D. H. Dolan, "Accuracy and precision in photonic Doppler velocimetry," Review of Scientific Instruments, vol. 81, May 2010.

[29] Mercier, P.; Benier, J.; Frugier, P.A.; Debruyne, M.; Crouzet, B. "Nitromethane ignition observed with embedded PDV optical fibers" EPJ web of conferences 10, 00016 (2010); DOI: 10.1051/epjconf/20101000016

[30] Hare, D.E.; Goosman, D.R.; Lorenz, K.T.; Lee, E. L. "Application of the Embedded Fiber Optic Probe in High Explosive Detonation Studies: PBX-9502 and LX-17", 2006. UCRL-CONF-222509. Hare, D.E.; Garza, R.G.; Stand, O.T.; Whitworth, T.L.; Holtkamp, D.B. "Embedded Fiber Optic Probes to Measure Detonation Velocities using the PDV; 14th Intn'l Detonation Symp. Coeur d' Alene Apr 11-16, 2010.

R1-C.2: Compatibilities & Simulants: Explosive Polymer Interactions

I.   PARTICIPANTS

Faculty/Staff			
Name	**Title**	**Institution**	**Email**
Jimmie Oxley	Co-PI	URI	joxley@uri.edu
Jim Smith	Co-PI	URI	jsmith@chm.uri.edu
Sze Yang	Co-PI	URI	syang@chm.uri.edu
Gerald Kagan	Post-Doc	URI	gkagan@chm.uri.edu
Graduate, Undergraduate and REU Students			
Name	**Degree Pursued**	**Institution**	**Month/Year of Graduation**
Jon Canino	PhD	URI	12/2014
Maria Donnelly	PhD	URI	4/2015
Michelle Gonsalves	PhD	URI	5/2018
Guang Zhang	PhD	URI	8/2015
Jeff Canaria	PhD	URI	5/2020
Rebecca Levine	PhD	URI	5/2018
Devon Swanson	PhD	URI	5/2017

II.   PROJECT DESCRIPTION

A.   Overview and Significance

The aim of this project is to develop new methods for those involved in the Homeland Security Enterprise (HSE) to collect, handle and store explosives. Because there are many applications where explosives must interact with other materials, a number of approaches have been developed. To date, the applications of this study have been safe trace explosive sources for canine and instrument training and explosive sampling devices (swabs), which are effective at pick up and release of explosive residue.

Military explosives are rarely used pure, meaning without a plasticizer or other formulating agent. So, too, homemade explosives (HMEs), may require admixture with other materials. Considering only use by the HSE, understanding how HMEs react with other materials is necessary for a number of applications: safe handling and storage of HME; creation of better swabs; creation of better vapor concentrators; creation of canine training aids; and creation of trace and bulk simulants. Whatever the reason, for the sake of safety and for proper selection of materials, we must understand their interactions. This project has focused on finding the best materials for such devices as canine training aids, swab material and pre-concentrators. One successful application of our studies is polymer encapsulation to facilitate handling of volatile, sensitive explosives, e.g. triacetone triperoxide (TATP). This approach promises canine handlers and instrument vendors with safe, store-able access to hazardous explosives. It has been received with enthusiasm. We are presently negotiating licensing with a commercial vendor.

Along with the discovery of potential applications, metrics for assessment are being developed. Our studies have employed a closed vapor chamber as a metric for sorption. The quantity of a sorbed explosive is determined by exhaustive extraction. Desorption of explosives in many applications is accomplished by heating. A thermogravimetric analyzer (TGA) coupled with infrared and/or mass spectrometry determines desorption quantity, purity and the presence of decomposition products. Atomic Force Microscopy (AFM), using the jump-off point, has been used as a way to measure the adhesive forces between the polymer and explosive.

R1-C.2 has resulted in two papers authored at URI [1, 2] and two from our partner at a minority-serving-institution (MSI) [3, 4], as well as a provisional patent [5]. Both our MSI partner and our group have been awarded further Department of Homeland Security (DHS) funding for certain aspects of this research [6, 7]. This work has also resulted in a graduate student award [8] and partnerships with three vendors supporting trace explosive detection.

B.   State-of-the-Art and Technical Approach

This project uses a variety of tools to determine compatibility of various materials with explosives. In addition to standard laboratory analysis methods, this project has explored the use of reaction and titration calorimetry, AFM, TGA-IR, and various gas and liquid chromatographs as tools to aid this work. This project has also investigated new methods to package sensitive HME and novel ways to collect explosives residues with the goal of an on-off collection methodology. For example, this project has focused on safe and long-lived canine training aids for peroxide explosives, and exploring methods to encapsulate these hazardous materials. Scientists at NIST have since reported a similar approach and sent us a congratulatory email after seeing our presentation at the Trace Explosive Detection conference (April 2014). Recently, their paper has been sent to us for review (see reference [10]); in fact in the last year we have been asked to review over 40 papers dealing with explosive, suggesting our expertise is valued in this field. The following sections B.1-B.3 discuss the various elements of the R1-C.2 effort.

B.1.   Encapsulation and coating of energetics

In the explosives detection community, there is a need for an insensitive, storage-stable source of HMEs and in particular the high-sensitive, peroxide explosives. To meet the demand for safe forms of TATP, we have sublimed TATP onto scrupulously clean filter paper. While this approach fulfilled immediate needs of canine trainers and instrument suppliers, preparation was arduous; and the aids were effective for only about 90 minutes. To enhance the work- and shelf-life of the product, we developed a method to encapsulate TATP. The approach, best matching our laboratory resources, was emulsification. A polymer shell-coating material was added, with stirring, to the dispersed phase solvent; i.e. dichloromethane, DCM. Once all the shell material had dissolved, TATP was added. When the TATP had completely dissolved in the polymer solution, the entire solution was added to water with 2% of polyvinyl alcohol and stirred at ~900 rpm until the DCM evaporated, allowing the formation of solid plastic microspheres (~1hr). Additional water was added with stirring to aid filtration and solid microspheres were recovered by vacuum filtration.

While there were batch-to-batch variations, typically the microspheres contained 20-25wt% TATP. The amount of TATP, the temperature at which it was released from the microsphere, and the purity of its signature was assessed using thermogravimetric analysis (TGA) with the off-gas analyzed by infrared (IR) spectroscopy. With TGA, it was possible to distinguish between release of pure explosive, explosive decomposition products and polymer decomposition products. It also allowed the researcher to select the scent. Figure 1 on the next page (red) shows an IR spectrum of evolved gas from heating polycarbonate beads of TATP; for comparison, pure TATP vapor is the blue trace. The scent sources prepared in this fashion are easier to produce than the previous ones, but the main benefit is that encapsulated TATP has been shown to be stable for up to three years. Figure 2 on the next page shows the TGA traces of TATP encapsulated in polystyrene-fresh and 2.5 years old. The TATP content remained at 16.0%, as judged by TGA.

A total of nine polymers were investigated for encapsulation of TATP (see Table 1 on the next page). While polystyrene remained an acceptable encapsulating polymer, for a variety of reasons, polycarbonate became the material of choice. Our top choices in encapsulated TATP were tested by actual aging or by accelerated aging (see Fig. 2). Thermal stability proved to be exceptional (see Table 2 on the next page).

This work resulted in a paper [9], a student homeland security innovation award of $10,000 [10], and partnership with a vendor desiring to design and market the heating device. Future work includes a rigorous calibration of heating schemes for releasing TATP upon demand; working with the vendor to design the heating device for TATP and HMTD heating specification; determining the most appropriate polymer for encapsulation of HMTD (hexamethylene triperoxide diamine).
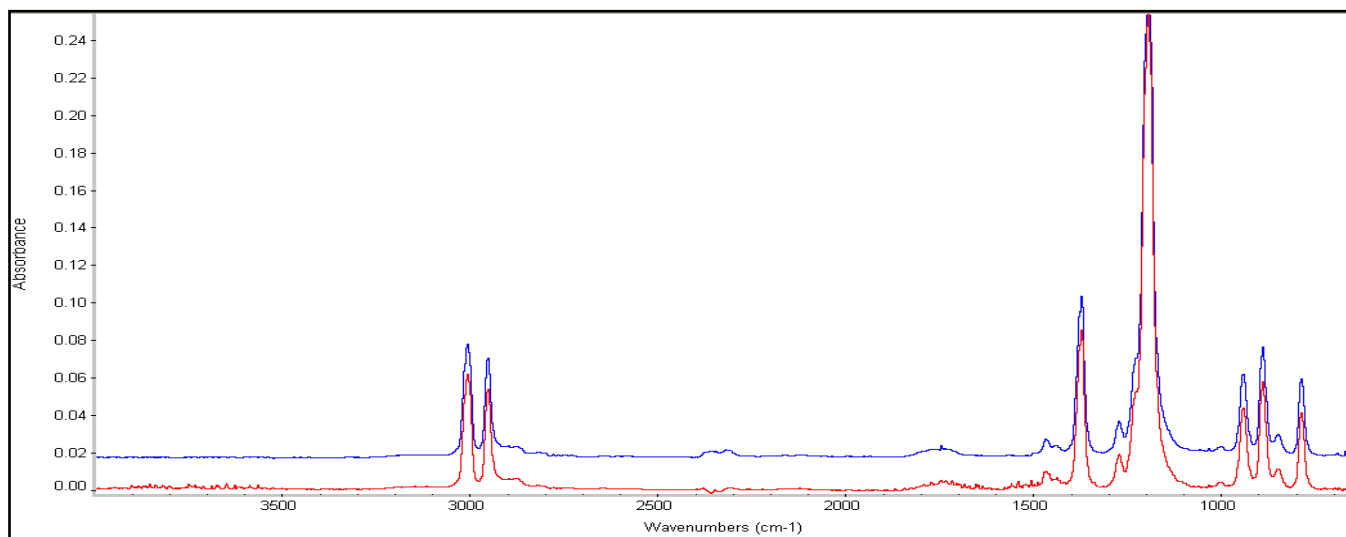

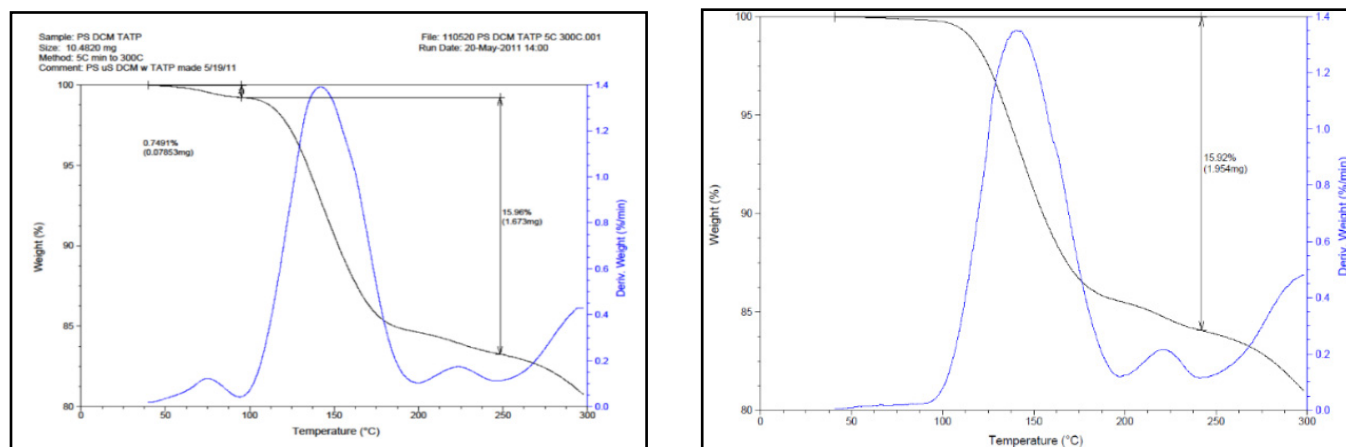**Figure 1: IR spectrum TGA off-gas of beads (red) and pure TATP (blue).**

Figure 2: Polystyrene bead of TATP, fresh, 16.0% (left) and aged 873 days, 15.9% (right).

Polymer	Tg 20°C/min (°C)	TATP Start Loss 2°C/min (°C)	TATP Max Loss 2°C/min (°C)	TATP Max Loss 20°C/min (°C)	DSC Max Endotherm 20°C/min (°C TATP)	DSC Max Exotherm 20°C/min (°C TATP)	DSC Max Endotherm 20°C/min (°C DADP)	DSC Max Exotherm 20°C/min (°C DADP)	DADP Start Loss 2°C/min (°C)	DADP Max Loss 2°C/min (°C)	Polymer Decomp (°C)	Release Type
Triacetonetriperoxide (TATP)	-	-	-	-	98	238	-	-	-	-	-	-
Diacetonediperoxide (DADP)	-	-	-	-	-	-	133	253	-	-	-	-
Poly(D,L-lactide-co-glycolide) (PLGA)	45-50*	~46, 60	-	-	-	-	-	-	-	-	-	A**
Polyethylmethacrylate (PEM)	63*	65	142	-	-	-	-	-	-	-	-	B
Poly(vinyl butyral-co-vinyl alcohol-co-vinyl acetate) (PVBVAVA)	64	77	93	102	89	-	-	-	-	-	-	A
Poly(4-methyl styrene) (P4MS)	104*	75	~124, 190	-	-	-	-	-	-	-	-	A
Polymethylmethacrylate (PMMA)	105*	77	154	-	-	-	-	-	-	-	-	B
Polystyrene (PS)	109	77	152	163	63	231	-	-	-	-	443*	A
Polycarbonate (PC)	148	88	135	168	87	-	132	-	103, 134	160	480-485*	A
Polysulfone (PSf)	190	139	167	183	93	184	-	-	149	197	530-535*	C
Polyetherimide (PEI)	220	140	195	197	93	199	-	-	-	-	-	C

* Literature Value   **Polymer Decomposes at Room Temperature

Table 1: Polymers investigated for encapsulation of TATP.

Polymer	% TATP Initial	238 Days	322 Days	432 Days	446 Days	771 Days	873 Days
Polystyrene	16.0	-	-	15.8	-	-	15.9
Polysulfone	19.7	-	19.6	-	-	19.6	-
Polycarbonate	25.7		-	-	25.5	-	-

Table 2: Storage stability of encapsulated TATP.

B.2. New explosive collection techniques

Current sampling techniques are inefficient and invasive. In an effort to make the release of explosives optimal, we focused on the challenge that pickup is sub-optimal. To counteract inefficient pickup, swabbing greater surface area may increase the mass of explosive collected but only if there is explosive contamination over the whole surface. Screening of hands, headdresses and medical appliances requires physical contact that can be embarrassing and invasive and may expose passengers and screeners to biohazards. To avoid being intrusive or causing physical harm (medical devices), TSA operators may not swab certain areas otherwise of interest. Swabbing can also damage (scratch) some surfaces.

The aim of this work is to create a reversibly switching surface that can be used in a swab to maximize both pick up and release of analyte particles in a detector. Modern explosives swabs suffer from the fact that they can only either adhere analyte well and release it poorly, or adhere analyte poorly but release it well. Both aspects are important to adequate delivery of analyte to a detector system. Thus, we aim to overcome this obstacle by creating a surface that changes adhesion upon application of a small electric charge (less than that of a 9 V battery) or heat. Three approaches are being considered. Approach 1 and 2 do not required direct contact. While not considered non-contact by the DHS definition (i.e. standoff of greater than 2 inches), the switchable swab would attract explosive particles from a distance of ½ inch away from the contaminated surface. This obviates the need for actual physical contact with a surface, and therefore speeds the sampling process, provides for greater privacy, may increase the overall swab lifetime, and may minimize collection of certain types of interfering compounds. These advantages, coupled with higher pickup and release efficiencies, will make for speedier, more pleasant, and more economical checkpoint operations while improving trace detector performance. Approach 3 involves new material synthesis, specifically creation of self-assembled monolayers.

B.2.a. Approach 1

This proposed triboelectric enhancement would require no major change in the swabbing materials nor sensor hardware but would allow a change in the technique as the swab would no longer need to be rubbed over a surface. Triboelectric charging, a subset of contact electrification, is a well-known phenomenon, e.g. children rub balloons in their hair to make the balloon stick to the wall. Therefore, it is surprising that so much of the basic theory is subject to debate, even to the point of whether the charge is generated by transferring electrons, ions, or nanoparticles [11]. Nevertheless, static electricity is exploited in applications from laser jet printers to industrial air cleaners [12]. Electrostatic precipitators have been used for many years for dust and other particle collection [13]. Moreover, though there must be a balance of charge between the two neutral surfaces that are rubbed together to create the positive and negative charges, these charges can persist long after the two surfaces are physically separated [12]. However, the electrostatic precipitator imparts a net charge to the particle [13]. In contrast, our technique charges the collector, which temporarily induces a dipole in the particle. This dipole dissipates as soon as the charge on the collector is neutralized. The precipitator charges the particles; the enhanced swab only redistributes charge temporarily so that the particle is attracted to the collector.

The concept is to enhance the pickup and release efficiency of current swabs used by TSA for the collection of particulate explosives from a variety of surfaces. This enhancement approach can be applied to any swab material of low conductivity, e.g. plastic or cloth. Such a material will be statically charged, e.g., by triboelectric effect or corona discharge. The statically charged swab attracts the explosive particulate through space. However, when the swab is inserted into the inlet of the detection instrument, the static charge is dissipated; thus, it is no longer attractive to the particulate and the analyte is readily released into the inlet. Because the particulate was never pressed into the substrate or the material of the swab by rubbing, it is readily collected and released into the detector. This concept is demonstrated in Figure 3. A Teflon swab charged by rubbing on a polyamide fabric picks up an easily visible amount of pentaerythritol tetranitrate (PETN). This method of charging develops up to -7 kV of static charge on Teflon.
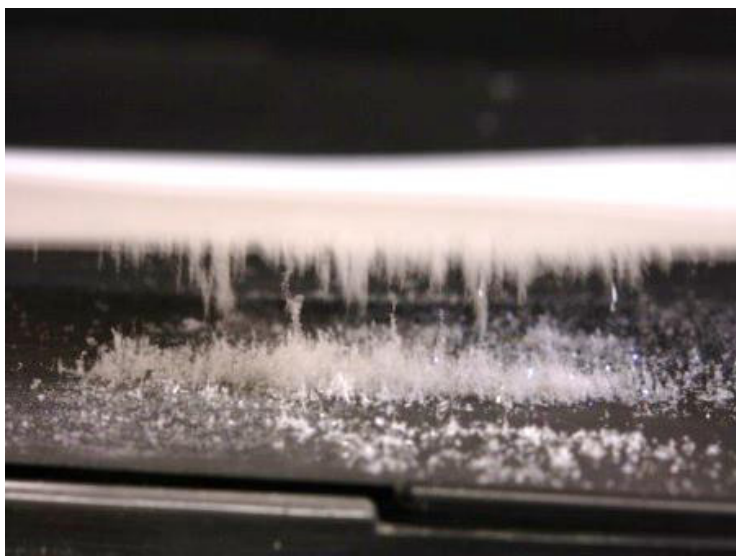
Figure 3: Bulk PETN attraction to statically-charged Teflon.

Figure 4 on the next page illustrates two points: 1) the larger the charge on the swab, the more particles are picked up; and 2) particle size does not appear critical. In Figure 4, the pickup efficiency is demonstrated on sugar particles ranging ~150 μm to ~800 μm in size. In Figure 5, on the next page, this is demonstrated for TNT (2,4,6-trinitrotoluene). (Note macroscopic pickup is more visual, but microscopic pickup has also been demonstrated (vide infra)).

Figure 4: Pickup of sucrose of two particle sizes.

Figure 5: Pickup of TNT of two particle sizes.

Figures 3 to 5 illustrate static generated by contact electrification attracting explosives on the macroscale. In such testing, we have demonstrated the technique is effective on several substrates including glass, polymer resin, card stock, rough vinyl, and human hair. Moreover, the technique is easily employed on the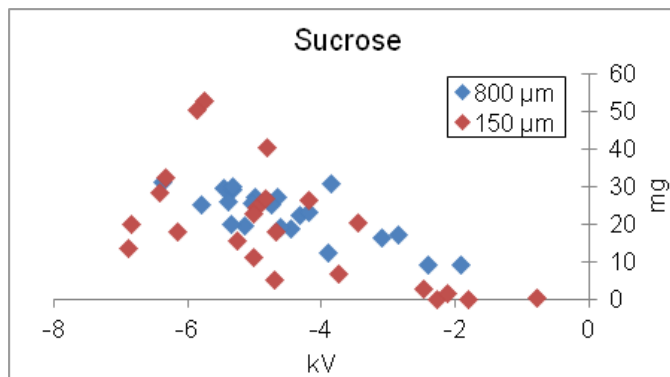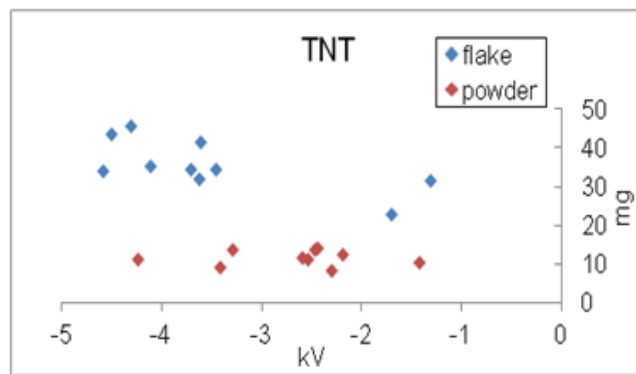 microscale. For example, when strands of hair which had been purposely exposed to explosive vapor were swabbed with a charged and an uncharged swab, the charged swab resulted in detection on the FLIR Fido X3 while the uncharged swab did not (see Fig. 6). (Our premise is that the explosive vapor adhered to dust particles which were subsequently attracted to the charged swab.) Additionally, when a C-4 fingerprint was analyzed using a charged swab, it resulted in detection on a Morpho Itemizer IMS (ion mobility spectrometer). It should be noted that all swabbing experiments were performed at 3 mm standoff.
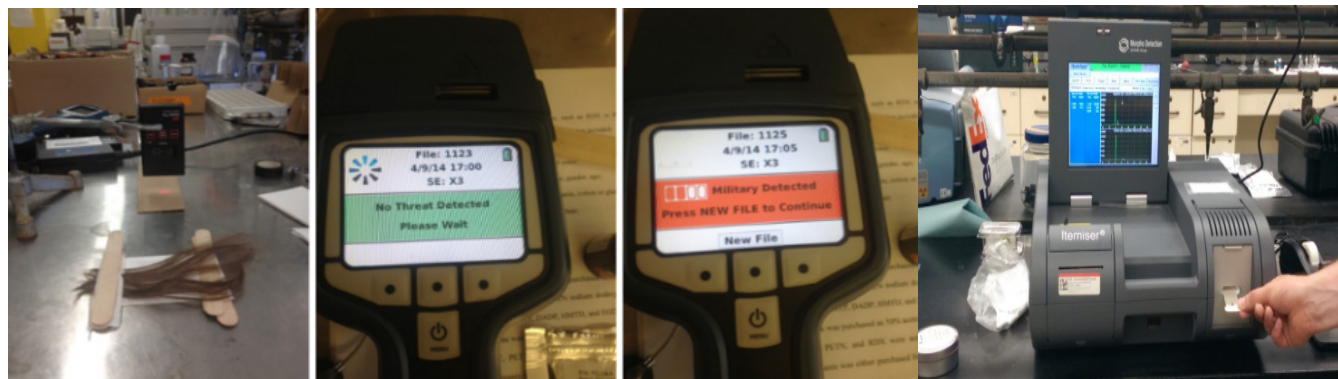

Figure 6: Setup of TNT-exposed hair, depressors for set standoff (left), "No hit" with uncharged (middle left), & "hit" with charged swab (FLIR FidoX3, middle right). Hit with charged swab (Morpho Itemizer, right).

Electrostatically charged swab materials will reduce the introduction of interfering and masking compounds to the detector inlet. Most of these compounds are not very volatile, have high molecular weights, and typically adhere strongly to surfaces, e.g. oils on skin or hair and common plasticizers. During contact sampling, these compounds are typically collected from the surface along with the explosive particles. Electrostatically enhanced sampling appears to provide some selectivity based on the strength of surface adherence. Loose explosive particles are more likely to be picked up by electrostatically charged swabs than oils. Figure 7 on the next page illustrates the effect. The left and middle sets of bars represent "clean" glass (blanks) and "clean" hair. With the non-charged contact swabs (blue), the interfering compounds on the hair caused a background response four times as large as the response on glass. The charged swab, which did not need to contact the hair, did not pick up these interfering compounds. Thus, the hair background was as clean as with the blanks on the glass slide. On the other hand, when explosives were present, as in a TNT contaminated thumbprint (right bars), the charged swabs collected almost as well as the uncharged contact swabs. While this was a small data set, charged swab sampling appears to reduce background response significantly while

response to explosive was only slightly reduced. Swabs in this case were Nomex.
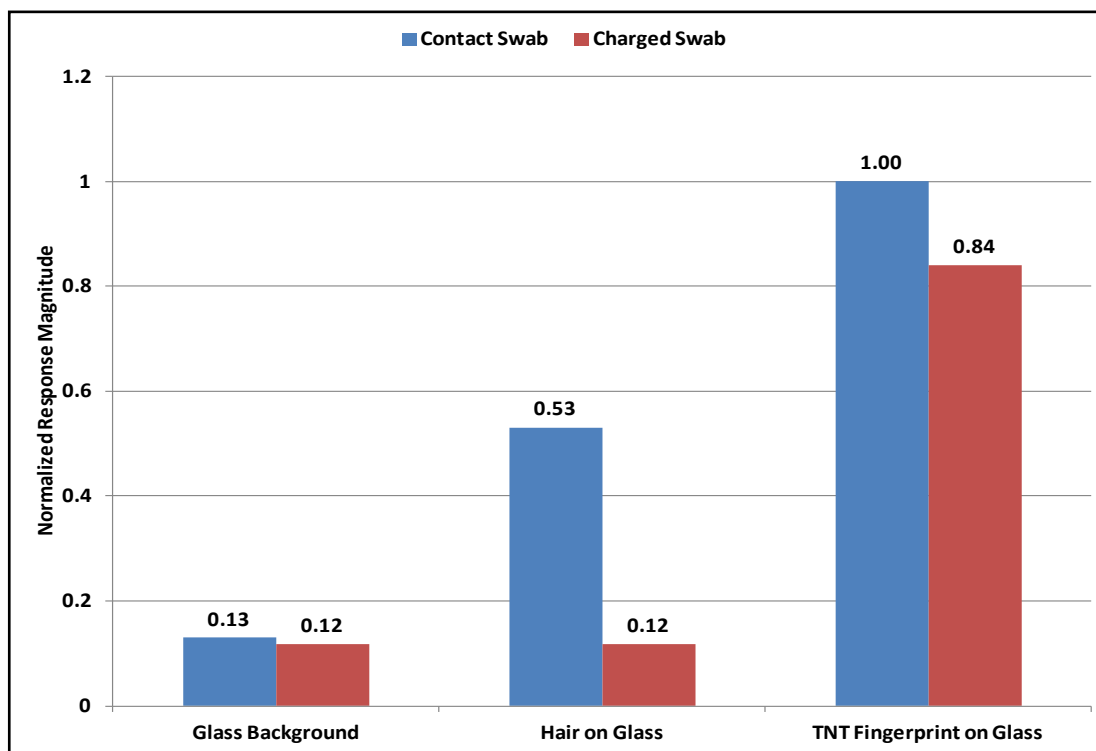

Figure 7: Fido X3 response to Nomex swabs-contact, uncharged (blue) vs. non-contact, charged (red). Substrates include blank glass slide (left), blank hair (middle), and TNT thumbprint (right).

Non-obtrusive detection of trace amounts of illicit materials has long been a goal of detection companies and security firms. Though detector technology continues to improve, a key challenge remains in collection and release of sufficient analyte, e.g., explosives or precursors, into the detector. In fact, many detection companies choose swabs with the best release profile rather than the best collection profile. Hence, materials such as Teflon, Nomex, and metal mesh have been employed. An electrostatically enhanced swab improves the collection efficiencies of these poorly collecting materials. When the swab is placed in the desorber, the charge is dissipated and desorption occurs. Because the collection is done near-field, there is less wear on the swab material, and therefore the swab has a longer life-time. Furthermore, because the swab does not rely on physical adhesion of particles, the particles are readily released when the static field is dissipated. Thus, more residue can be collected, and more residue can be released, facilitating faster and more accurate identification of threat materials. The breadth of explosives and precursors attracted by this method will yield operational benefits in speed and ease with which objects may be screened with greater scrutiny for threat materials. Our swabbing technique will deliver a collection enhancement greater than 50% over comparable sampling techniques currently in use. Desorption efficiency are greater than 90%. Table 2 (D.1) shows that reproducible release in macroscopic samples is 97% (standard deviation less than 3%). Charging time is less than 5 seconds. Desorption time is unchanged from traditional swabbing methods. No additional instrument maintenance or downtime is required. Temperatures tolerated by the swab depend on its chemical makeup, but an electrostatically enhanced Teflon swab is compatible with thermal desorption systems operating at greater than 400 °C.

In near-field mode, the sampled surface is not impacted. We have demonstrated operation on several surface substrates. The near-field mode also spares wear on the swab and enhances its life-time, reducing swab costs below threshold. Reuse of a swab for which there was no alarm is simply a matter of recharging. As a side

benefit, it has been noted that in the near-field mode less contamination is collected on the swab (see Fig. 7). Shelf life for Teflon or Nomex swabs is greater than one year.

B.2.b. Approach 2

Triboelectric charging of swabs presents a number of challenges: potential contamination during charging due to active rubbing of one surface on another; the time required for charging; and maintenance of the charge under high humidity conditions. Creating a swab with an electret surface overcomes these difficulties. An electret is defined as a "piece of dielectric material exhibiting quasi-permanent electrical charge"[14]. Quasi-permanence means that a significant decay in charge does not occur in the time scale of the experiments (years). The electret can extend from the surface into layers of the material (10 to 100 microns). Electrets are created by exposing a dielectric material to an electrical field, thus polarizing it. The magnitude of the charge created on the dielectric material is dependent on the resistance and chemical stability of the material. When heated and exposed to a strong electrostatic field, the polar molecules at the surface of the dielectric (polymer) align themselves (see Fig. 8). The dielectric surface molecules solidify and maintain charge on cooling.
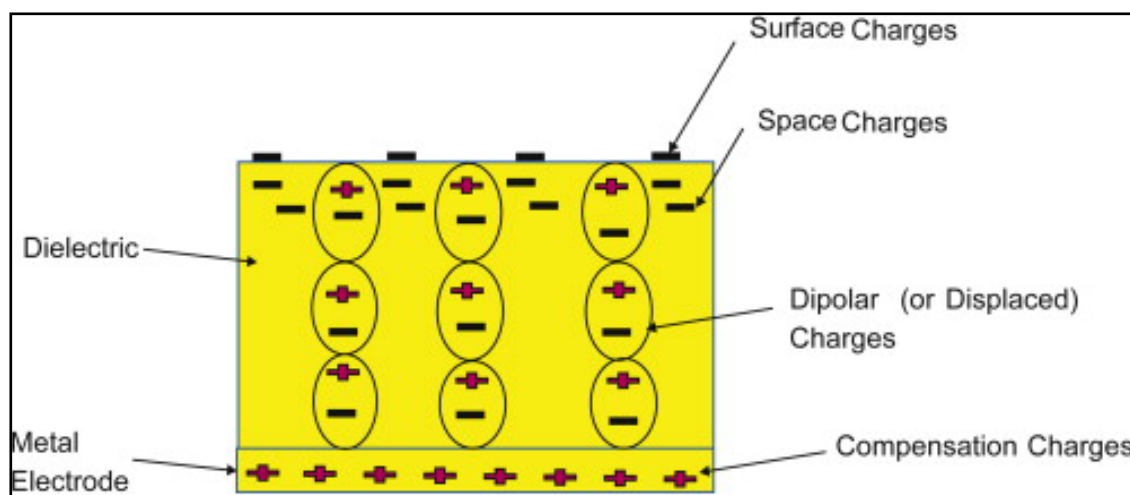
Figure 8: Notional diagram of electrets from [15].

Swabs that are electrets can be created and used in a completely non-contact fashion; thus, reducing the possibility of contamination. The electrets should accept and maintain a charge similar in magnitude to that created by tribocharging (7-12kV). Our initial approach to making electrets would charge Teflon, β-PVDF, or Nomex using an external electric field, e.g., a tip-to-plane corona charging apparatus (see Fig. 9 on the next page). Charging will be performed at elevated temperatures, just under the glass-transition point of the polymer, in order to increase their thermal stability. The apparatus will be purged with dry nitrogen to ensure low humidity. If higher voltage charging is required (> 30 keV), the chamber would be filled with a high dielectric gas such as SF_6; however, need for this high a charging apparatus is not expected.

Swab materials created by Approach 1 (triboelectric charging) will be compared to those created by Approach 2 (electrets). Both of these approaches create a swab that does not require direct contact, and neither approach transfers charge to the operator or the surface being swabbed.

Figure 6.8: Schematic illustration of the tip-to-plane corona charging system with gas supply.
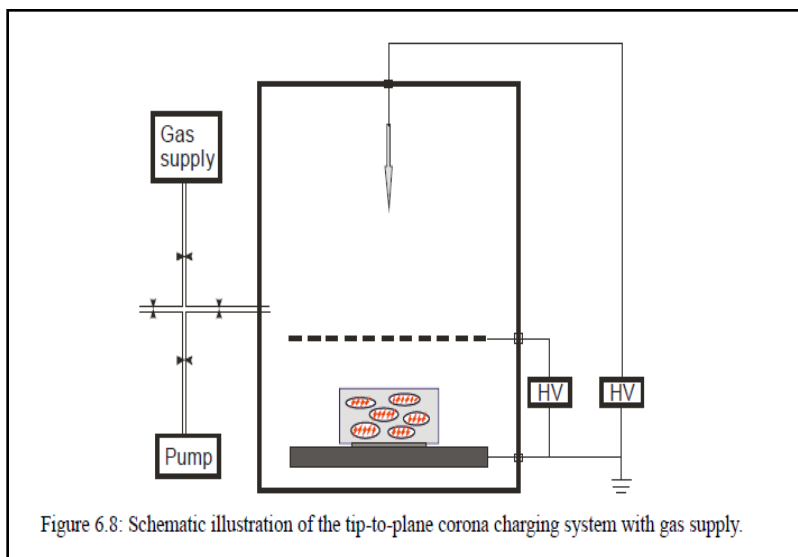
Figure 9: Charging chamber for creating electrets from [16].

B.2.c.   Approach 3

Lahann has reported that a hydrophilic/hydrophobic surface can be created by allowing (16-mercapto)hexa-decanoic acid (MHA) to form a self-assembled monolayer (SAM) on gold sputtered on silicon nitride [17]. The MHA was modified with an acid labile globular head group to produce low-surface packing density and conformational freedom. After SAM formation, the head group is removed to leave a carboxylic acid, which is deprotonated to the carboxylate. This negatively charged carboxylate is electrostatically attracted to or repelled from the gold surface to which it is bound. This attracting/repelling behavior is based on electric potential (see Fig. 10). When a positive potential is applied to the gold, the negatively charged head group is attracted to the surface, revealing an aliphatic (hydrophobic) backbone. Application of a negative potential repels the carboxylate group to its maximum extent, revealing a charged (hydrophilic) face.

Figure 10: A representation of the reversibly switching surface reproduced from [8].

Synthesis of the MHA ester and creation of the SAM on the gold surface was a multi-step process. We are presently simultaneously characterizing the MHA SAM created and investigating metrics available to us for

probing its "switching" properties. Surface analyses explored include reflectance-infrared microscopy, Energy Dispersive X-ray Spectroscopy (EDS), Scanning Electron Microscopy (SEM), and Atomic Force Microscopy (AFM).

B.2.d.   Summary

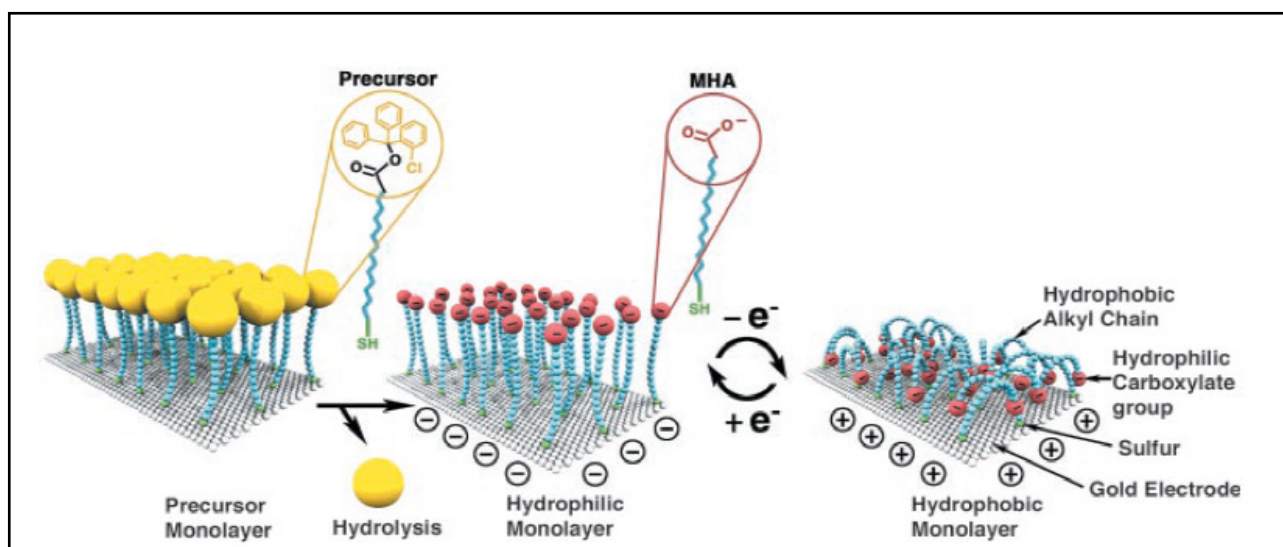The enhancement proposed herein would require no major change in the swabbing materials nor sensor hardware but would require a change in the operational protocol as the swab would no longer need to be rubbed over a surface. Each of the approaches to switchable swabs would require a different operational protocol. Approach 1 would require the swab be charged before each sample collection. Inserting the swab into the detection device would trigger the release of the analyte. In Approach 2, the swab would be permanently charged at the factory, and sample release would be accomplished by heating in the detection device desorber. The swab could immediately be reused. Approach 3, like Approach 1, would require an alignment before every use, and switching would be accomplished at the inlet of the detection device. The enhanced swab would attract explosives particles from a distance of ½ inch away from the contaminated surface. This obviates the need for actual physical contact with a surface and, therefore, speeds the sampling process, provides for greater privacy, may increase the overall swab lifetime and may minimize the collection of certain types of interfering compounds. These advantages, coupled with higher pickup and release efficiencies, will make for speedier, more pleasant and more economical checkpoint operations while improving trace detector performance.

This work resulted in a DHS research award under BAA EXD 13-03 (Advanced Swabs for Near-Field Sampling) with subcontractors, FLIR and DSA.

B.3.   Metrics for explosive-polymer interactions

The interactions of energetic materials and polymers have important implications in safety, long-term storage and performance of explosives and explosive mixtures. AFM was used to investigate adhesion forces, at the molecular scale, of eight energetic materials [(1,3,5-trinitroperhydro-1,3-5-triazine (RDX), octahydro-1,3,5,7-tetranitro-1,3,5,7-tetrazocine (HMX), pentaerythritol tetranitrate (PETN), and 2,4,6-trinitrotoluene (TNT)), energetic salts (potassium chlorate and potassium nitrate), and homemade explosives (hexamethylene triperoxide diamine (HMTD) and triacetone triperoxide (TATP))], on seven common polymers: polyethylene (PE), polyvinylalcohol (PVA), polystyrene (PS), poly(4-vinyl phenol) (P4VP), poly(2,6-dimethylphenylene oxide) (PPO), poly(2,6-diphenyl-p-phenylene oxide) (Tenax®) and polytetrafluoroethylene (Teflon®). Teflon was the least adhesive polymer to all EMs, while no distinct trend could be elucidated for the other polymers.

Typically, AFM is used to generate topographic images of surface features from atomic to micron scale [18]. However, AFM can also generate force curves between the cantilever tip and sample surface [19-23]. These force curves yield adhesive parameters for the two test materials. By using the AFM cantilever and sample stage, an explosive particle affixed to the cantilever is pressed into a sample material, or the sample material is deposited onto the cantilever tip and pressed into a monolayer of explosive [24] (see Fig. 11 on the next page). Previous work on energetic materials and AFM focused on adhesion to terminal group-functionalized self-assembled monolayers [25], and metal coupon finishes [26].

Commercial polymers were acquired and flattened on glass slides by gentle heating and pressing with a silicon wafer of defined roughness (RRMS ~2 nm). This approach was particularly difficult with the polymers acquired as powders. PE, PS, and PVA yielded RRMS ranging from 15 to 45 nm, while Teflon gave a value of 342 nm. Explosive microcrystallites were adhered to tipless cantilevers using a micromanipulator and polarized light microscope. Particle size was estimated using an ocular micrometer; more accurate estimates of particle size were obtained by scanning electron microscopy (SEM). A microdrop of UV-curing glue (Loctite 352, Henkel) was used to adhere the energetic microcrystallite (~40 micron long) to the cantilever. Tips

were inspected by SEM imaging. Each energetic tip was tested against Teflon, PE, PS, and PVA, while some tips were tested against all polymer surfaces. If the energetic tip appeared damaged, it was replaced and all measurements were rerun.

Before force curves were taken and after each polymer set, the modified cantilever was calibrated using the Thermal K function available on an Agilent 5500 AFM. Though many methods exist for calculating a cantilever spring constant, this function employs thermal fluctuations of the cantilever as harmonic oscillation [29-33]. One 50 μm x 50 μm area was raster scanned at 1 μm/s to collect force measurements at <20% relative humidity. Because the polymer surface was easily deformed, the vertical displacement of the force curve was adjusted after every few force curve measurements to prevent indentation of the polymer.

Force measurements were taken using native tipped cantilevers, tipless cantilevers with only glue, a tipless cantilever with a polystyrene microsphere, and tipless cantilevers with fully adhered energetic microcrystallites. The order of polymers examined against a given tip was altered to show that one data set had no effect on another; repeat measurements of an initial polymer were conducted after collecting measurements from a second polymer for the same reason. After collection of a number of force curves (usually 1000), unrepresentative curves were culled for two primary reasons. First, significant indentation of the polymer after the jump-to-contact point was occasionally unavoidable, causing plastic deformation to the polymer or energetic material particle or transfer of significant amounts of polymer onto the particle. After the deformation or transfer, each successive force curve would be obtained with a unique particle (or polymer-coated particle), hindering comparison to other polymer force curves and other force curves within the same polymer set. Second, surface roughness of polymer substrates was potentially too high, causing unrepresentative adhesion or detector saturation. Representative force curves were baseline-normalized and calibrated using the measured cantilever deflection sensitivity and force constant; then a histogram was created to determine the adhesion force with highest frequency. A representative histogram is shown in Figure 12. Quantitative force measurements were collected for a virgin tipped cantilever and polystyrene microsphere on Teflon, PE, PS, and PVA (see Table 3 on the following page). Results confirm that none of the energetic adhesions resulted from artifacts of cantilever, glue, or polymer-polymer adhesion. In fact, the obtained polystyrene-polystyrene adhesion force from the PS microsphere (335 nN) closely correlates to a previously calculated force (314 nN) [34].
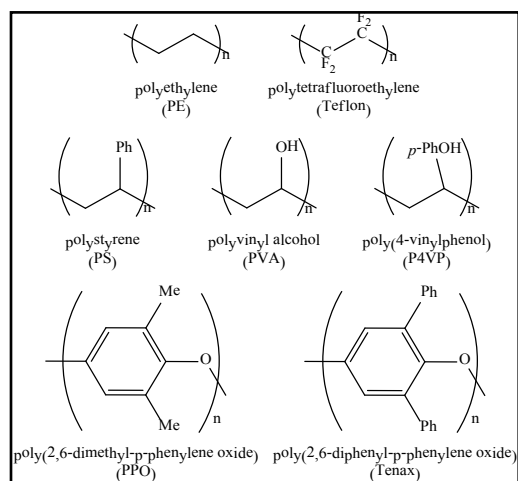
Figure 11: Monomers units of polymers used.
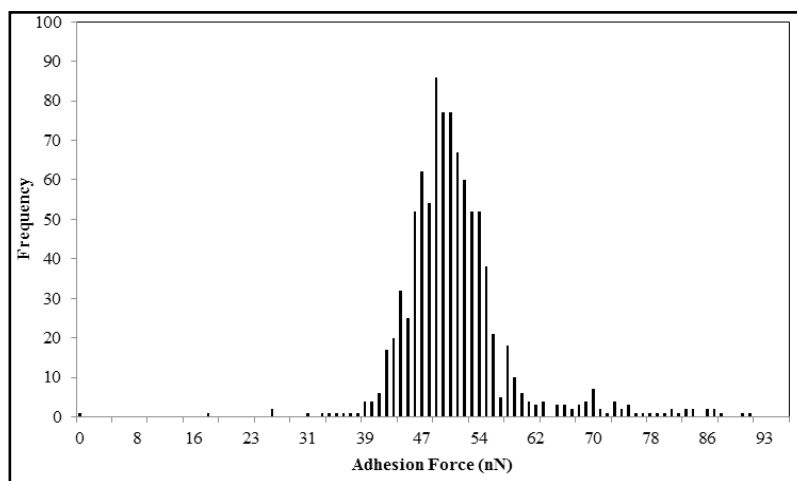
Figure 12: Force histogram of KNO3 v. polyethylene.

Quantitative force measurements were collected for eight energetic materials on the seven polymer substrates. AFM data sets were run over a period of 18 months. Table 3 on the following page presents the data collected over the last two intervals in order to exhibit the degree of reproducibility using different energetic material tips and different polymer substrates. Table 3 shows both the number of scans and the standard de-

viations. As is typical for AFM measurements, standard deviations were large (see Table 4 on the next page). In cases where the standard deviation was larger than the measured force, the data are shown, with shadowing, but not included in the averages. Examining the trends across the seven polymers, Teflon and P4VP had the lowest adhesion forces for all eight energetic materials. The average force exhibited with these two surfaces was almost as small as that observed with the bare cantilever. For Teflon, low adhesion force values are not surprising because it is valued for its "nonstick" properties. Its higher relative surface roughness (RRMS 342 nm) may account for values with high standard deviations. In addition, the small values observed with P4VP could be attributed to high surface asperities throughout a rough substrate. We encountered great difficulty in creating a smooth surface for this material, acquired as a powder, and the resulting surface could have been so rough as to only create a miniscule contact area and subsequent low adhesion force. The other five polymers had average adhesion forces ranging from 108 to 127 nN, which, considering the standard deviations, were essentially identical.

The eight energetic materials studied represent the major classes of military explosives, as well as the improvised peroxide explosives and energetic oxidizers: nitrate ester (PETN); nitroarene (TNT); nitramine (RDX and HMX); peroxides (HMTD and TATP); and salts (KNO3 and KClO3). (As explained above, shadowed data were not included in the averages). While the data in Table 3 on the next page allowed us to detect some differences among the polymer substrates, the diverse structural differences among the energetic materials could not be distinguished from adhesion measurements. For each energetic, the data sets collected in May were averaged separately from those collected in Sept/Oct. Our purpose in averaging the two data sets separately was to see the magnitude of the differences in measured adhesion another researcher might observe using the same chemical but different microcrystal on the tip and same polymer but different surface preparation. The overall average for a given energetic material across all polymers is shown in the far right column in Table 3 on the next page. Little distinction is seen among them.

Two polymers, Teflon and P4VP, stand out as having low adhesion to the energetics. This feature, especially in P4VP, deserves further examination. However, there was generally little difference in the adhesion of the various energetics to a variety of polymers. This lack of differentiation among chemicals with diverse functional groups suggests that the difference in functionality of the energetics is not the main factor affecting the adhesion forces. Macro scale considerations such as lattice structure, surface area, and surface roughness may have a greater effect on adhesion forces than the purely van der Waals-dominated interactions assumed herein.

Energetic Material	Teflon			PE			PS			PVA			P4VP			PPO			Tenax			Date	Ave. Set	Ave. All
	Force (nN)	St Dev	Scans	Force (nN)	St Dev	Scans	Force (nN)	St Dev	Scans	Force (nN)	St Dev	Scans	Force (nN)	St Dev	Scans	Force (nN)	St Dev	Scans	Force (nN)	St Dev	Scans			
HMTD	15	23	680	71	88	815	50	15	429	130	81	512	22	13	1035	103	47	948				May-14	76	
	119	85	953	186	70	948	152	51	895	184	14	973										Oct-14	160	118
HMX	40	31	906	95	48	907	52	77	969	80	50	976	43	16	679	74	82	859	185	40	803	May-14	89	
	31	23	968	113	15	974	59	26	967	59	26	967										Sep-14	66	101
RDX	86	124	940	98	44	937				77	73	855	42	56	818				56	60	932	May-14	88	
	41	24	983	117	83	978	270	94	941	101	93	967										Oct-14	132	117
PETN	23	17	804	87	32	952	98	44	937										17	8	938	May-14	56	
	99	49	944	161	17	980	125	26	934	238	48	976										Sep-14	156	106
TNT	10	22	835	81	55	935	205	82	863	60	5	1009	69	72	872	176	72	837	33	56	793	May-14	131	
	14	14	1081	89	35	936	100	32	636	26	57	964										Sep-14	95	119
KClO$_3$	51	55	528	328	82	989	49	16	434							149	77	818	149	75	706	May-14	169	
	22	40	951	118	21	998	85	59	954	110	43	944										Oct-14	104	141
KNO$_3$	46	30	1007	171	23	999	154	28	1003	70	47	908	43	22	941	58	31	889	125	56	377	May-14	95	
	41	24	976	49	24	952	85	21	980	44	7	982										Sep-14	55	81
TATP	28	34	1081	85	70	376	94	36	942	137	58	877										Oct-14	105	105
Ave.	55			127			117			108			36			122			119					

Table 3: Energetic materials on polymer adhesion force summary.

Reference	Tip	Substrate	Adhesion Force (nN)	Standard Deviation/Error
8	Energetics	Functionalized monolayers	20-130	10-50
9	Energetics	Acrylic coatings	16-110	5-24
18	Polystyrene	Polypropylene	250-400	40%
19	Polystyrene Latex	Silicon	127	21
20	Polystyrene	Silica	1000-2000	N/A

Table 4: Typical adhesion forces and standard deviations.

C.   Major Contributions

A primary consequence of this research is safety. Workers using explosives handle them with inert material, e.g. a container, a gloved hand, a detection instrument. They must be assured there are no unanticipated hazards. Second, most detection instruments contain plastic parts and many ETDs require pre-concentrators or swabs. Not only will this project seek the best way to evaluate the wealth of modern materials available, but it is likely to point to some of the best choices in these areas. This impacts both trace and bulk detection.

TATP has been successfully encapsulated both for canine training aids and for calibration of trace detection equipment. HMTD is presently being studied.

A non-contact swab has achieved sufficiently promising results to win additional funding.

AFM has been used to examine explosive/polymer interactions, and calorimetry is presently being employed for the same purpose.

D.   Milestones

Our present approach to TATP canine training aids is presently being adapted to another peroxide explosive, HMTD. Whether this approach can be adapted to the low-melting HME erythritol tetranitrate (ETN) is a subject of present experimentation.

Efforts toward switchable swabs have just begun. In terms of specially prepared polymers, we have synthesized a polymer which should have the desired characteristics. However, complete characterization of that polymer must be done before the "switchable" properties can be confirmed and applied to the target materials.

We are also examining charged swabs for their pick-up and release capabilities. We have taken a two-prong approach, using electrostatics, a temporary charge, as well as electrets, for a more permanent approach. Both approaches need to be tested for long term viability.

E.   Future Plans

All three areas outlined above continue to be the subject of active research.

Coating and encapsulation of materials will continue to be of interest. Not only will we investigate encapsulation of energetic materials, but also the encapsulation of potential additives to energetics. For example, we have shown that addition of parts-per-million (ppm) amounts of generally-recognized-as-safe (GRAS) metals to 3% or 12% hydrogen peroxide (HP) prevents its concentration by heating, instead promoting its decomposition. Furthermore, at ppm levels, the metals do not affect the stability of hydrogen peroxide at room temperature. Applying the same approach to 30% HP requires elevated levels of metals which would negatively influence shelf-life. This could be avoided by encapsulating the metals with a coating which can be degraded by heating. Thus, at room temperature, the 30% HP would be stable, but if heated, rather than concentrate the HP, the heat would remove the polymer coating from the metals and expose the HP to their degrading effect. This requires that the polymer be compatible with both the metal and the HP and that it can be removed or softened by heating; hence, the need for metrics.

Work on switchable polymers and swabs, which has just begun and will continue, including electrostatics and electrets. In addition, each task requires its own metrics. Last year, we investigated vapor chamber exposure followed by total extraction (solvent). That tool we now thoroughly understand in terms of use and limitation. This year we have examined AFM, and in coming year's calorimetry will be explored.

III.   EDUCATION AND WORKFORCE DEVELOPMENT ACTIVITY

A.   Course, Seminar or Workshop Development

"Advanced Studied in Explosives" course was offered for the first time in spring of 2015 with 15 graduate students in attendance.

In May 2015, a hands-on course entitled "Explosive Analysis" was offered for the first time; six members of the HSE came to URI to attend.

Graduate student Devon Swanson was selected to give an award talk at the Trace Explosive Detection conference for his work on AFM of explosives (April 2015, Pittsburgh).

Dr. Smith presented "An Introduction to the Properties of Explosive and Trace Detection" at the IEEE HST '15 ALERT Tutorial Session: Introduction to Explosives/Threat Screening Tools and Technologies in April 2015.

Courses were presented for the Army, Navy, Air Force, and the Transportation Security Administration (TSA-TSIF, 10 classes and 200 people) and TSA explosive specialists (TSA-TSS-E, 5 classes and 110 people).

A.1.   Invited Lectures

Thermal Stability and Chemistry of Difficult Energetic Materials", New Trends in Research Energetic Materials; Pardubice, CZ, April 11, 2015.

JANNAF, December 10, 2014, Academic Research to Real Life Application, ABQ

7th Annual CBRNe Convergence, October 28-30 2104, New York, NY, tutorial to first responders

Recognizing Improvise Drug vs Explosive Labs, 23rd Annual Haz-Mat Training Conf. September 18, 2014, Plymouth, MA, tutorial to first responders

B.   Student Internship, Job or Research Opportunities

Each URI project supports one or more graduate students. This is their best learning experience. Undergraduates are also supported on the projects as their class schedules permit.

A newly minted PhD from our group, Jon Canino, accepted a position at Signature Science and is working at the Transportation Security Laboratory in New Jersey.

C.   Interactions and Outreach to K-12, Community College, Minority Serving Institution Students or Faculty

We have continued our K-12 outreach by hosting high school teachers in the summer and providing chemical magic shows at schools K-12. High school teachers conduct research in URI labs for 8 to 10 weeks under the mentorship of a graduate student. As a result, two have gone back to seek advanced degrees.

In addition, in the summer of 2014, we hosted 2 forensic scientists from Qatar and a West Point cadet for several weeks. For the summer of 2014, we hosted a professor from Tuskegee University and one of her students. In summer of 2015, we hosted two Navy midshipmen and a Penn State engineer, and air force employee will be placed at URI to begin work on a master's degree.

D.   Training to Professionals or Others

We trained 110 TSS-E (TSA explosive specialists) in five classes and approximately 230 other people involved in the homeland security industry in 12 classes, one of which was created to meet the needs of the U.S. Army forensic laboratory.

IV.   RELEVANCE AND TRANSITION

A.   Relevance of Research to the DHS enterprise

- R1-C2 "encapsulation/coating" addresses safe samples of explosive. Evidence that this program has importance are as follows:
    - o   Requests from ETD (explosive trace detection) equipment vendors for product information;
    - o   Requests to license the vapor scent product;
    - o   An innovation award from the National Homeland Defense Foundation of $10,000 for the vapor scent product.
- R1-C2 novel sampling addresses novel, non-contact, switchable sampling of explosives. Metrics include:
    - o   New initiative received DHS award (see overview and references therein).

B.   Potential for Transition

- R1-C2 addresses safe samples of explosive. We receive requests to license the vapor scent product.

- R1-C2 addresses sampling of explosives. A DHS award under BAA EXD 13-03 (see overview and references therein) with transition partners FLIR and DSA is presently being negotiated.

C.   Transition Pathway

- R1-C2 addresses safe samples of explosive. We receive requests to license the product and are working with a potential vendor, although the product is presently available for free to those requesting it.

- R1-C2 addresses sampling partners are in place for transitioning this work.

D.   Customer Connections

We have been distributing the scent product for free to a number of users. This puts a customer base in place for future sales.

V.   PROJECT DOCUMENTATION

A.   Peer Reviewed Journal Articles

1. Oxley, "Explosive Detection: How We Got Here and Where Are We Going?" International Journal of Energetic Materials and Chemical Propulsion; 2014, 13(4): 373-381.

2. Oxley, J.C.; Smith, J.L.; Canino, J.N. "Insensitive TATP Training Aid by Microencapsulation" J. Energetic Materials; 2015, 33(3), 215-228.

B.   Other Publications

Pending-

1. Oxley, J.C.; Smith, J.C.; Swanson, D.; Kagan, G. "Adhesion Forces of Energetic Materials on Polymer Surfaces, submitted to Propellants, Explosives, Pyrotechnics.

2. Oxley, J.C.; Smith, J.L.; Porter, M.; Colizza, K.; McLennan, L. ; Zeire, Y.; Kosloff, R.; Dubikova, F. "Synthesis and Degradation of Hexamethylene triperoxide diamine (HMTD)", submitted to Propellants, Explosives, Pyrotechnics.

3. Oxley, J.; Smith, J.; Donnelly, M.; Rayome, S. "Thermal Stability Studies on IMX-101 (Dinitroanisole/Nitroguanidine/NTO)", submitted to Propellants, Explosives, Pyrotechnics.

C.   Other Conference Proceedings

1. Smith, J. "An Introduction to the Properties of Explosive and Trace Detection." IEEE HST '15 Tutorial Session: Introduction to Explosives/Threat Screening Tools and Technologies, April 2015.

D.   Other Presentations

1. Seminars
   a. Devon Swanson (presenter) with J Oxley; J. Smith; G. Kagan "Adhesion Forces of Energetic Materials on Polymer Surfaces" Trace Explosive Detection April 2015; Pittsburgh

2. Poster Sessions—for ALERT events

3. Short Courses-listed under education

E.   *Student theses or dissertations produced from this project*

1. PhD Chemistry: Jon Canino Dec. 2014 Polymer Systems and Explosives

2. PhD Chemistry: Maria Donnelly May 2105 Thermal Stability & Sensitivity of Energetic Formulations

F.   *New and Existing Courses Developed and Student Enrollment*

New or Existing	Course/Module/ Degree/Cert.	Title	Description	Student Enrollment
New	Certificate	Explosive Analysis	Lab Analysis of Explosives	6*
New	Graduate credit	Explosive Analysis	Mass Spectroscopy; Thermal; Shock	15
Existing	Certificate	Pyrotechnics	Raytheon K-Tech ABQ	12
Existing	Certificate	Fundamentals	Fundamentals - Alcoa	12
Existing	Certificate	Air Blast	Air Blast - Huntsville	14
Existing	Certificate	Materials Characterization	Picatinny	14
Existing	Certificate	Fundamentals	TSIF Fundamentals	50
Existing	Certificate	Fundamentals	Fundamentals Eglin	28
Existing	Certificate	Fundamentals	URI Fundamentals	32
Existing	Certificate	Air Blast	Air Blast - LANL	15
Existing	Certificate	Materials Characterization	Materials Characterizations - Navy	18
Existing	Certificate	Stability, Compatibility	Stability, Compatibility - Navy	18

* Included DHS personnel

G.   *Requests for Assistance/Advice*

1. From DHS

   a. On call for a variety of TSA TSS-ES personnel

   b. Oxley is part of the DHS-formed Inter-Agency Explosive Terrorism Risk Assessment Working Group (IExTRAWG)

2. From Federal/State/Local Government

   a. Singapore, India, Turkey Defense groups ask questions, request classes; class request from India in review at Dept of State.

   b. We have been asked to support Brookhaven National Lab in some of their international outreach.

VI.   REFERENCES

[1] Oxley, J.C.; Smith, J.L.; Canino, J.N. "Insensitive TATP Training Aid by Microencapsulation" J. Energetic Materials; 2015, 33(3), 215-228. 10.1080/07370652.2014.985857

[2] Oxley, J.C.; Smith, J.C.; Swanson, D.; Kagan, G. "Adhesion Forces of Energetic Materials on Polymer Surfaces, submitted.

[3] Gan, Y. X.; Yazawa, R. H.; Smith, J. L.; Oxley, J. C.; Zhang, G.; Canino, J.; Ying, J.; Kagan, G.; Zhang, L., Nitroaromatic explosive sorption and sensing using electrochemically processed polyaniline-titanium dioxide hybrid nanocomposite. Materials Chemistry Physics 2014, 143 (3), 1431-1439 DOI .10.1016/j.matchemphys. 2013.11.059

[4] Johnson, S.C.; Gan, Y, X.; Calderon, S.B.; Smith, J.L.; Oxley, J.C. "Measuring the Electrochemical Response of a Titanium Dioxide Nanotube Electrode to Various Chemicals as Explosive Components" International Research Journal of Pure and Applied Chemistry 2015; 5(2) 119-130. DOI: 10.9734/IRJPAC/2015/14263

[5] Jimmie Oxley; James Smith; Jonthan Canino March 2013. Provisional Patent. U.S. Patent App. No. 14/215,768 "Non-Detonable Explosive Simulant Source"

[6] DHS MSI award of $50,000 for "Electrochemically Synthesized Nanocomposites for Explosive Detection and Mitigation" by Dr. Y.X. Gan.

[7] DHS contract negotiations in progress for "Advanced Swabs for Near-Field Sampling" under BAA EXD 13-03

[8] First-Place Team 8th Annual National Security Innovation Contest; April 2014 for Safe Training Aids for Bomb-Sniffing Dogs; prize $10,000.

[9] Oxley, J.C.; Smith, J.L.; Canino, J.N. "Insensitive TATP Training Aid by Microencapsulation" J. Energetic Materials; 2015, 33(3), 215-228 and references therein.

[10] First-Place Team 8th Annual National Security Innovation Contest; April 2014 for Safe Training Aids for Bomb-Sniffing Dogs; prize $10,000.

[11] Lacks, D. J.; Sankaran, R. M., Contact electrification of insulating materials. Journal of Physics D: Applied Physics 2011, 44 (45), 453001.

[12] Smyth, C. P., Dielectric behavior and structure: dielectric constant and loss, dipole moment and molecular structure. McGraw-Hill: 1955.

[13] Jonassen, N., Electrostatics, International Thomson Publishing: 1998.

[14] Sessler, G.M. Electrets, Laplacian Press: Morgan Hill, California, 1998.

[15] Singh, R.; A review of developments in thermal techniques for charge profile measurements in polymer electrets. Journal of Electrostatics. 2014, 72, 322-329.

[16] Fang, P. PhD. Dissertation, University of Potsdam, 2010.

[17] Lahann, J.; Mitragotri, S.; Tran, T-N; Kaido, H.; Sundaram, J.; Choi, I.; Hoffer, S.; Somorjai, G.A.; Langer, R., A Reversibly Switching Surface. Science 2003, 299 (5605), 371-374.

[18] G. Binnig, C. F. Quate, and Ch. Gerber, "Atomic force microscope," Phys. Rev. Lett, vol. 56, pp. 930-933, March 1986.

[19] H.-J. Butt, B. Cappella, and M. Kappl, "Force measurements with the atomic force microscope: technique, interpretation and applications," Sur. Sci Rep., vol. 59, pp. 1-152, October 2005.

[20] W. A. Ducker, T. J. Senden, and R. M. Pashley, "Direct measurement of colloidal forces using an atomic force microscope," Nature, vol. 353, pp. 239-241, September 1991.

[21] A. Janshoff, M. Neitzert, Y. Oberdörfer, and H. Fuchs, "Force spectroscopy of molecular systems — single molecule spectroscopy of polymers and biomolecules," Angew. Chem. Int. Edit., vol. 39, pp. 3212-3237, September 2000.

[22] Y. I. Rabinovich and R. H. Yoon, "Use of atomic force microscope for the measurements of hydrophobic forces between silanated silica plate and glass sphere," Langmuir, vol. 10, pp. 1903-1909, June 1994.

[23] G. V. Lubarsky, M. R. Davidson, and R. H. Bradley, "Elastic modulus, oxidation depth, and adhesion force of surface modified polystyrene studied by AFM and XPS," Surf. Sci., vol. 558, pp. 135-144, June 2004.

[24] Y. Gan, "Invited review article: a review of techniques for attaching micro- and nanoparticles to a probe's tip for surface force and near-field optical measurements," Rev. Sci. Instrum., vol. 78, pp. 081101-1 - 081101-8, August 2007.

[25] Y. Zakon, N. G. Lemcoff, A. Marmur, and Y. Zeiri, "Adhesion of standard explosive particles to model surfaces," J. Phys. Chem. C, vol. 116, pp. 22815-22822, November 2012.

[26] M. N. Chaffee-Cipich, B. D. Sturtevant, and S. P. Beaudoin, "Adhesion of explosives," Anal. Chem.,vol. 85, pp. 5358-5366, June 2013.

[27] J. C. Oxley, J. L. Smith, P. R. Bowden, and R. C. Rettinger, "Factors influencing triacetone triperoxide (TATP) and diacetone diperoxide (DADP) formation: Part I," Propell. Explos. Pyrot., vol. 38, pp. 244-254, April 2013.

[28] J. C. Oxley, J. Zhang, J. L. Smith, and E. Cioffi, "Mass spectra of unlabeled and isotopically labeled hexamethylene triperoxide diamine," Propell. Explos. Pyrot., vol. 25, pp. 284-287, December 2000.

[29] J. L. Hutter, J. Bechhoefer, "Calibration of atomic-force microscope tips," Rev. Sci. Instrum., vol. 64, pp. 1868-1873, July 1993.

[30] A. Torii, M. Sasaki, K. Hane, and S. Okuma, "A method for determining the spring constant of cantilevers for atomic force microscopy," Meas. Sci. Technol., vol. 7, pp. 179-184, February 1996.

[31] C. T. Gibson, G. W. Watson, and S. Myhra, "Determination of the spring constants of probes for force microscopy/spectroscopy," Nanotechnology, vol. 7, pp. 259-262, September 1996.

[32] N. A. Burnham et al., "Comparison of calibration methods for atomic-force microscopy cantilevers," Nanotechnology, vol. 14, pp. 1-6, January 2003.

[33] S. M. Cook et al., "Practical implementation of dynamic methods for measuring atomic force microscope cantilever spring constants," Nanotechnology, vol. 17, pp. 2135-2145, May 2006.

[34] B. Cappella, and G. Dietler, "Force-distance curves by atomic force microscopy," Surf. Sci. Rep., vol. 34, pp. 1-104, 1999.

[35] E. R. Beach, G. W. Tormoen, J. Drelich, and R. Han, "Pull-off force measurements between rough surfaces by atomic force microscopy," J. Colloid Interf. Sci., vol. 247, pp. 84-99, 2000.

[36] K. Cooper, A. Gupta, and S. Beaudoin, "Simulation of the adhesion of particles to surfaces," J. Colloid Interf. Sci., vol. 234, pp. 284-292, 2001.

[37] M. Reitsma, V. Craig, and S. Biggs, "Elasto-plastic and visco-elastic deformations of a polymer sphere measured using colloid probe and scanning electron microscopy," J. Int. Adhes. Adhes., vol. 20, pp. 445-448, 2000.